

How Real Estate Responds to Regulatory Changes over the Long Run: Evidence from the Closure of Hong Kong's Downtown Airport

Jingwen Zheng*

December 5, 2024

Click [here](#) for the most recent version

Abstract

City governments increasingly view relaxing building height limits, or “upzoning,” as a key strategy to promote compact and affordable cities, yet evidence on its effectiveness is mixed. To evaluate the determinants of upzoning effectiveness, I study two distinct upzoning events in urban Hong Kong. In 1989, the city implemented the first modest upzoning along a newly narrowed flight path to the downtown airport. In 1998, following the closure of the downtown airport, the city undertook the second, large-scale upzoning, which is *one of the largest in history worldwide*. My spatial regression discontinuity design at upzoning borders before and after each upzoning event yields three key findings about developers’ responses over the course of three decades. First, the modest upzoning did not elicit a strong supply response in urban areas where building height limits were binding. Second, in response to the large-scale upzoning, *within a decade*, developers closed the initial gaps in building height, volume, and quality between the two sides of the upzoning borders. Third, developers deferred maintenance and investment before the airport closure, as evidenced by a rapid deterioration in flat quality, suggesting they anticipated the larger upzoning. This anticipation likely moderated their response to the first modest upzoning and accelerated the convergence of the built environment after the second. These results indicate that in a rapidly growing city, upzoning can drive vertical development and housing supply in areas where zoning is binding. However, its effectiveness depends on the extent of upzoning and developers’ expectations of future zoning changes.

*Jingwen Zheng: The Trachtenberg School of Public Policy and Public Administration, George Washington University (GWU), jzheng@gwu.edu. I would like to thank Leah Brooks, Remi Jedwab, Paul Carrillo and Tanner Regan for their invaluable guidance. Special thanks to Arnab Basu, Marco Gonzalez-Navarro, Matthew Turner, and Anthony Yezer for inspiring conversations, and seminar participants at the GWU Development Tea Workshop, 2024 NARSC, 2024 APPAM, and 2024 SMU-Jinan Conference on Urban and Regional Economics for their feedback. This research was generously funded by the Sigur Center for Asian Studies and the Cosmos Club. I’m thankful for the support provided by the staff at the University of Hong Kong library and various Hong Kong government agencies during my fieldwork.

1. Introduction

It is now conventional wisdom that cities' failure to allow for housing growth leads to increased housing prices and stifles economic growth (Baum-Snow, 2023; Molloy et al., 2020; Paciorek, 2013). To accommodate more housing, economists often recommend relaxing stringent zoning regulations—such as those governing building heights, floor area ratios (FAR), and housing types—in already-developed areas, allowing developers to respond to underlying market forces. Can such upzoning effectively incentivize a supply response? Answering this question is challenging for several reasons. First, the selection of upzoning locations within a city is not random; it is typically influenced by pre-existing conditions, such as housing prices and proximity to public transit. Second, the average scale of upzoning in cities is generally small, and upzoning often involves changes to multiple density parameters simultaneously (e.g., zone types and allowable densities), making it difficult to isolate the impact of a major zoning shift. For example, Chicago relaxed FAR by 17%, New York by 23%, and Mumbai by 10-50%. São Paulo not only relaxed the built area ratio by 36% but also updated zone types.¹ Third, capital investment is generally a slow process and requires an extended time horizon to fully understand the effects of upzoning.

This paper addresses these challenges by examining two distinct upzoning events in urban Hong Kong. In 1989, the city implemented a modest upzoning along a newly narrowed flight path to the downtown airport, made possible by advancements in airplane navigation technology.² Concurrently, the government announced plans to build a new airport farther from the city center to replace the downtown airport. In 1998, the downtown airport's closure prompted a large-scale upzoning in central urban areas.³ Both events occurred during a period of rapid economic and urban expansion in Hong

¹The average scale of upzoning in the referenced cities was derived from analyses in the following studies: Freemark (2020); Peng (2023); Anagol et al. (2021); Nagpal and Gandhi (2023).

²Advancements in airplane navigation technology reduced the need for strict building height restrictions enforced along a wide flight path for airplanes approaching and landing at the downtown airport. In response, the government narrowed the flight path and relaxed height limits, particularly in areas outside the narrowed path.

³The airport closure eliminated the need for building height restrictions to ensure safe aircraft operations in urban Hong Kong.

Kong—a city with one of the most expensive housing markets, facing challenges such as limited land availability and an urgent need for affordable housing.

The first upzoning increased height limits by 43% in regulated urban areas—a scale on the higher end compared to typical upzoning events in other cities today. The second upzoning, following the downtown airport’s closure, increased height limits by 212%, making it *one of the largest in history*. This second upzoning enabled additional building volume equivalent to 790 Empire State Buildings in urban Hong Kong. Specifically, the city increased height limits within the flight path, previously capped at an average of 37 meters, by more than ten times to 463 meters, allowing for the construction of skyscrapers. For context, the Empire State Building stands at 443 meters. These two zoning shifts, which focused solely on building heights in already-developed urban areas, provide a unique opportunity to analyze the scale and speed of developers’ responses over the course of three decades.

I measure developers’ responses by collecting and digitizing granular, novel datasets spanning three decades, focusing on two types of outcomes. The first outcome is developer construction quantity, measured by maximum building height, total building footprint, and total building volume within 30m × 30m grid cells for the years 1988, 1998, 2008, and 2023. Among these, total building volume is the best measure of developers’ overall supply response. I constructed this dataset using building height data from the Hong Kong government, supplemented by historical aerial photographs from 1988 onward. The second outcome measures construction quality and amenity investment by developers, using the asset price per sq ft of floor space from geo-coded private residential flat transactions between 1991 and 2020, along with associated flat features. I further enrich these outcomes with digitized data on building height limits from various periods, as well as information on elevation, slope, the locations of public facilities, and the distribution of low-quality housing.

I use a spatial regression discontinuity design to examine developers’ responses to changes in building height restrictions. The unit of observation is either grid cells (for quantity analysis) or transactions (for quality analysis), categorized as inside or outside the narrowed flight path. The running variable is the distance of each observation to

the nearest narrowed flight path border. Identification relies on local and temporal changes in building height restrictions around these borders. The key assumption is that neighboring areas on either side of the narrowed flight path borders share comparable underlying locational fundamentals, such as slope, elevation, proximity to the central business district, and proximity to the downtown airport. The primary difference lies in the building height limits enforced on the two sides of the borders during the period preceding the downtown airport's closure—specifically, between the first and second upzoning events—and their associated impacts (e.g., building structures and population density).⁴ Assumption tests confirm an average height limit difference of approximately 30 meters between the two sides during this period. Meanwhile, height limits were similar across the narrowed flight path borders before the first upzoning and after the second upzoning. Other locational fundamentals, including topography and key amenity indicators, also remained similar across the borders. Importantly, these flight path borders, where height limits were stricter and binding inside the flight path between the first and second upzoning events, do not overlap with any administrative boundaries.

My analysis first demonstrates that developers responded strongly to the 1998 large-scale upzoning in already-developed urban areas, closing initial gaps in building height, volume, and quality across the flight path borders *within a decade*. Before the airport's closure, neighborhoods just inside the flight path—subject to stricter height limits—had buildings approximately 7 meters shorter (equivalent to two to three stories) and smaller in volume relative to those outside the flight path. Within a decade of the airport's closure, these disparities disappeared. Building volume inside the flight path increased by 77% more than in areas outside, driven by a 33% greater rise in maximum building height and a 34% larger expansion in footprint. The asset price per sq ft of floor space ("floor space price") was similar across the flight path borders both before and after the closure, when accounting for flat quality. However, quality-unadjusted floor space prices, initially lower inside the flight path, equalized post-closure, reflecting an improvement in flat quality, as

⁴In 1989, the first upzoning relaxed height limits more outside the narrowed flight path, while stricter restrictions remained inside. In 1998, after the airport closure, the second upzoning increased height limits more inside, resulting in similarly lenient limits on both sides. This suggests that height limits should have been similar across the borders before the first upzoning and after the second, differing only between the two upzoning events.

supported by data on flat amenities and the distribution of low-quality housing.

In contrast, the 1989 modest upzoning did not elicit a strong supply response, as changes in building volume were similar across the flight path borders after this first upzoning. Although much smaller than the subsequent large-scale upzoning, a 43% increase is substantial enough to expect some response based on prior evidence. For example, in Mumbai, a 10-50% increase in FAR led to a 28% rise in housing supply, while in New York City, a 23% increase in FAR resulted in a 6% increase in housing floor space (Nagpal and Gandhi, 2023; Peng, 2023). Yet, my findings indicate that a comparable 43% relaxation in building height limits failed to spur significant housing construction in urban Hong Kong.

Additionally, earlier findings indicate that the gap in flat quality across the flight path borders, which existed prior to the airport's closure, closed afterward. This suggests the potential presence of planners' blight, where anticipation of future policy changes negatively impacts property values and development decisions (Dennis and Halsey, 1972). In 1989, when the first modest upzoning occurred, the government also announced plans to build a new airport farther from the city center to replace the downtown one. In anticipation of major zoning changes following the airport's closure, developers deferred maintenance and investment within the flight path, leading to a noticeable decline in flat quality before the closure.⁵ This is evidenced by initially similar quality-unadjusted floor space prices across the flight path borders when the airport decision was announced, which later fell to 30% lower inside the flight path as the closure approached.

From the developers' perspective, the decision to redevelop already-developed urban areas depends on both redevelopment costs (e.g., demolition, land acquisition, permits and regulatory fees, reconstruction) and expected future returns. Assuming similar redevelopment costs for a given lot and attributing additional returns to rents from the extra structure that can be built, my findings suggest that a 43% increase in allowable building heights may not be sufficient to incentivize redevelopment, especially in the

⁵In the 1993 Review of Building Density & Height Restrictions in Kowloon & New Kowloon Report, the Hong Kong Planning Department noted that, after the downtown airport's closure, there would be no air safety reasons to limit development in Kowloon—the main urban area where height limits had historically been enforced to ensure safe aircraft operation. This suggests that the general public, including developers, was aware of potential forthcoming policy changes, though the specifics remained uncertain.

presence of planners' blight, whereas a 212% increase does. Developers' anticipation of future significant upzoning likely moderated their response to the first modest upzoning and accelerated the subsequent rapid convergence in building height, volume, and quality after the second large-scale upzoning.

I contribute to three main strands of literature. First, I illuminate the elasticity of developers' response to the relaxation of land use restrictions by leveraging two distinct upzoning events within a single jurisdiction, using a regression discontinuity design. Previous studies have examined the causal effects of zoning using cross-metropolitan variations in zoning rules and, more recently, block-level variations along municipal borders (Turner et al., 2014; Song, 2021; Kulka et al., 2023; Kulka, 2019). Recent studies have also begun to explore within-city upzoning policies and their impacts on housing supply (Freemark, 2020; Anagol et al., 2021; Liao, 2022; Greenaway-McGrevy, 2023; Büchler and Lutz, 2024). I contribute to this literature by estimating the average treatment effects of two upzoning events, each with a different scale, in central urban areas, using local and temporal variations in height limits around flight path borders. My approach advances our understanding of the effectiveness of upzoning in incentivizing housing supply by demonstrating how the scale of upzoning and developers' anticipation of future zoning changes interact to shape supply response. Additionally, my data analysis, spanning over three decades, provides a long-term perspective on developers' behavior in urban areas with binding height restrictions. This work also relates to the literature that uses theoretical models to understand how land-use regulation affects urban density and housing prices (Bertaud and Brueckner, 2005; Brueckner and Singh, 2020; Yezer, 2024).

Second, I show that large-scale relaxation of land use restrictions can drive convergence in the built environment, even between areas that previously had significantly different restrictions. Researchers have theoretically analyzed the role of durable capital in urban redevelopment, showing that durable capital inhibits investment (Brueckner, 1982; Braid, 2001; Glaeser and Gyourko, 2005). More recent empirical work by Hornbeck and Keniston (2017) uses the Great Boston Fire of 1872 to demonstrate that negative spillovers from outdated buildings discouraged reconstruction and substantially constrained Boston's growth before the fire. Henderson et al. (2021) further indicates that

institutional friction in land use conversion contributes to the persistence of outdated informal housing in Nairobi. My work demonstrates that significant relaxation of land use constraints can effectively incentivize developers to demolish old buildings and construct taller ones, breaking the persistence of durable structures. Additionally, my findings on the convergence of the built environment within a decade of large-scale upzoning offer insights into how quickly durable housing can be replaced and urban transformation can occur after major zoning changes.⁶

Finally, I demonstrate that expectations of future upzoning can moderate developers' construction response, even from a relatively sizable relaxation of land use regulations. The existing literature highlights the trade-offs developers face between the immediate benefits of redevelopment and the option value of waiting for more favorable conditions amid policy uncertainty (Capozza and Helsley, 1990; Clapp and Salavei, 2010; Clapp et al., 2013; McMillen and O'Sullivan, 2013; Munneke and Womack, 2020). In particular, Chau and Wong (2014) observes that Hong Kong developers are highly sensitive to this option value due to the region's regulatory volatility. The unique setting of Hong Kong—where two upzoning events occurred nine years apart, with developers aware during the first upzoning that strict building height limits might no longer be needed for air safety reasons following the downtown airport's closure—enabled a detailed examination of how developers adjusted their maintenance and investment strategies in anticipation of major zoning changes. My findings deepen our understanding of how expectations of future upzoning and the associated option value can influence redevelopment dynamics in evolving policy environments. To the best of my knowledge, this study provides the first empirical evidence of planners' blight risk arising from developers' deferral behavior in response to zoning policy changes.

The rest of this paper is organized as follows: Section 2. describes the institutional background. Section 3. discusses the conceptual framework and outlines the theoretical predictions to be tested. Section 4. introduces the novel datasets used in this study, and

⁶This finding also contrasts with existing studies suggesting that historical urban structures—such as lot sizes, transportation patterns, and central locations—tend to persist and shape contemporary urban layouts (Takeda and Yamagishi, 2024; Brooks and Lutz, 2019; Jedwab et al., 2017; Yamasaki et al., 2021; Michaels et al., 2021).

section 5. describes the empirical strategy. Section 6. presents the main results, including a discussion on the role of developers' anticipation. Finally, Section 7. concludes the paper.

2. Institutional Background

Zoning regulations in Hong Kong, particularly those governing building heights, have influenced the urban landscape since the 1950s. Initially, these regulations were enforced in Kowloon to ensure the safe operation of the downtown-located Kai Tak Airport in its eastern part. After the airport's closure and the subsequent opening of Chek Lap Kok Airport farther from the city center, these stringent height restrictions were relaxed, allowing for greater vertical development in Kowloon. Figure 1 illustrates the locations of Kai Tak and Chek Lap Kok airports relative to Hong Kong's main urban areas. As depicted, Kowloon—one urban area where building height limits were enforced—is located just north of Hong Kong Island. Its commercial hub at the southern tip is well connected to the Central Business District (CBD) on Hong Kong Island via ferries, the cross-harbour tunnel, and the Mass Transit Railway (MTR). This section outlines four distinct eras of building height limits in Kowloon, each defined by major regulatory reforms.

2.1. Era 1 - 1957-1989: Downtown Airport Restricts Urban Heights

The initial building height regulation was implemented in the 1950s to ensure the safe operation of aircraft at Kai Tak Airport. Originally developed in the 1920s, the airport featured a distinctive single runway that necessitated precise pilot maneuvers to avoid buildings and mountainous terrain during landings. The Hong Kong government enacted the Hong Kong Airport (Control of Obstructions) Ordinance in 1957, imposing height restrictions on newly constructed buildings in most areas of Kowloon (Ho, 2018).⁷

These height restrictions were most stringent along the airport's take-off and landing

⁷Only the northeastern part of the Kowloon region, which is further from the airport and consists mostly of uninhabited mountainous areas, is not regulated.

paths and diminished with increasing distance from the airport, as shown in Panel A of Figure A.1 in Appendix A.⁸

2.2. Era 2 - 1989-1998: Narrowed Flight Path

In October 1989, the Hong Kong government announced its decision to replace Kai Tak Airport with a new facility at Chek Lap Kok, located far from the city center. This decision, based on a thorough feasibility study, reflected the limitations of Kai Tak's expansion potential amid Hong Kong's increased urban development and air travel demand.⁹ The announcement led to widespread expectations among the public and developers that the stringent height restrictions in Kowloon would be fully lifted after the airport's relocation, although the specifics remained uncertain.

At the same time, advancements in navigation technologies led the government to update the Hong Kong Airport (Control of Obstructions) Ordinance in 1989, narrowing the flight path's coverage compared to previous decades. This change concentrated the most stringent height restrictions within a smaller area (see Panel B of Figure A.1), while certain areas, particularly those outside the updated flight path, experienced a relaxation of building height limits.¹⁰ As a result, the average height limit in regulated areas of Kowloon increased from 58 meters above the Hong Kong Principal Datum (mPD) in Era 1 to 83 mPD in Era 2, allowing for a 43% increase in potential building volume for a given lot size.¹¹

⁸The Building Authority, however, retained the power to grant exemptions on a case-by-case basis as per the Building Regulations. For instance, developers who included public facilities, such as passages or multi-story car parks alongside new construction, could exceed height limits pending thorough review and approval by the Building Authority.

⁹Prior to its closure, Kai Tak Airport ranked third in passenger volume globally and had the highest freight volume.

¹⁰The regulated areas in Kowloon during Era 2 were larger than in Era 1, partly due to extensive land reclamation along the western coast and the addition of specified height limits in the northeastern mountainous areas.

¹¹The Hong Kong Principal Datum (HKPD) is the geodetic reference system used for mapping and surveying in Hong Kong, with the Mean Sea Level approximately 1.3 meters above HKPD. The abbreviation "mPD" refers to meters above the Hong Kong Principal Datum.

2.3. Era 3 - 1998-2008: The Sky's the Limit

In July 1998, the new airport at Chek Lap Kok officially replaced Kai Tak Airport, and the government announced the complete removal of all building height limits previously associated with Kai Tak's operation.¹² Meanwhile, the government implemented a new set of height controls to ensure the safe operation of the new airport. Panel C in Figure A.1 depicts the building height limits in Kowloon after the airport relocation. As shown, in Era 3, after the closure of Kai Tak Airport, the height limits associated with the new airport, which is located far from the city center, became much looser, all exceeding 300 mPD.

This change represents one of the *largest* upzonings in already-developed urban areas in history. The flight landing path, where height limits were most stringent, was upzoned from an average height limit of 37 mPD before the airport's relocation to 463 mPD post-relocation—an 11-fold increase. In all regulated areas of the Kowloon region, the average height limit increased from 151 mPD to 471 mPD, resulting in a 212% increase in potential building volume for a given lot size. The building height restrictions post-airport relocation are effectively equivalent to having no restrictions at all, enabling the construction of very tall buildings. To get a sense of scale, the tallest tower in the United States, One World Trade Center in New York City, stands at 541 meters.

2.4. Era 4 - 2008-Present: Re-imposing Height Limits

Following the removal of stringent building height limits, the construction of tall structures proliferated in Kowloon, leading to several issues that attracted the attention of the Hong Kong government. These issues included the rapid increase of exceptionally tall buildings in low-density areas, the development of "wall-effect" structures, and the absence of view corridors and breezeways.

To address these concerns, the Town Planning Board, the primary government agency responsible, began incorporating building height limits in outline zoning plans

¹²Here is the link to the government announcement: <https://www.info.gov.hk/gia/general/199807/10/0710062.htm>

to regulate future constructions.¹³ Beginning in 2008, regulated building height limits were formally introduced and clearly specified in the outline zoning plan maps for most planning scheme areas in Kowloon.¹⁴ These limits were established based on existing building heights, land use types, and other density planning considerations. The re-imposition of building height limits was a response to the rapid construction of tall buildings during Era 3 (1998-2008, "Sky's the Limit") and has continued to influence building construction in subsequent years. Panel D in Figure A.1 shows the specified building height limits for regulated land lots in Kowloon in Era 4.

2.5. Three Regulatory Transitions

Three key regulatory transitions stand out after reviewing the four distinct eras of building height regulations in Kowloon since the 1950s. The first, *Regulatory Transition 1: First Upzoning in 1989*, occurred in 1989 when the flight path was adjusted, mainly easing height restrictions for areas that were heavily constrained in Era 1 (1957-1989, "Downtown Airport Restricts Urban Heights") but fell outside the newly defined path in Era 2 (1989-1998, "Narrowed Flight Path"). The second, *Regulatory Transition 2: Second Upzoning in 1998*, occurred in 1998 when all height limits associated with the operation of Kai Tak Airport were removed, both inside and outside the updated flight path, leading to substantial upzoning in urban centers. The third, *Regulatory Transition 3: Downzoning in 2008*, began around 2008, with the re-imposition of height limits for individual land lots, marking a shift back from the earlier period of deregulation.

3. Conceptual Framework

In this section, I present a simple conceptual framework to understand the levels and changes in building height and asset price per sq ft of floor space ("floor space price")

¹³Outline Zoning Plans delineate proposed land uses and major road systems for individual planning scheme areas.

¹⁴For instance, in 2008, planning scheme areas in Kowloon such as Ho Man Tin, Tsim Sha Tsui, Southwest Kowloon, and Hung Hom incorporated building height limits in their outline zoning plans. Similarly, planning scheme areas such as Mongkok, Shek Kip Mei, Yau Ma Tei, Cheung Sha Wan, Wang Tau Hom, and Tung Tau followed suit in 2010.

in regulated urban areas across three regulatory transitions. First, drawing on the monocentric city model developed by Alonso (1964), Mills (1967), and Muth (1969), Arnott and MacKinnon (1977), and later extended by Wheaton (1974), Brueckner et al. (1987), and Bertaud and Brueckner (2005), I briefly discuss spatial equilibrium in cities with and without spatially varying building height restrictions.¹⁵ Then, using this established model, I compare levels and changes in equilibrium building height and floor space price across narrowed flight path borders during each regulatory transition and propose hypotheses for empirical testing.¹⁶

3.1. City without Building Height Restrictions

The standard monocentric model assumes a city on level terrain, housing a central business district (CBD) and a fixed population of N identical residents, all of whom work in the CBD. Each resident earns an income of y per period and commutes to the CBD from their residence on a radial road network, with a distance of x to the CBD incurring a cost of t per round-trip mile per period. The disposable income of an inhabitant living x miles from the CBD is then $y - tx$.

The utility function for each individual is denoted as $v(c, q)$, depending on the consumption of a composite non-housing good c and housing square footage q . The asset price per sq ft of floor space is represented by p . The consumer's budget constraint is thus $c + pq = y - tx$. By replacing c using this budget constraint, utility is $v(y - tx - pq, q)$. Consumers maximize their utility by choosing q and taking p as given. To attain locational equilibrium, realized utility across the city must be uniform ($\max v(y - tx - pq, q) = u$).

In terms of housing supply, developers produce floor space using a combination of land and capital with constant-return technology. Housing output per unit of land, measured in floor space, is $h(S)$, where S is the capital-to-land ratio, and h is the intensive form of the production function. The function $h(S)$ is a linear transformation of building height H , with $h(S) = \frac{wH(S)}{\gamma}$. Here, w is the fraction of land used for housing development

¹⁵Conceptual frameworks introduced in recent empirical papers also discuss the theoretical impacts of upzoning, e.g., Greenaway-McGrevy (2023).

¹⁶Narrowed flight path borders refer to the borders of the flight path used in Era 2 (1989-1998, "Narrowed Flight Path"), which were updated and narrowed from those in Era 1 (1957-1989, "Downtown Airport Restricts Urban Heights").

rather than open space around the structure per unit of land and it falls between 0 and 1 ($w \in [0, 1]$). The parameter γ is a positive constant that applies uniformly to all buildings in the city, converting total heights into the number of floors.¹⁷ Normalizing the price of capital to one, profit per sq ft for a housing developer is given by $ph(S) - S - r$, where r is the land rent per unit of land. Given the asset price per sq ft of floor space p , the developer selects S to maximize profit, meeting the first-order condition $ph'(S) = 1$. The zero-profit condition yields land rent of $r = ph(S) - S$.

The conditions on both the consumer and production sides help derive the effects of distance to the CBD x and utility u on the key variables. As the distance to the CBD x increases, housing square footage q increases, while asset price per sq ft of floor space p , capital-to-land ratio S , and land rent r decrease ($\frac{\partial q}{\partial x} > 0$, $\frac{\partial p}{\partial x} < 0$, $\frac{\partial S}{\partial x} < 0$, $\frac{\partial r}{\partial x} < 0$). Similarly, as utility u increases, housing square footage q also increases, while asset price per sq ft of floor space p , capital-to-land ratio S , and land rent r decrease ($\frac{\partial q}{\partial u} > 0$, $\frac{\partial p}{\partial u} < 0$, $\frac{\partial S}{\partial u} < 0$, $\frac{\partial r}{\partial u} < 0$).¹⁸

The utility level is ultimately endogenous, determined by two urban equilibrium conditions: the urban land rent per unit of land r at \bar{x} must equal the agricultural rent r_a , and the city's population N must fit within \bar{x} . These two conditions are as follows:

$$r(\bar{x}_0, u_0) = r_a \quad (1)$$

$$\int_0^{\bar{x}_0} \theta x \frac{wH(S(x, u_0))}{\gamma q(x, u_0)} dx = N \quad (2)$$

\bar{x}_0 and u_0 are the equilibrium values of \bar{x} and u , respectively, and $\theta \leq 2\pi$ represents the fixed number of radians of land available for housing. Based on this model, the blue curve in Figure 2 illustrates the equilibrium building height in a city without any building height restrictions. The equilibrium building height follows a concave pattern—starting high in the CBD and gradually decreasing as the distance from the center increases, eventually flattening out toward the city's periphery. This pattern arises because, as the

¹⁷It is assumed that $h(S)$ is concave, with the properties $h' > 0$ and $h'' < 0$. Since $h(S) = \frac{wH(S)}{\gamma}$, the function $H(S)$ also exhibits concavity, with $H' > 0$ and $H'' < 0$.

¹⁸For a more in-depth discussion, please refer to Bertaud and Brueckner (2005), pages 111-113.

distance from the CBD x increases, the asset price per sq ft of floor space p decreases, reducing the incentive for developers to invest heavily in the land. Consequently, the capital-to-land ratio S also declines with x , resulting in shorter building heights H .¹⁹

3.2. City with Spatially Varying Building Height Restrictions

Cities often enforce spatially varying building height restrictions. In my empirical case, the operation of the airport in urban areas caused building height limits that varied by proximity to flight paths and distance from the airport (see Figure 2 for an example). Building on Bertaud and Brueckner (2005), I introduce building height limits \hat{H}_i enforced in neighborhood block i .²⁰ There are n such blocks in the city, each with a fixed height limit of \hat{H}_i . Let u_m and \bar{x}_m represent the equilibrium utility and the distance from the periphery to the city center, respectively, for the city with spatially varying building height restrictions. Now the equilibrium conditions not only include that the urban land rent per unit of land at \bar{x}_m equals the agricultural land rent and the city population N fits within \bar{x}_m , but also that within block i , there is a point where the building height freely chosen by developers equals the building height limit enforced (Please refer to detailed discussion in Appendix B).

Based on the model's properties, a city with spatially varying building height limits must expand to accommodate population N , resulting in a larger city radius compared to an unrestricted city ($\bar{x}_m > \bar{x}_0$). This expansion raises transportation costs and reduces residents' disposable income, leading to a lower equilibrium utility level than in an unrestricted city ($u_m < u_0$). As discussed earlier, when utility decreases, the asset price per sq ft of floor space increases.²¹ Therefore, the lower utility in a city with spatially varying height limits implies a higher asset price per sq ft of floor space at all locations compared to a city without such restrictions.

Further, depending on the distance from the CBD, the height limits in a neighborhood block may be binding, partially binding, or not binding at all (see Figure A.2 in Appendix

¹⁹Recall that $\frac{\partial p}{\partial x} < 0$ and $\frac{\partial S}{\partial x} < 0$, and the function $H(S)$ is concave, with $H' > 0$ and $H'' < 0$.

²⁰For a detailed discussion on the introduction of a uniform building height limit in the city, please refer to Bertaud and Brueckner (2005).

²¹Recall $\frac{\partial p}{\partial u} < 0$.

A). Here, “binding” means that the enforced building height limit is lower than the equilibrium height developers would choose in the absence of such restrictions. In a neighborhood block where the height limit is binding, developers will construct buildings exactly at the height limit of \hat{H}_i (Figure A.3a in Appendix A). As a result, the equilibrium height in this block would be lower in a restricted city compared to an unrestricted city. In a neighborhood block where the height limit is not binding, the building height in the restricted city will exceed that in the unrestricted city due to the lower utility level in the restricted city. Specifically, $H_i(S(x, u_m)) > H_i(S(x, u_0))$ within the range where S is freely chosen, although the building height in the restricted city will remain below the prescribed height limit \hat{H}_i , as shown in Figure A.3b.²² In a neighborhood block where the height limit is partially binding, there exists a point x_e^i at which the height limit transitions from binding to nonbinding, representing a combination of the two aforementioned situations (Figure A.3c).

3.3. Neighborhood-level Predictions

To align the conceptual framework with the empirical strategy and estimation, I focus on neighborhoods inside and outside the updated flight path borders of Era 2 (1989-1998, “Narrowed Flight Path”). For each regulatory transition, I compare building height limits across the borders and predict, based on the model’s properties, the differences in equilibrium building height across the borders before and after each transition, as well as changes during the transition. Throughout, I assume that height limits inside the flight path are binding prior to the downtown airport’s closure, meaning the enforced height limit is below the equilibrium height that developers would choose without restrictions. Finally, I predict differences in asset price per sq ft of floor space (“floor space price”) across the borders in each Era.

²²Note that $\frac{\partial S}{\partial u} < 0$.

3.3.1. Building Height and Volume

First Upzoning in 1989. In Era 1 (1957-1989, "Downtown Airport Restricts Urban Heights"), both sides of the updated flight path borders fell within the old flight path and were therefore subject to the same tight height limits. Given the binding height limits inside the old flight path, developers are predicted to build only up to the height limit on both sides of the updated flight path borders. As shown in Panel A of Figure 3, the equilibrium building heights in Era 1, marked by the orange lines, are the same across the updated flight path borders of Era 2, denoted by x_{b2} .

Following the narrowing of the old flight path and the first relaxation of height limits in 1989, neighborhoods inside the updated flight path continued to face strictly binding limits in Era 2 (1989-1998, "Narrowed Flight Path"). In contrast, neighborhoods located outside experienced a greater relaxation in height limits, resulting in lower height limits inside the updated flight path compared to outside. According to the theoretical model, developers respond to the relatively larger upzoning outside the flight path, where limits had previously been binding, by constructing taller buildings. As illustrated in Panel A of Figure 3, the equilibrium height in Era 2, marked by the blue lines, is predicted to be lower inside the updated flight path than outside. The green arrow further indicates a smaller increase in building height within the updated flight path compared to outside after the first upzoning.

In the theoretical model, the built-up area per unit of land (w), or building footprint per unit of land, is assumed to be uniform across the city. Since building volume is the product of footprint and height, the relative change in building volume inside the updated flight path compared to outside is expected to mirror the change in building height. Therefore, the following discussions do not specifically address building footprint and volume.

Second Upzoning in 1998. After the second upzoning, the newly enforced height limits related to the operation of the new airport were very loose in Era 3 (1998-2008, "Sky's the Limit"), effectively equivalent to having no height limits at all on either side of the updated flight path borders. This implies a larger upzoning inside the updated

flight path borders than outside. The city is expected to re-establish equilibrium building heights to meet the conditions defined by Equations (1) and (2) for an unrestricted city. In Panel B of Figure 3, the equilibrium building heights in Era 3, marked by the blue lines, are expected to be similar in these spatially proximate neighborhoods across x_{b2} , gradually decreasing from neighborhoods closer to the CBD to those further away.²³ Neighborhoods inside x_{b2} experienced more substantial upzoning during the second upzoning and are therefore expected to see a greater increase in building heights compared to those outside, as indicated by the green arrow in the same figure.

Notably, while the height limits inside the updated path are assumed to be binding, the height limits outside the path in Era 2 (1989-1998, "Narrowed Flight Path"), following the first upzoning in 1989, may be binding, partially binding, or not binding. Consequently, neighborhoods outside x_{b2} may experience a smaller increase in height than those inside, or even a slight decrease, after the second upzoning in 1998, depending on whether the previous height limits outside the path in Era 2 are binding (see Figure A.4 for further details). Nevertheless, this does not alter the prediction that neighborhoods inside x_{b2} will experience a greater increase in building heights compared to those outside after the second upzoning.

Downzoning in 2008. During the third regulatory transition, the government re-imposed building height limits based on the existing heights in each street block from the mid-2000s; these limits were no longer influenced by the flight path factor from Era 2. As a result, the building height limits in Era 4 (2008-present, "Re-imposing Height Limits") are expected to be similar across the flight path borders. In Panel C of Figure 3, the equilibrium building heights in Era 4, marked by the blue lines, transition smoothly across x_{b2} , showing no differential changes in height on either side of the borders following the 2008 downzoning.

²³This panel illustrates the scenario where neighborhoods outside the flight path are closer to the CBD. Panel C of the same figure also illustrates this scenario.

3.3.2. Floor Space Price

The floor space price, defined as the asset price per sq ft of floor space, is predicted to be similar across the updated flight path borders of Era 2 for each Era. This uniformity in the model arises because the floor space price depends on the distance from the CBD, rather than on local building height restrictions. The equilibrium conditions for each Era ensure equal utility across all locations. In neighborhoods very close to x_{b2} , commuting costs are the same due to the similar distance from the CBD, and housing unit sizes are also similar. Therefore, residents in these neighborhoods have identical disposable incomes after accounting for commuting costs, resulting in the same floor space price across the borders.

The model assumes consistent housing unit quality across these proximate neighborhoods. However, in reality, quality may differ across borders due to various factors. For instance, in Era 2, stricter building height limits inside the updated flight path may have led developers to adopt different development and maintenance strategies inside versus outside the path. Consequently, the floor space price, if unadjusted for quality, could vary across borders.

To summarize my discussion, Figure 4 presents the differences in building height limits inside versus outside the updated flight path borders in each Era (Column (1)). It also provides predictions for equilibrium building height and asset price per sq ft inside versus outside the updated flight path borders for each Era, as well as the relative changes in equilibrium building height across regulatory transitions (Columns (2) to (4)).

4. Data

To test the theoretical predictions about developers' responses, I construct detailed and novel datasets spanning three decades (1988-2023). I focus on Kowloon, Hong Kong, where building height limits were enforced from the 1950s until 1998 due to the operation

of Kai Tak Airport.²⁴ Appendix D provides a comprehensive description of all datasets used for analysis, including their sources, processing methods, and variables.

Spatial Unit. To have a consistent spatial unit across different datasets, I overlay 30-meter by 30-meter grids over the Kowloon region. These grid cells serve as the main spatial unit of analysis for all building-related analyses. This grid size typically covers around one to two building towers along with their podiums, allowing for a detailed capture of changes in building footprints across Eras. For each grid cell, I assign building height limits in each Era and incorporate other important control variables (e.g., elevation, slope, distance to various locations) based on the geolocation of the centroid of each grid cell. Additionally, I calculate the maximum building height, building footprint, and total building volume for each grid cell in each Era.

Building Height Limits. Mapping the building height limits enforced across different eras is essential for understanding changes in flight path borders and the associated height limits both inside and outside the flight path. To determine the building height limits for each 30-meter by 30-meter grid cell in each Era, I first georeferenced and digitized the Airport Height Control Maps for Era 1, Era 2, and Era 3.²⁵ For Era 4, I used zoning plans that include height limits for each regulated land lot. I then calculated the building height limits at the centroid of each grid cell using specific height restriction zones, landing gradient ratios, and fixed reference points from the maps.²⁶

Building Height, Footprint, and Volume. I measure key building characteristics within each grid cell—specifically, maximum building height, total building volume, and total building footprint—in each Era. Maximum building height is the height of the tallest building in a grid cell, capturing the extensive margin of development by indicating whether developers respond to height limits. Total building volume, a combination of

²⁴I use the administrative boundary of Kowloon as defined in the 2021 Census. It is important to note that major land reclamation activities took place during the 1980s and 1990s, resulting in the expansion of the Kowloon region along the coast over the years.

²⁵These maps were primarily obtained from the library at the University of Hong Kong and the Government Records Service of Hong Kong.

²⁶The height limit at the centroid of each grid cell serves as a proxy for all locations within the grid cell. This method does not introduce measurement errors for zones with fixed height limits. However, for grid cells in zones where height limits vary with distance, measurement errors of up to 4.06 meters may occur for locations other than the centroid.

building height and footprint, is the overall built space within a grid cell and measures the intensive margin of supply response. It shows how developers adjust both vertical and horizontal dimensions to optimize the use of available space under zoning regulations. Total building footprint, which measures the ground area covered by buildings in a grid cell, provides insight into developers' land use intensity strategies.

To construct these variables, I first obtained and cleaned a dataset from the Lands Department of Hong Kong, which includes geographical coverage, top height, and current status for all buildings constructed since the 1940s. I then used historical satellite imagery and aerial photos from the 1980s to the present to determine the presence or absence of buildings in December 1988, July 1998, January 2008, and January 2023 - the end points of each target Era. This method aids in understanding the life cycles of buildings where time information is missing (approximately 26.2% of the total built-up area) and in creating comprehensive building footprint maps for Kowloon for each Era. To address remaining missing height information—affecting 13.1% of the built-up area for the 1988 map, 6.4% for the 1998 map, 3.4% for the 2008 map, and 2.4% for the 2023 map—I imputed these values using the heights of the nearest buildings.²⁷ Finally, I divided each year's building footprint into 30m × 30m grid cells to construct the key dependent variables: maximum building height, total building footprint, and total building volume within each grid cell.²⁸

Private Residential Flat Transactions. I measure the asset price per sq ft of floor space in Era 2, Era 3, and Era 4 using all private residential flat transactions from 1991 to 2020.²⁹

²⁷I will include the imputed heights in my main analysis but also exclude them in robustness checks to test sensitivity.

²⁸For grid cells without any built-up area, all these variables were coded as 0. Additionally, to track changes in maximum building height, total building footprint, and total building volume within each grid cell for the periods 1988-1998, 1998-2008, and 2008-2023, I calculated both the differences and log ratios of these variables. Specifically, for calculating the log ratios, I adjusted the maximum building height, total building volume, and total building footprint for the years 1988, 1998, 2008, and 2023 by adding 1 to account for observations with values of 0. Then, I computed the natural logarithm of the ratio of these variables between years. For example, the log ratio for maximum building height between 1998 and 1988 is calculated as

$$\log \left(\frac{\text{maximum building height in 1998} + 1}{\text{maximum building height in 1988} + 1} \right).$$

²⁹The data source is EPRC Limited, a credible source for private residential flat transactions in Hong Kong, as verified by numerous well-published research papers on the Hong Kong housing market. The dataset was compiled using electronic transaction data from the Land Registrar of Hong Kong and

Each observation in the dataset represents a unique transaction in the private residential flat market.³⁰ The dataset includes variables covering transaction details (e.g., sale date, price, first-/second-hand market), property features (e.g., swimming pool, clubhouse), and flat unit characteristics (e.g., floor, unit, gross/net area in square feet, number of bedrooms, number of living rooms). I geocoded each transaction using location information.³¹ Then, I excluded transactions with an age less than -3 years or transactions without available price information, representing 0% and 0.5% of the total transactions in Kowloon during this period, respectively.³² I deflated the transaction prices using the Private Domestic Property Price Index released by the Rating and Valuation Department of Hong Kong (with 1999 as the base year).³³ Given that 23.6% of the transactions lack available unit size information, I excluded these transactions when using the asset price per sq ft of floor space as the outcome but tested the sensitivity by including all of them and using the asset price per unit instead.

Other Geographical Datasets. I combine my data on building height limits, building characteristics, and private residential flat transactions with various other census and geographical data. This includes the share of households living in different housing types at the street-block level for 1996, 2006, and 2016 (corresponding to Eras 2, 3, and 4, respectively)³⁴, as well as data on slope, elevation, MTR station locations, coastal lines, and public facility locations. Data Appendix D provides detailed information.

supplemented with additional information such as housing unit characteristics. The earliest year available for this data is 1991, so Era 1 cannot be assessed.

³⁰Hong Kong has three main types of permanent housing: private permanent housing, public rental housing, and subsidized sale flats. These account for 56.8%, 28.5%, and 14.7% of the total housing stock, respectively (Census and Statistics Department of Hong Kong, 2022). Private residential flats constitute the largest proportion of private permanent housing, including flats and apartments in multi-story blocks or houses constructed by the private sector for residential purposes.

³¹I used the Location Search API Service provided by the Hong Kong CSDI Portal for geocoding, as it generally provides more accurate geographical coordinates in Hong Kong compared to Google or ArcGIS Pro's geocoding API services.

³²Pre-sales of flat units rarely occur more than three years before completion.

³³In my main sample, I deflate the floor space price using the Private Domestic Property Price Index. The results are identical when using the Consumer Price Index released by the World Bank (with 2010 as the base year).

³⁴The street block level in Hong Kong refers to street block groups containing 1,000 or more residents. According to the 2016 Census, Hong Kong has 1,622 such street blocks. By comparison, the U.S. Census Bureau uses a similar geographic unit called a "census block group," typically containing between 600 and 3,000 residents.

5. Empirical Strategy

I now turn to empirical tests of my hypotheses about developers' behavior in the wake of building height regulation changes. Directly comparing neighborhoods can be problematic. For instance, neighborhoods under the updated flight path are at different distances from the CBD compared to those outside the flight path and much farther away. Additionally, these neighborhoods may have different topographical features that affect both the type and height of buildings that can be constructed.

To address this issue, I employ a spatial regression discontinuity (RD) design. This approach compares neighborhoods that are spatially close but located just on opposite sides of the updated flight path borders of Era 2 (1989-1998, "Narrowed Flight Path"). The primary distinction between these neighborhoods lies in the building height limits enforced during Era 2, just before the closure of the downtown airport, and the resulting outcomes, such as building structures and population density. I will show that other underlying locational fundamentals, including elevation, slope, and certain amenities (e.g., proximity to MTR stations and coastlines) are similar across these borders. In addition, the spatial RD borders are independent of other administrative planning considerations. Indeed, none of these flight path borders overlap with any administrative boundaries.

By comparing neighborhoods very close to either side of these borders, I can isolate and estimate the effects solely attributable to changes in height limits, for the first upzoning due to the narrowed flight path and the second upzoning from the closure of the downtown airport. In this section, I elaborate on my border and sample selection criteria, empirical specifications, and assumption tests.

5.1. RD Border Selection

Zoning regulation boundaries are typically not randomly determined; they are often tied to demographic or neighborhood characteristics and may overlap with roads or administrative borders. In my case, however, the RD boundaries are de facto flight path borders, shaped by the locations of flight landing and takeoff paths as well

as advancements in navigation technology, rather than factors like topography or demographic characteristics influencing the inherent attractiveness of the land.

Following my conceptual framework, I limit the sample to flight path borders with significant variation in height limits on two sides of the border in Era 2, and with binding limits inside the flight path. Therefore, among all flight path borders demarcating different zones from Era 2, I apply the following two selection criteria: 1) flight path borders that demarcate zones with a distinct difference in building height limits exceeding 10 meters in Era 2; and 2) the stricter side of the border must have a height limit of less than 80 meters. Based on these criteria, I further exclude four borders that overlap with parks, depots, or oceans, because these areas have no scope for developers' response.

These criteria yield 24 flight path borders.³⁵ I further restrict the sample to grid cells (the unit of analysis for buildings) and flat transactions in Kowloon that are within a narrow bandwidth of 360 meters (approximately a 5-minute walk) on either side of the updated flight path borders.³⁶ Figure A.5 shows the selected borders and the grid cells located just inside and outside these borders within a 360-meter bandwidth.

5.2. Empirical Specification

I follow Gelman and Imbens (2019) by using a semiparametric RD design.³⁷ For each grid cell i adjacent to border j , I estimate:

$$Y_{ij} = \alpha + \beta_1 \text{Treat}_{ij} + \beta_2 \text{Dist}_{ij} + \beta_3 \text{Treat}_{ij} \times \text{Dist}_{ij} + \beta_4 \text{Design Controls}_{ij} + \omega_j + \mu_{ij}. \quad (3)$$

³⁵Note that not all 24 borders have private residential flat transactions on each side in different Eras. For the analysis of floor space price, I limit the borders to those with at least 30 transactions on each side in Era 2, Era 3, and Era 4, respectively.

³⁶Given Hong Kong's high density, I use a bandwidth that provides enough sample size and captures relevant variation in building height limits in Era 2, while keeping neighborhoods geographically comparable and minimizing the influence of confounding factors. I will also conduct and report sensitivity analyses using larger and smaller bandwidths.

³⁷Gelman and Imbens (2019) argue that using global high-order polynomials in regression discontinuity analysis is flawed due to three major issues: it produces noisy estimates, is highly sensitive to the choice of polynomial degree, and results in poor coverage of confidence intervals. Consequently, they recommend using estimators based on local linear or quadratic polynomials, or other smooth functions.

Y_{ij} is various building-related outcomes, including maximum building height, total building volume, and total building footprint within a grid cell for the years 1988, 1998, 2008, and 2023, corresponding to Era 1, Era 2, Era 3, and Era 4, respectively.³⁸ Additionally, I use the logarithmic ratios of these building characteristics for the periods 1988-1998, 1998-2008, and 2008-2023 as outcomes to directly capture changes driven by each regulatory transition.³⁹ This approach helps control for potential unobservable variations across grid cells that are constant over time.

Treat_{ij} is the main regressor of interest, indicating whether the centroid of grid cell i lies **inside** the nearest updated flight path border j of Era 2. Dist_{ij} is the running variable, which measures the distance (in meters) from grid cell i to the nearest flight path border j . $\text{Design Controls}_{ij}$ is a vector of additional controls potentially endogenous to future building construction and development, including distance to the CBD, distance to the downtown airport, elevation, and slope. Including these controls improves precision and reduces standard errors. ω_j is a vector of border fixed effects that ensures I only compare the initially less strict side of the border with their nearest stricter side. μ_{ij} denotes the error term. I cluster standard errors at $150\text{m} \times 150\text{m}$ grids, roughly the average size of one neighborhood in Kowloon. In this specification, β_1 captures the differences in outcomes across the updated flight path borders of Era 2.

Next, I include all private residential flat transactions from 1991 to 2020 in a single RD difference-in-differences regression. This approach ensures that the hedonic pricing of different flat unit features on the asset price per sq ft of floor space remains consistent over time, reducing bias and improving the comparability of treatment effects across different periods. For each transaction i adjacent to border j in year t , I estimate:

$$\begin{aligned}
 Y_{ijt} = & \alpha + \beta_1 \text{Treat}_{ijt} + \beta_2 \text{Dist}_{ijt} + \beta_3 \text{Treat}_{ijt} \times \text{Dist}_{ijt} + \sum_{k=1}^2 (\beta_{4,k} \text{Treat}_{ijt} \times \text{Post}_{ijt,k} + \\
 & \beta_{5,k} \text{Post}_{ijt,k} + \beta_{6,k} \text{Dist}_{ijt} \times \text{Post}_{ijt,k} + \beta_{7,k} \text{Treat}_{ijt} \times \text{Dist}_{ijt} \times \text{Post}_{ijt,k}) + \\
 & \beta_8 \text{Controls}_{ijt} + \omega_j + \gamma_t + \mu_{ijt}.
 \end{aligned} \tag{4}$$

³⁸Table A1 in Appendix A presents the summary statistics for these outcome variables.

³⁹Considering the data transformation involved in this process (see footnote 28), I will also use direct changes in values between years as outcomes in my robustness checks.

Y_{ijt} is the log of the asset price per sq ft of floor space for transaction i adjacent to border j in year t . This specification introduces a $\text{Post}_{ijt,k}$ dummy, indicating whether transaction i occurred in the post-airport closure period k . Specifically, $\text{Post}_{ijt,1}$ is a dummy for Era 3 (1998-2008, "The Sky's the Limit"), and $\text{Post}_{ijt,2}$ is a dummy for Era 4 (2008-2023, "Re-imposing Height Limits").⁴⁰ Controls_{ijt} includes four types of controls: a. design controls, such as slope, elevation, distance to CBD, and distance to the downtown airport, exactly the same as in Equation (3); b. flat size controls, such as unit size, inclusion of a car park, and multiple floors; c. flat quality controls, such as building age, number of bedrooms and living rooms, floor level, presence of a clubhouse or swimming pool in the building, and first-hand transactions; d. access to public facilities, such as proximity to MTR stations, bus stops, schools, parks, markets, and health facilities.⁴¹ γ_t is year fixed effects that control for variations across different years. The standard errors are clustered at $150\text{m} \times 150\text{m}$ grids.

Notably, β_1 captures the differences in the asset price per sq ft of floor space across the borders in Era 2, while the sum of β_1 and $\beta_{4,1}$ captures the differences in Era 3. The sum of β_1 and $\beta_{4,2}$ captures the differences in Era 4. This regression is run with and without flat quality controls to examine how quality-adjusted and unadjusted floor space prices differ across borders.

One potential issue that could lead to underestimated effects is that, in Era 2, buildings straddling the updated flight path borders had to comply with the stricter height limits inside the flight path, even if part of the building was located outside. To address this, I exclude grid cells within a 60-meter band just outside the flight path border from the sample of all observations within a 360-meter bandwidth on either side of the border. This "donut RD" approach is my preferred specification for analyzing building features and floor space prices.

⁴⁰Era 2 includes transactions from 1991 to July 9, 1998, which is one day before all building height limits associated with the downtown airport were removed. Era 3 includes transactions from July 10, 1998, to December 31, 2007. Era 4 includes transactions from 2008 to 2020.

⁴¹Table A2 in Appendix A provides details of these variables.

5.3. Assumption Tests

RD estimates rely on the assumption that the only sharp change at the border is the policy of interest. Thus, my identification depends on two key assumptions: 1) building height limits in Era 2 change discontinuously across the flight path borders, and 2) all other underlying locational fundamentals—such as topography, distance to the coastline, and distance to the nearest MTR station—remain continuous across these borders. Additionally, since the updated flight path borders of Era 2, which demarcate height limit zones, were only applicable in Era 2, building height limits in Eras 1, 3, and 4 should transition smoothly across these borders.

To test these assumptions, I first estimate Equation (3) without controls, using building height limits in Era 2 as the dependent variable. Figure 5 presents the predicted regression line based on the RD estimates, along with the binned-average residuals for the building height limits of Era 2.⁴² Negative-value distance bins represent neighborhoods just outside the flight path. At the borders, there is an approximately 30-meter difference in building height limits on either side, supporting the validity of the first assumption.

In line with my theoretical framework, I also need to confirm that the building height limits in Era 2 were effectively enforced. Specifically, within the narrowed flight path during Era 2, the height limits should be binding, meaning buildings would be constructed precisely up to the height limit. To test this, I examine whether new buildings constructed just inside the updated flight path borders during Era 2 adhered to the height limits enforced at that time.

In Figure 6, I plot the maximum building height (y-axis) for 1988, 1998, 2008, and 2023—corresponding to Eras 1, 2, 3, and 4, respectively—against the building height limits (x-axis) enforced during Era 2, using data from grid cells within a 360-meter bandwidth of selected flight path borders. Each point represents a grid cell, with orange dots indicating cells inside the updated flight path and blue dots representing those outside. Darker shades of orange and blue in Panels B, C, and D indicate grid cells with new constructions, resulting in updated maximum building heights during the respective

⁴²Note that all estimates in the figure have been adjusted by adding the sample mean of 79.3 meters above the Hong Kong Principal Datum (mPD).

era. The red line in each panel represents points where the maximum building height equals the Era 2 height limit, as they have the same values on both the x- and y-axes. If many dots are above this line, it suggests that the height limits are not effectively enforced, as developers do not comply with the regulation and build taller than the limit. If most dots are located on or below the line, it indicates that the Era 2 limit is well enforced. Specifically, if many dots are on or just below the line, it suggests that the Era 2 limit is binding in these grid cells, as developers build precisely up to the height limit.

Panel B of Figure 6 provides clear evidence of the effective enforcement of height limits in Era 2. Grid cells with changes in maximum building heights during this Era, represented by darker orange and blue dots, generally had new maximum heights at or below the red line. This indicates that newly constructed buildings in Era 2 complied with the height limits.⁴³ Specifically, many darker orange dots representing grid cells inside the updated flight path were at or just below the red line, suggesting the binding nature of these limits within the flight path during Era 2.⁴⁴ Overall, only a small number of grid cells slightly exceeded the height limits, primarily due to measurement errors, special government approvals, or historical buildings subject to earlier regulations.⁴⁵ In the same figure, Panel A shows that grid cells, particularly those outside the updated flight path, had maximum building heights in Era 1 that were well below the more relaxed limits subsequently enforced in Era 2. Panels C and D further confirm that the height limits established in Era 2 were no longer enforced in Eras 3 and 4, as evidenced by numerous grid cells with new maximum heights exceeding the Era 2 limits (represented by points above the red line), both inside and outside the flight path borders.

Finally, I examine the remaining assumptions, including whether underlying

⁴³Some grid cells had new maximum heights in Era 2 significantly below the limits due to factors such as building types (e.g., short public structures), other regulations unrelated to airport operations, or nonbinding limits.

⁴⁴For an analysis of the binding status both inside and outside each updated flight path border in the sample, please refer to Figure A.6 in Appendix A.

⁴⁵Detailed investigations revealed that discrepancies were caused by: 1) measurement errors, where using grid cell centroids to calculate height limits resulted in inaccuracies of 0.06 to 4.06 meters for certain locations; 2) special approvals granted to public structures such as housing, parks, and universities located farther from the old downtown airport; and 3) historical buildings near Kowloon Walled City that were 4-6 meters above the height limit. Notably, reasons 2 and 3 together accounted for only 0.59% of the sample, while reason 1 accounted for 2.51%.

locational fundamentals transition smoothly across the updated flight path borders, as well as the continuity of height limits in Eras 1, 3, and 4. To do this, I estimate Equation (3) without controls, using standardized measures of locational fundamentals and the building height limits enforced in Eras 1, 3, and 4 as the dependent variable, respectively. Figure 7 presents the standardized RD coefficients for locational fundamentals, including elevation, slope, and distance to the CBD, the downtown airport, the nearest MTR stations, and the coastline. The estimates for these variables are mostly within 0.1 standard deviation and are all statistically insignificant, indicating smooth transitions of locational fundamentals across the borders. The same figure also shows that building height limits in Eras 1, 3, and 4 are similar on two sides of the updated flight path borders. Together, these findings support the validity of the assumptions underlying my empirical strategy.

6. Main Results

I now test the predictions outlined in my conceptual framework, as summarized in Columns (2) through (4) of Figure 4. The first subsection analyzes building characteristics during each regulatory transition, the second examines the asset price per sq ft of floor space, and the third explores the role of developers' anticipation.

6.1. Building Height, Volume and Footprint

This subsection investigates differences in the levels and changes in maximum building height, total building volume, and total building footprint across the flight path borders of Era 2 during each regulatory transition. Maximum building height refers to the height of the tallest constructed building within a grid cell, reflecting developers' response to regulatory changes by increasing building heights. Total building volume in a grid cell serves as the best measure of the overall supply response. And total building footprint in a grid cell captures developers' strategies for land use intensity. The discussion opens with a brief review of the theoretical predictions for equilibrium building height during

each regulatory transition and proceeds to the empirical findings and their analysis.

6.1.1. Regulatory Transition 1: First Upzoning in 1989

Building Height. According to my conceptual framework, there are three key predictions regarding equilibrium building height during the first upzoning in 1989. First, before the first upzoning, the equilibrium building height in Era 1 (1957–1989, “Downtown Airport Restricts Urban Heights”) should be similar across the updated flight path borders. Second, after the first upzoning, the equilibrium building height in Era 2 (1989–1998, “Narrowed Flight Path”) is predicted to be lower inside the updated flight path compared to outside. Third, neighborhoods within the updated flight path should see a smaller increase in equilibrium building height compared to those outside after the first upzoning.

To test these predictions, I estimate the coefficient of interest (β_1) from Equation (3) using grid cells within a 360-meter bandwidth of the updated flight path borders. The outcome variables include the constructed building height, measured as the maximum building height in a grid cell in 1988 and 1998 (Eras 1 and 2), and the change in constructed building height, measured by the log ratio of maximum building height in a grid cell between 1998 and 1988. The estimated coefficient (β_1) quantifies the differences in these outcomes across the borders. Panel A of Table 1 presents these estimates. Column (1) includes only border fixed effects. Column (2) adds design controls, including slope, elevation, distance to the CBD, and distance to the downtown airport. Column (3), my preferred specification and sample, further excludes grid cells within a 60-meter donut just outside the flight path.

Panel A1 in Table 1 shows no significant difference in building heights inside versus outside the updated flight path in 1988, as all estimates in Columns (1) through (3) are statistically insignificant. This result aligns with my theoretical prediction. In 1998, approximately a decade after the first upzoning, the same panel further indicates that building heights were statistically lower—by 5.5 to 7 meters—inside the flight path compared to outside, consistent with the theoretical prediction. Comparing Columns (1) and (2), the estimates are nearly identical (-5.5 vs. -5.6 meters), but the inclusion

of locational fundamentals in Column (2) improves precision and reduces standard errors. In Column (3), accounting for buildings that straddle the updated flight path borders increases the estimated height difference to 7.0 meters. This suggests that such buildings attenuate the estimated effect, leading to an underestimation of the overall impact observed in Columns (1) and (2).⁴⁶

The identified 5.5 to 7-meter difference in building heights—equivalent to approximately 2 to 3 stories—between the two sides of the updated flight path borders in 1998 is small compared to the 30-meter difference in enforced height limits at the time. Several factors may explain this discrepancy. First, the height limits outside the flight path were not binding in some areas, meaning developers may not have built to the maximum allowable height, resulting in smaller actual height differences than the enforced limits suggest. Second, capital investment and urban renewal are inherently slow processes, and nearly a decade after the first upzoning may not have provided sufficient time for developers to fully respond. Furthermore, developers may have been hesitant to respond strongly to this modest upzoning—at 43%—possibly weighing the costs and benefits of redevelopment or anticipating a more significant relaxation of height limits following the airport’s closure.

Panel A2 of Table 1 reports relative changes in constructed building height inside the flight path compared to outside during the first upzoning. My estimates, presented in Columns (1) through (3), indicate no statistically significant differential change in building height across the borders, although the estimates are negative. Using my preferred specification and sample, the estimate is -12.7 log points, or -11.9 percent, but it is not statistically significant. This result contrasts with the predictions of my conceptual framework, which anticipated a smaller increase in building heights inside the flight path relative to the outside. The finding is somewhat unexpected, given that a 43% relaxation in height limits, while modest in Hong Kong’s history, might seem substantial in other contexts. However, this change does not appear to sufficiently incentivize developers to construct taller buildings in areas outside the flight path, despite the greater relaxation of

⁴⁶Panels A and B of Figure A.7 in Appendix A visually illustrate these findings. Using my preferred specification and sample (Column (3) of Panel A1), the figure depicts comparable building heights at the border in Era 1 and shorter heights inside the flight path in Era 2.

height limits compared to inside.

Building Volume and footprint. Total building volume is the best measure of overall supply response. Column (1) of Panel A in Table 2 presents the key coefficient of interest (β_1) from Equation (3), estimated using my preferred specification and sample. The outcome variables include the total building volume in a grid cell in 1988 and 1998 (Eras 1 and 2) and the log ratio of total building volume between 1998 and 1988. Panel A1, Column (1), shows that building volume levels in 1988 and 1998 exhibited patterns similar to those of building heights across the updated flight path borders. In 1988, building volume was comparable across the flight path borders, while in 1998, it was statistically 2,112.6 cubic meters smaller inside the flight path borders.

During the first upzoning, the estimated change in total building volume was 19.2 percent (or 21.3 log points) lower inside the flight path compared to outside, although this difference was not statistically significant (Panel A2, Column (1) of Table 2). This result aligns with the earlier finding of no differential changes in building heights across the borders during the first upzoning, providing further evidence that the modest relaxation of height limits did not elicit a significant supply response.

Evidence from prior literature suggests that a 43% relaxation in height limits can be substantial enough to prompt a supply response. For example, in Mumbai, a 10-50% relaxation in building height limits, measured by Floor Area Ratio (FAR), led to a 28% increase in housing supply, while in New York City, a 23% increase in FAR resulted in a 6% increase in housing floor space (Nagpal and Gandhi, 2023; Peng, 2023). In contrast, my findings indicate that a comparable 43% relaxation in building height limits failed to elicit a significant supply response from developers in Hong Kong. This raises the question of whether the 43% relaxation was still too small to economically incentivize developers, or if other factors, such as expectations of a future, larger relaxation of height limits, led developers to delay investment in areas experiencing a modest upzoning. I will discuss this further in subsection 6.3..

In Column (2) of Panel A in Table 2, the results further demonstrate that the building footprint in a grid cell was similar across flight path borders in both 1988 and 1998 (Eras 1 and 2), with no significant differential changes observed during the first upzoning.

This supports my model's assumption of comparable built-up areas across the flight path borders.

6.1.2. Regulatory Transition 2: Second Upzoning in 1998

Building Height. There are two theoretical predictions regarding the second upzoning in 1998. First, following the second upzoning, the equilibrium building height in Era 3 (1998–2008, "The Sky's the Limit") should be similar across the flight path borders of Era 2. Second, neighborhoods inside the flight path are expected to experience a larger increase in equilibrium building height compared to those outside.

To evaluate these predictions, I estimate the coefficient of interest (β_1) from Equation (3), using grid cells within a 360-meter bandwidth of the flight path borders. The dependent variables are the constructed building height in 2008 (Era 3) and the change in building height between 1998 and 2008, measured as the log ratio of maximum building height in a grid cell in 2008 to that in 1998. Panel B of Table 1 presents the results. In Panel B1, estimates across all specifications and samples show no statistically significant difference in building height across the borders in 2008, indicating a convergence of building heights on both sides.⁴⁷ This finding aligns with the theoretical prediction.

The rapid convergence in building height from 1998 to 2008 reflects significantly larger increases in building height in neighborhoods inside the flight path compared to those outside, following the second large-scale upzoning. Panel B2 in Table 1 shows that building heights inside the flight path grew 17.6 to 32.7 percent more than those outside, consistent with my theoretical prediction. Adding design controls raises this estimate from 17.6 to 19 percent (or 16.2 to 17.4 log points), as seen in Column (1) versus Column (2). When accounting for buildings straddling the borders (Column (3)), the greater increase inside the flight path reached 32.7 percent (or 28.3 log points), nearly doubling the effect size compared to Column (2).

Building Volume and Footprint. Panel B of Table 2 reports the key coefficient of interest (β_1) from Equation (3), estimated using the preferred specification and sample.

⁴⁷Panel C of Figure A.7 in Appendix A visually illustrates this convergence using my preferred specification and sample.

The outcomes include total building volume and footprint in a grid cell in 2008 (Era 3) and the log ratio of total building volume and footprint in 2008 to that in 1998.

Panel B1, Column (1), shows that the initial gap in building volume observed in 1998 (Era 2) had fully closed by 2008 (Era 3). This convergence was driven by a 76.5 percent (or 56.8 log points) greater increase in building volume in neighborhoods just inside the flight path borders compared to those outside (Panel B2, Column (1)). This result highlights a strong and rapid supply response from developers to the large-scale upzoning, effectively closing the building volume gap between the two sides of the flight path borders within a decade.

Panel B1, Column (2), indicates that the total building footprint remained similar across the flight path borders in 2008. However, neighborhoods just inside the flight path experienced a 34 percent (or 29.3 log points) larger expansion in building footprint compared to those outside (Panel B2, Column (2)). This finding suggests that developers responded to the large-scale upzoning not only by constructing taller buildings but also by intensifying land use, leading to a substantial increase in building volume.

Prior literature, both theoretical and empirical, emphasizes how durable capital inhibits investment, resulting in the persistence of older building structures (Brueckner, 1982; Braid, 2001; Glaeser and Gyourko, 2005; Hornbeck and Keniston, 2017; Henderson et al., 2021). My findings demonstrate that significant relaxation of land use constraints can incentivize developers to demolish aging buildings and construct taller ones, breaking the persistence of durable building stock. Moreover, the rapid convergence of the built environment—achieved within a decade of large-scale upzoning—demonstrates that durable housing can be replaced in a relatively short time frame when major zoning changes provide strong incentives.

6.1.3. Regulatory Transition 3: Downzoning in 2008

Building Height. My theoretical model predicts that, first, building heights remain similar across the borders in Era 4 (2008–2023, “Re-imposing Height Limits”), even after the downzoning rollout in 2008, and second, no differential change in building height occurs on either side of the borders during this regulatory transition. I test these

predictions by estimating the coefficient (β_1) from Equation (3), using the sample within a 360-meter bandwidth of flight path borders. This estimated coefficient captures cross-border differences in outcomes, including constructed building heights in 2023 (Era 4) and changes observed between 2008 and 2023. Panel C of Table 1 reports these estimates.

In Panel C1, building heights in 2023 (Era 4) were similar on both sides of the flight path borders across all specifications, consistent with my theoretical prediction.⁴⁸ This pattern in Era 4 mirrors that of Era 3, where constructed building heights transitioned smoothly across the flight path borders. Panel C2 further indicates no differential changes in building heights across the borders during this regulatory transition, as predicted by the conceptual framework.

Building Volume and Footprint. Panel C of Table 2 presents the coefficient (β_1) from Equation (3), estimated using the preferred specification and sample for outcomes including total building volume and footprint in a grid cell in 2023 (Era 4), as well as the log ratio of total building volume and footprint in 2023 to that in 2008. Panel C1 indicates that both building footprint and volume were comparable across the flight path borders in 2023. Furthermore, Panel C2 shows no differential changes in building footprint or volume before and after the 2008 downzoning.

These findings collectively indicate that the convergence in building height and volume on both sides of the borders, driven by the second large-scale upzoning in 1998, persisted over the long term—25 years after the second regulatory transition.

In Appendix C, I show that my main results, including differences in building height across the borders in different Eras and supply responses to each regulatory transition (best captured by the log ratio of building volume between Eras), are robust to several checks addressing concerns related to identification, border selection, and data issues.

First, the main results were estimated using a donut RD design with specific choices of bandwidth and excluded donut size, raising concerns about robustness to other choices. Figures C.1 and C.2 show that the main results are robust to different bandwidth choices,

⁴⁸Panel D of Figure A.7 in Appendix A illustrates the predicted regression lines and binned-average residuals for building heights in 2023, corresponding to Era 4, using my preferred specification and sample.

while Figures C.3 and C.4 demonstrate robustness to various excluded donut sizes outside the flight path. Another concern is the potential spillover effects of buildings across neighborhoods (Turner et al., 2014; Hornbeck and Keniston, 2017; Redding and Sturm, 2016). Larger and taller buildings can create externalities, such as increased traffic or shadowing, impacting nearby areas on the stricter side of the border. To address this, I run the main regressions by excluding donuts on both sides of the flight path borders. Figures C.5 and C.6 show that the main results still hold when different sizes of donuts are excluded on both sides of the borders and also confirm minimal spillover effects.

Next, I assess the robustness of my results to border selection criteria. In subsection 5.3, I already tested that height limits were binding below 80 meters inside the flight path during Era 2 (1989-1998, 'Narrowed Flight Path'), as shown in Figure 6. To further test the sensitivity of the main results to my border selection criteria, I run the main regressions using stricter cut-offs of 60 and 70 meters inside the flight path in Era 2 as the main border selection criteria. Figure C.7 shows that the results remain consistent overall, while indicating a greater increase in building volume outside the path compared to inside following the first modest upzoning. Additionally, my theoretical predictions on building height across the borders in each Era hinge on binding height limits inside the path during Era 2. When limits are non-binding inside the path, no differences in building height across the borders are expected in this period. I test this by using observations spatially close to borders that have height limits of 80 meters or more on the stricter side. Table C1 shows similar building heights across these borders in all Eras, further confirming the theoretical predictions and the choice of an 80-meter cut-off.

Finally, I address data-related concerns that could affect my results. Specifically, some borders in my main analysis have no observations for bandwidths over 200 meters due to limited geographical coverage of building height limit zones. Additionally, some borders lack private residential flat transactions on either side of the flight path borders in certain Eras, and some buildings have missing height information that requires imputation. Figure C.8 shows that the results remain consistent when excluding borders without observations for bandwidths over 200 meters and when excluding observations with imputed building heights. The result identifies a longer response period to the second

large-scale upzoning when borders without enough flat transactions nearby are excluded from the analysis. Furthermore, to capture the supply response, I use the log ratio of building volume between Eras. To address concerns about the data transformation involved in calculating the log ratio, I also use changes in building volume levels between Eras (in cubic meters) directly as the outcome. Panels B1 to B3 in Figures C.2, C.4, C.6, and Panel C in Figures C.7 and C.8 show consistent patterns when using level changes in building volume compared to my main results that use the log ratio of building volume between Eras.

6.2. Floor Space Price

I now test the model's prediction that the asset price per sq ft of floor space ("floor space price") never differs across the flight path borders in each Era. Due to data limitations, I compare prices only from Era 2 onward.

6.2.1. Era 2 - 1989-1998: Narrowed Flight Path

Floor Space Price. To examine how the asset price per sq ft of floor space changes across the flight path borders in Era 2, I estimate Equation (4) using transactions from 1991 to July 1998 within a 360-meter bandwidth of the flight path borders. Panel A of Table 3 reports the key coefficient (β_1) from Equation (4), capturing differences in the log of the asset price per sq ft of floor space across the flight path borders in Era 2, with and without flat quality controls. The results indicate that, when controlling for flat quality, there was no statistically significant difference in floor space prices across the flight path borders in Era 2, consistent across all specifications and samples (Columns (1) to (3)). This finding aligns with the theoretical prediction of equal floor space prices across the borders, based on the model's assumption of identical quality and sizes of flat units spatially close to either side of the borders.

If we allow flat quality to vary, we may expect differences in flat quality across the borders in Era 2. Neighborhoods inside the flight path had stricter height limits in Era 2, which likely led developers to invest in and maintain residential flats differently. In

a second regression, reported in Panel A of Table 3, floor space prices appeared lower in neighborhoods inside the flight path compared to those outside in Era 2, without controlling for flat quality. Columns (1) and (2) show a 17.1 percent (or 18.7 log points) to 18.3 percent (or 20.2 log points) lower floor space price inside the flight path. The effect size remains similar in Column (3) but is not statistically significant. The lower unadjusted floor space price inside the flight path suggests lower flat quality in these neighborhoods in Era 2.

Other Flat Features. To further support the findings on flat quality differences across the borders, I use direct quality indicators such as building age and clubhouse availability as outcome variables and estimate Equation (4) without controlling for flat quality, size, or access to public facilities. Column (1) of Panel A, Table 4, shows that buildings inside the flight path were, on average, 7 years older according to my preferred specification and sample. Column (2) of Panel A indicates that the likelihood of having access to a clubhouse was lower inside the flight path during Era 2. These indicators suggest that flat quality was inferior inside the flight path during Era 2, with developers offering fewer amenities in areas with stricter height restrictions.

A potential explanation for this behavior is planners' blight—where the anticipation of future policy changes negatively impacts current property conditions, value, and development decisions (Hagman, 1972; Dennis and Halsey, 1972). In this case, developers, anticipating future redevelopment opportunities with taller buildings after the airport closure, may have allowed the housing inside the flight path to deteriorate. I explore this hypothesis in greater detail in subsection 6.3..

Finally, Columns (3) and (4) in Panel A show no differences in the share of households living in informal or private permanent housing across the flight path borders in Era 2. This suggests that housing types (informal vs. private permanent) were consistent across the borders. Therefore, the observed differences in flat quality and amenities across the borders are more likely due to developers' investment and maintenance strategies, rather than differences in housing composition.

6.2.2. Era 3 - 1998-2008: The Sky's the Limit

Floor Space Price. To compare floor space prices across the borders in Era 3 after the closure of the downtown airport and the second large-scale upzoning, I estimate Equation (4) using transactions from July 1998 to Dec. 2007 within a 360-meter bandwidth of the borders. In Panel B of Table 3, I report the key coefficient of interest ($\beta_1 + \beta_{4,1}$) from equation (4), which captures the differences in the log of the asset price per sq ft of floor space across the flight path borders in Era 3, both with and without flat quality controls. The results across all specifications indicate no statistically significant differences in quality-adjusted floor space prices across the flight path borders in Era 3, consistent with theoretical predictions. When flat quality is not controlled for, the prices also show no statistically significant difference across the borders, although the estimates are negative and lower compared to those that include quality controls. This seemingly suggests an improvement in flat quality inside the flight path in Era 3 compared to Era 2, as shown by the comparison with the results in Panel A of Table 3.

Other Flat Features. To further substantiate this finding, I examined the building age and the availability of a clubhouse. As shown in Panel B, Table 4, there was no statistically significant difference in building age across the flight path borders (Column (1)) or in the availability of a clubhouse (Column (2)). This suggests an improvement in flat quality inside the flight path following the second large-scale upzoning in 1998, as developers constructed newer buildings with better amenities in neighborhoods just inside the flight path, compared to the previous Era.

Additionally, although the estimates for household shares living in informal or private permanent housing were not statistically different across the borders, I find that the share of households living in informal housing was 6 percentage points lower inside the flight path borders compared to outside (Column (3)), while the share of households living in private permanent housing was 13 percentage points higher inside the flight path borders (Column (4)). This suggests a potentially greater reduction in informal housing inside the flight path, further supporting the evidence of improved flat quality in these areas.

6.2.3. Era 4 - 2008-2023: Re-imposing Height Limits

Floor Space Price. To investigate differences in floor space price across the borders during Era 4, I estimate Equation (4) using transactions between 2008 and 2020 within a 360-meter bandwidth of the borders. Panel C of Table 3 presents the key coefficient of interest ($\beta_1 + \beta_{4,2}$) from Equation (4), capturing differences in the log of floor space price across the borders in Era 4, with and without flat quality controls. As shown, both quality-adjusted and quality-unadjusted floor space prices transitioned smoothly across the flight path borders in Era 4, regardless of the specification used. This result is consistent with my theoretical prediction.

Other Flat Features. Further analysis of building age and the availability of a clubhouse (Columns (1) and (2) in Panel C, Table 4) shows that by Era 4, there was no longer any significant difference in flat quality across the flight path borders. Additionally, the share of households living in informal housing was 7.4 percentage points lower in neighborhoods just inside the flight path compared to those outside (Column (3)), indicating a more pronounced improvement in flat quality within the flight path during this period. The share of households living in private permanent housing was 11 percentage points higher inside the flight path borders, though not statistically significant (Column (4)).

In Appendix C, I demonstrate that the pattern of results on floor space prices, both with and without flat quality controls, is robust to various checks addressing concerns regarding identification, border selection, and missing data. First, the bandwidth in an RD design sets the “window” around the cutoff where the data is considered to estimate the local treatment effect. Figure C.9 shows that my results are not sensitive to different bandwidth choices. Second, I exclude a 60-meter donut just outside the flight path in my main results to account for buildings intersecting flight path borders. Figure C.10 shows that my results hold when different sizes of excluded donuts just outside the flight path are used. Third, to further address potential building externalities, I test robustness by excluding donuts on both sides of the borders. Figure C.11 shows mostly consistent results but suggests a longer time frame for flat quality to converge across the

borders after the second upzoning when the excluded donut on each side exceeds 50 meters (totaling more than 100 meters). Fourth, I show that my main results are robust to different border selection criteria, specifically using 60 meters and 70 meters as cut-offs for defining binding height limits inside the flight path (see Figure C.12). Finally, missing data can lead to biased estimates if data gaps are non-random. Therefore, I assess robustness to missing data by using the log of asset price per unit as the outcome variable for my main regression, which includes all transactions regardless of the availability of unit size information. Figure C.13 shows that the results remain consistent when using price per unit compared to my main results using price per sq ft.

6.3. The Role of Developers' Anticipation: Deferred Maintenance and Investment

My earlier results show that the initial gap in flat quality during Era 2 (1989-1998, "Narrowed Flight Path"), measured by building age and clubhouse availability, closed after the downtown airport's closure and the resulting second large-scale upzoning. This suggests the potential presence of planners' blight—the negative impact on property conditions, values, and investment decisions caused by the anticipation of future policy changes (Hagman, 1972; Dennis and Halsey, 1972). Planners' blight often occurs when developers delay or reduce maintenance and investment in properties, expecting significant policy changes, such as upzoning or infrastructure projects, that make current investments less attractive compared to waiting for future opportunities. Developers likely see greater value in delaying investments, anticipating significant future gains from major policy changes—a manifestation of option value (Capozza and Helsley, 1990; Clapp and Salavei, 2010).

In 1989, the Hong Kong government narrowed the flight path and implemented the first modest upzoning. At the same time, they announced plans to build a new airport further from the city center to replace the downtown airport. Developers likely anticipated that, once the downtown airport closed, all associated restrictive building height limits in urban Hong Kong would be removed, although the specifics

were uncertain. In this scenario, developers faced the choice of either investing and redeveloping properties immediately or waiting for future zoning policy changes that would allow for even taller structures. Since the anticipated zoning changes were expected to be more substantial inside the flight path, the option value was higher there compared to outside. Based on this higher option value, developers were likely delaying maintenance and investment more inside the flight path than outside until the zoning changes materialized.

To explore this hypothesis, I compare floor space price, building age, and clubhouse availability across the flight path borders during the early (1991-1994) and late (1995-July 1998) periods of Era 2. If developers were indeed deferring maintenance and investment in anticipation of major zoning changes, we would expect flat quality to worsen more inside the flight path than outside, particularly as the closure of the downtown airport approached. Column (1) of Table 5 shows that the asset price per sq ft of floor space, with quality controls, remained similar across the borders in both periods. However, the quality-unadjusted floor space price, initially comparable across the borders in early Era 2, became about 29.5% (or 34.9 log points) lower inside the flight path compared to outside during late Era 2 (Column (2)). This decline in quality-unadjusted floor space price suggests a rapid deterioration in flat quality inside the flight path. I further test this with quality indicators such as building age and clubhouse availability. Column (3) of Table 5 shows that, while building age was initially similar across the borders, by the end of the period, buildings inside the flight path were approximately eight years older. Similarly, while the likelihood of having access to a clubhouse was comparable in early Era 2, flats inside the flight path were less likely to have clubhouse access by the end of Era 2 (Column (4)). These findings support the hypothesis that developers reduced maintenance and investment in anticipation of significant zoning changes.

The anticipation of major zoning changes likely helps explain the limited supply response to the first modest upzoning, as identified in subsection 6.1.. Developers had two choices after the first upzoning: redevelop immediately by adding three to four stories in areas that experienced modest upzoning or wait for future zoning changes that would allow them to build taller structures and achieve economies of scale. Expecting

larger-scale upzoning soon, developers likely delayed investments in areas undergoing modest upzoning while more actively preparing for pre-redevelopment activities (such as land acquisition) in areas expecting substantial upzoning later on. As a result, this anticipation likely moderated developers' response to the first modest upzoning and accelerated the rapid convergence in the built environment across the borders after the second large-scale upzoning.

7. Conclusion

Cities worldwide face significant challenges in providing enough housing to keep prices in check. Zoning regulations often contribute to limited supply. In response, cities have started loosening zoning rules, expecting upzoning to stimulate housing supply. My paper contributes to this debate by examining two distinct upzoning events in urban Hong Kong: a modest relaxation of building height limits driven by the narrowing of the downtown airport's flight path in 1989 and a large-scale relaxation after the downtown airport's closure in 1998. These events provide a unique opportunity to assess the nature and speed of developers' responses to different scales of upzoning in the same jurisdiction.

My findings show that developers responded strongly to the large-scale upzoning, quickly closing initial gaps in building height, volume, and quality between areas with previously differing height limits. In contrast, the modest upzoning did not trigger a significant supply response. Moreover, developers reduced maintenance and investment in anticipation of the second, larger-scale upzoning, leading to accelerated deterioration in flat quality in areas awaiting more substantial regulatory relaxation. The limited response to the first modest upzoning likely stems from two factors. First, the initial upzoning might be too modest to stimulate redevelopment in densely built urban areas like Hong Kong. Second, developers expected a more substantial upzoning in the near future, which moderated their response to the initial smaller-scale change.

These findings have important policy implications for cities worldwide grappling with housing supply and affordability challenges. This study demonstrates that

upzoning can effectively promote vertical development and increase housing supply in urban areas with binding zoning restrictions. However, to ensure zoning reforms lead to meaningful supply increases, policymakers must carefully design and implement them while also managing the risk of planners' blight that may accompany such changes. To mitigate the negative effects of planners' blight, one feasible approach is to set a sunset date to review and modify zoning regulations. This would demonstrate policymakers' commitment to current reforms and encourage developers to act promptly, rather than delay in anticipation of imminent changes.

References

- Alonso, William, "The historic and the structural theories of urban form: their implications for urban renewal," *Land economics*, 1964, 40 (2), 227–231.
- Anagol, Santosh, Fernando Vendramel Ferreira, and Jonah M Rexer, "Estimating the economic value of zoning reform," Technical Report, National Bureau of Economic Research 2021.
- Arnott, Richard J and James G MacKinnon, "Measuring the costs of height restrictions with a general equilibrium model," *Regional Science and Urban Economics*, 1977, 7 (4), 359–375.
- Baum-Snow, Nathaniel, "Constraints on city and neighborhood growth: the central role of housing supply," *Journal of Economic Perspectives*, 2023, 37 (2), 53–74.
- Bertaud, Alain and Jan K Brueckner, "Analyzing building-height restrictions: predicted impacts and welfare costs," *Regional Science and Urban Economics*, 2005, 35 (2), 109–125.
- Braid, Ralph M, "Spatial growth and redevelopment with perfect foresight and durable housing," *Journal of Urban Economics*, 2001, 49 (3), 425–452.
- Brooks, Leah and Byron Lutz, "Vestiges of transit: Urban persistence at a microscale," *Review of Economics and Statistics*, 2019, 101 (3), 385–399.
- Brueckner, Jan K, "Building ages and urban growth," *Regional Science and Urban Economics*, 1982, 12 (2), 197–210.
- and Ruchi Singh, "Stringency of land-use regulation: Building heights in US cities," *Journal of Urban Economics*, 2020, 116, 103239.
- et al., "The structure of urban equilibria: A unified treatment of the Muth-Mills model," *Handbook of regional and urban economics*, 1987, 2 (20), 821–845.
- Büchler, Simon and Elena Lutz, "Making housing affordable? The local effects of relaxing land-use regulation," *Journal of Urban Economics*, 2024, 143, 103689.
- Capozza, Dennis R. and Robert W. Helsley, "The stochastic city," *Journal of Urban Economics*, 1990, 28 (2), 187–203.
- Chau, KW and Siu Kei Wong, "Externalities of urban renewal: A real option perspective," *The Journal of Real Estate Finance and Economics*, 2014, 48, 546–560.
- Clapp, John M and Katsiaryna Salavei, "Hedonic pricing with redevelopment options: A new approach to estimating depreciation effects," *Journal of Urban Economics*, 2010, 67 (3), 362–377.
- , Piet Eichholtz, and Thies Lindenthal, "Real option value over a housing market cycle," *Regional Science and Urban Economics*, 2013, 43 (6), 862–874.
- Dennis, Norman and HA Halsey, "Public participation and planners' blight," (*No Title*), 1972.
- Freemark, Yonah, "Upzoning Chicago: Impacts of a zoning reform on property values and housing construction," *Urban Affairs Review*, 2020, 56 (3), 758–789.
- Gelman, Andrew and Guido Imbens, "Why high-order polynomials should not be used in regression discontinuity designs," *Journal of Business & Economic Statistics*, 2019, 37 (3), 447–456.
- Glaeser, Edward L and Joseph Gyourko, "Urban decline and durable housing," *Journal of political economy*, 2005, 113 (2), 345–375.

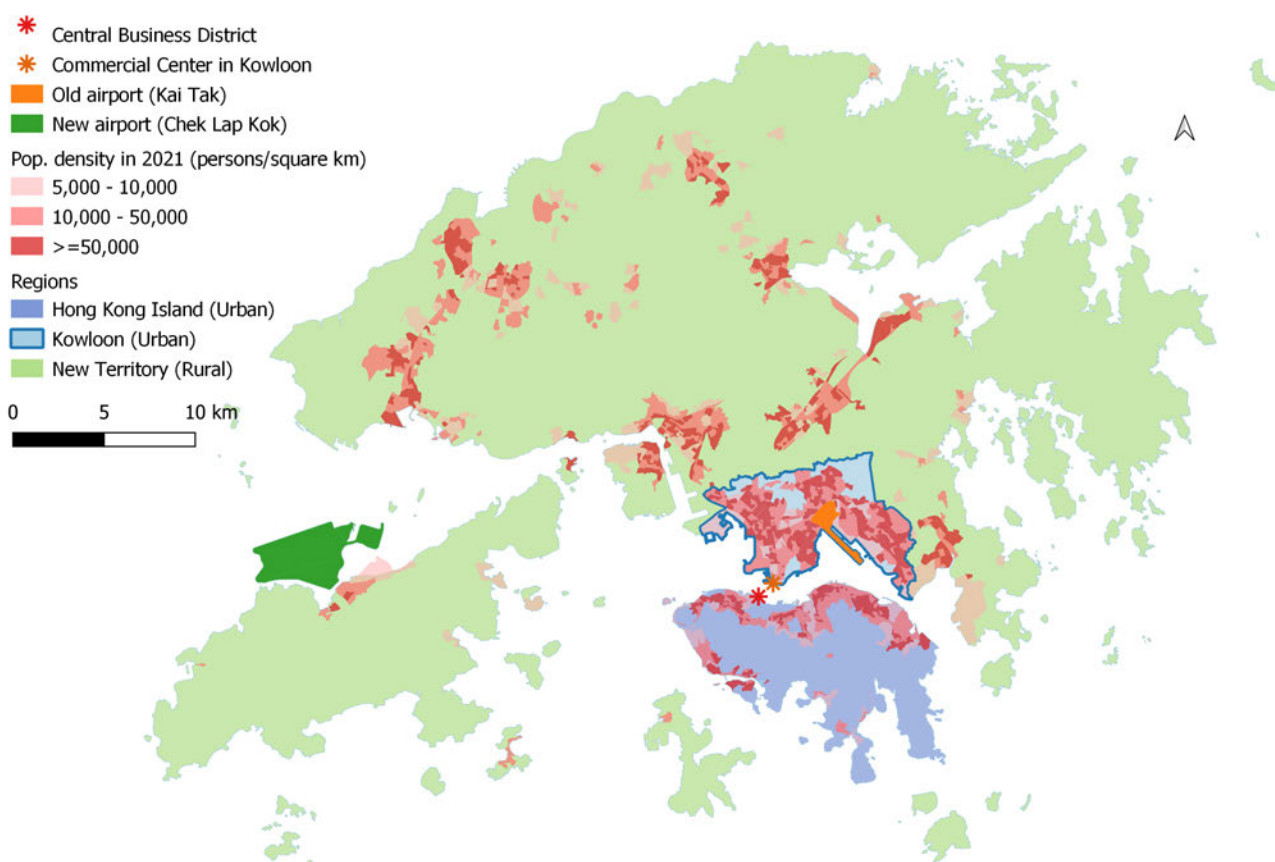
- Greenaway-McGrevy, Ryan, "Evaluating the Long-Run Effects of Zoning Reform on Urban Development," *Available at SSRN 4439532*, 2023.
- Hagman, Donald G, "Planning (Condemnation) Blight, Participation and Just Compensation: Anglo-American Comparisons," *Urb. Law.*, 1972, 4, 434.
- Henderson, J Vernon, Tanner Regan, and Anthony J Venables, "Building the city: from slums to a modern metropolis," *The Review of Economic Studies*, 2021, 88 (3), 1157–1192.
- Ho, Puiyin, *Making Hong Kong*, Edward Elgar Publishing, 2018.
- Hornbeck, Richard and Daniel Keniston, "Creative destruction: Barriers to urban growth and the Great Boston Fire of 1872," *American Economic Review*, 2017, 107 (6), 1365–1398.
- Jedwab, Remi, Edward Kerby, and Alexander Moradi, "History, path dependence and development: Evidence from colonial railways, settlers and cities in Kenya," *The Economic Journal*, 2017, 127 (603), 1467–1494.
- Kulka, Amrita, "Sorting into neighborhoods: The role of minimum lot sizes," in "Conference paper, APPAM 41st Annual Fall Research Conference, Denver, CO" 2019.
- , Aradhya Sood, and Nicholas Chiumenti, "Under the (neighbor) Hood: Understanding Interactions Among Zoning Regulations," *Available at SSRN 4082457*, 2023.
- Liao, Hsi-Ling, "The Effect of Rezoning on Local Housing Supply and Demand: Evidence from New York City," in "2022 APPAM Fall Research Conference" APPAM 2022.
- McMillen, Daniel and Arthur O'Sullivan, "Option value and the price of teardown properties," *Journal of Urban Economics*, 2013, 74, 71–82.
- Michaels, Guy, Dzhamilya Nigmatulina, Ferdinand Rauch, Tanner Regan, Neeraj Baruah, and Amanda Dahlstrand, "Planning ahead for better neighborhoods: Long-run evidence from tanzania," *Journal of Political Economy*, 2021, 129 (7), 2112–2156.
- Mills, Edwin S, "An aggregative model of resource allocation in a metropolitan area," *The American Economic Review*, 1967, 57 (2), 197–210.
- Molloy, Raven et al., "The effect of housing supply regulation on housing affordability: A review," *Regional science and urban economics*, 2020, 80 (C), 1–5.
- Munneke, Henry J and Kiplan S Womack, "Valuing the redevelopment option component of urban land values," *Real Estate Economics*, 2020, 48 (1), 294–338.
- Muth, Richard F, "Cities and Housing; The Spatial Pattern of Urban Residential Land Use.," 1969.
- Nagpal, Geetika and Sahil Gandhi, "Scaling Heights: Affordability Implications of Zoning Deregulation in India," 2023.
- Paciorek, Andrew, "Supply constraints and housing market dynamics," *Journal of Urban Economics*, 2013, 77, 11–26.
- Peng, Elsie], "The Dynamics of Urban Development: Evidence from Land Use Reform in New York," 2023.
- Redding, Stephen J and Daniel M Sturm, "ENE: EW DL," 2016.
- Song, Jaehee, "The effects of residential zoning in US housing markets," *Available at SSRN 3996483*, 2021.

- Takeda, Kohei and Atsushi Yamagishi, "The Economic Dynamics of City Structure: Evidence from Hiroshima's Recovery," Technical Report, Centre for Economic Performance, LSE 2024.
- Turner, Matthew A, Andrew Haughwout, and Wilbert Van Der Klaauw, "Land use regulation and welfare," *Econometrica*, 2014, 82 (4), 1341–1403.
- Wheaton, William C, "A comparative static analysis of urban spatial structure," *Journal of Economic Theory*, 1974, 9 (2), 223–237.
- Yamasaki, Junichi, Kentaro Nakajima, and Kensuke Teshima, *From samurai to skyscrapers: How historical lot fragmentation shapes Tokyo*, Graduate School of Economics Hitotsubashi University Teikoku Databank Center . . . , 2021.
- Yezer, Anthony M, "When Does Land Use Regulation Lower the Average Price of Housing in Cities?," *Available at SSRN 4896280*, 2024.

Main Figures and Tables

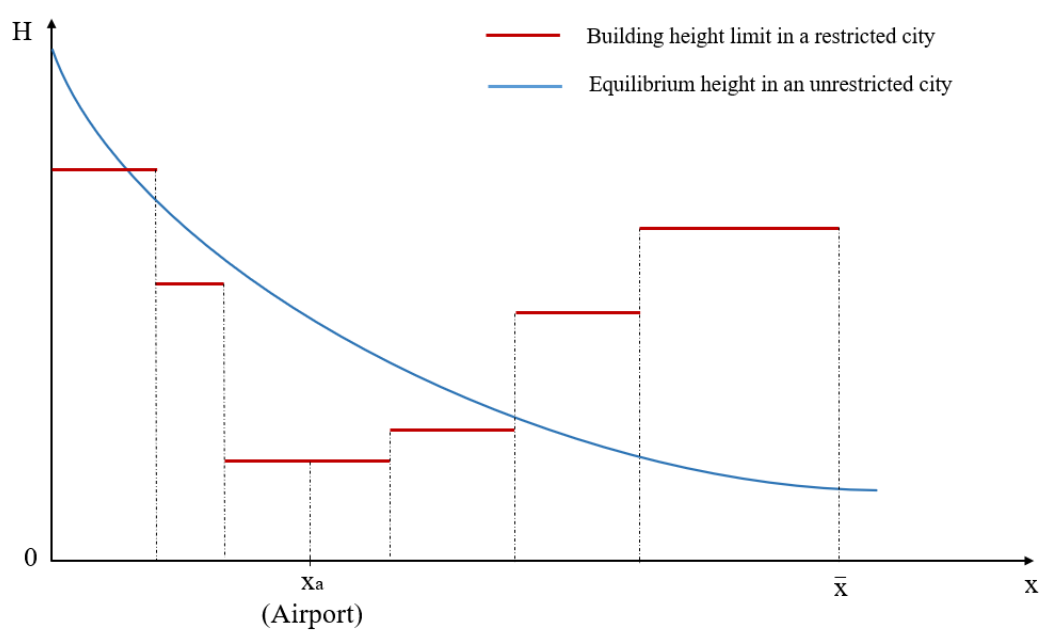
Figures

Figure 1: Hong Kong Territory



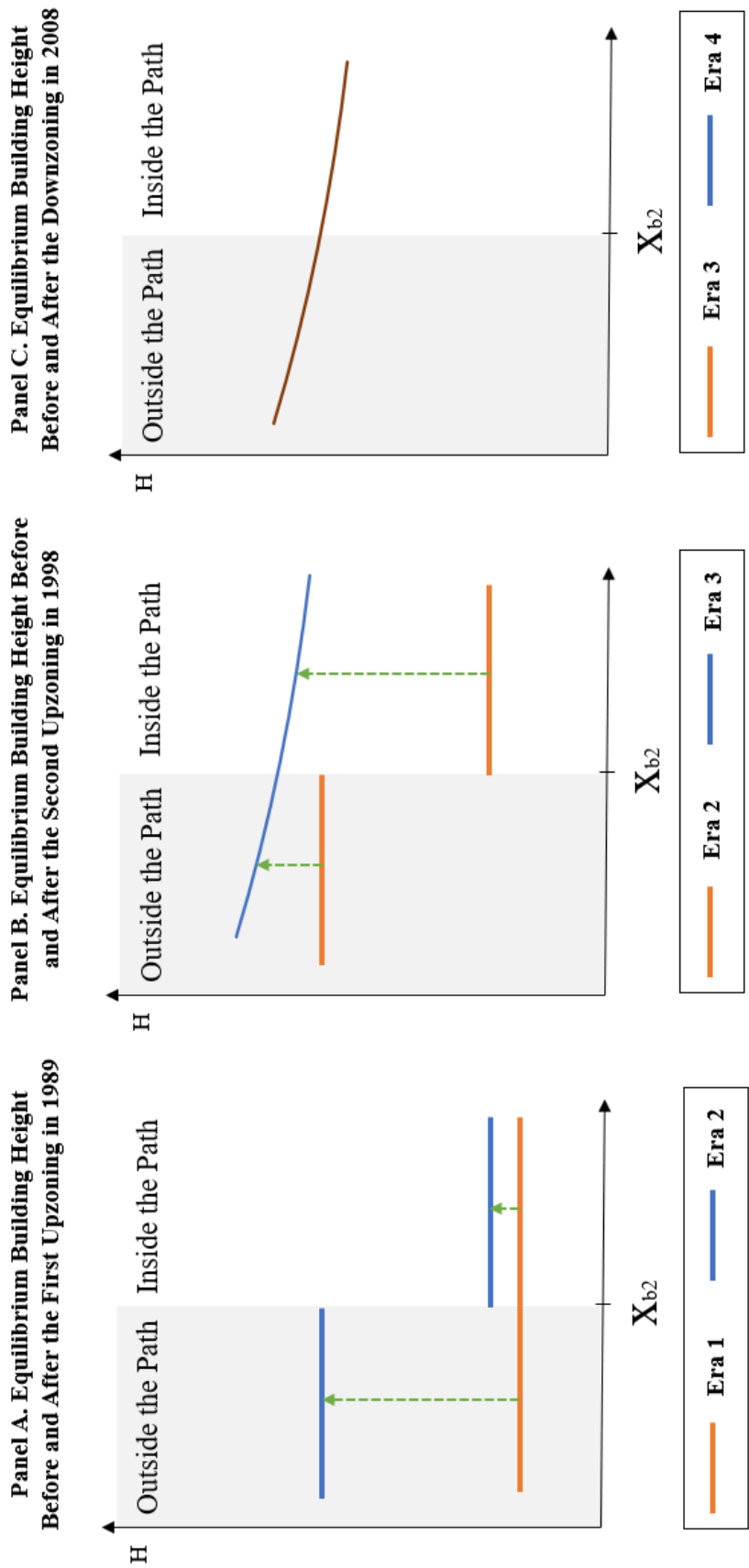
Notes: In Hong Kong, Kowloon and Hong Kong Island are urban areas, while the New Territories are considered rural. Kai Tak Airport, the old downtown airport, was located in eastern Kowloon, whereas the new airport is situated 25 km from the city center. Kowloon is where airport-specific building height restrictions were first implemented in the 1950s.

Figure 2: Building Height Restrictions in a City with a Downtown Airport



Notes: This figure illustrates how building height limits might be configured when an airport is located in the city center. In the graph, x_a marks the location of the airport. Height limits are most stringent along the flight path near the airport and become progressively less restrictive with increasing distance from the airport. The blue curve represents the equilibrium height in a city without height restrictions.

Figure 3: Equilibrium Building Height on Both Sides of the Updated Flight Path Borders Before and after Each Regulatory Transition



X_{b2} : Location of updated flight path borders in Era 2

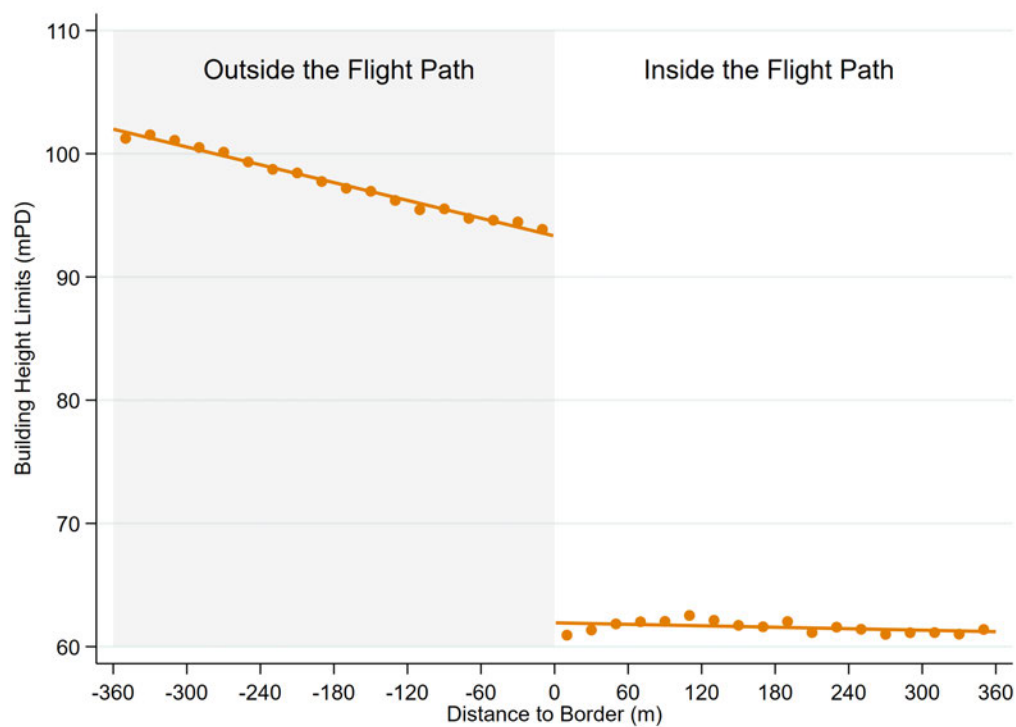
Notes: This figure shows the relative equilibrium building heights on both sides of the updated flight path borders in Era 2, denoted by x_{b2} , before and after each regulatory transition, along with the associated changes.

Figure 4: Summary of Theoretical Predictions for Key Outcomes Inside vs. Outside the Updated Flight Path During Each Regulatory Transition

	(1) Height Limits	(2) Equilibrium Height	(3) Changes in Equilibrium Height	(4) Floor Space Price
Era 1 - 1957-1989:				
Downtown Airport Restricts Urban Heights	0	0		0
Era 2 - 1989-1998:			Transition 1: 1 st Upzoning in 1989	
Narrowed Flight Path	↓	↓	↓	0
Era 3 - 1998-2008:			Transition 2: 2 nd Upzoning in 1998	
Sky's the Limit	0	0	↑	0
Era 4 - 2008-2023:			Transition 3: Downzoning in 2008	
Re-imposing Height Limits	0	0	0	0

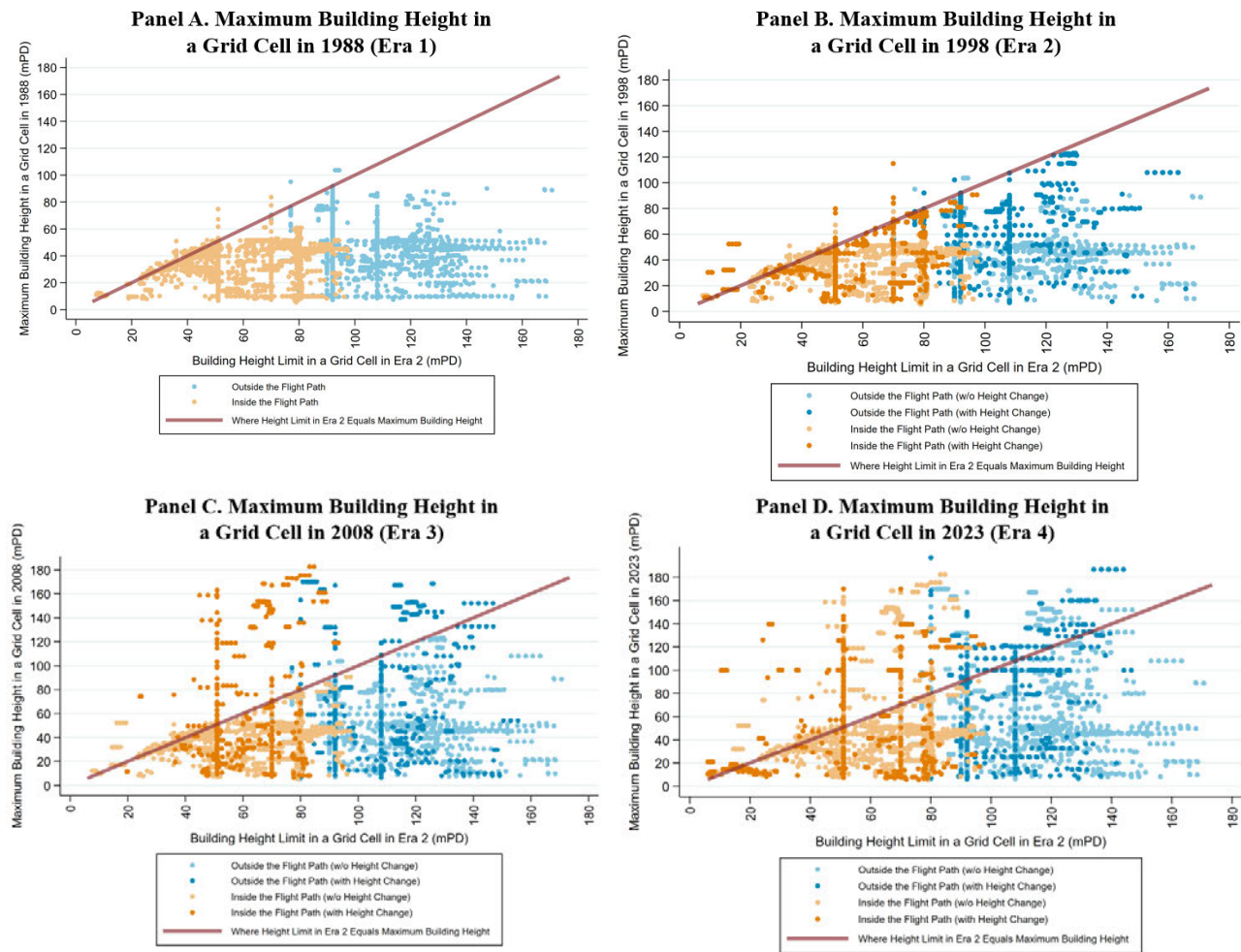
Notes: This figure first illustrates how height limits differed inside the updated flight path borders compared to outside in each Era (Column (1)). Based on the model properties, it then summarizes the differences in equilibrium height and asset price per sq ft of floor space (“floor space price”) inside versus outside the updated flight path borders in each Era, along with changes in equilibrium height. A value of 0 indicates no difference between locations inside and outside the updated flight path borders, while ↑ signifies a larger value inside the updated flight path compared to outside, and ↓ indicates a smaller value inside the updated flight path compared to outside.

Figure 5: Sharp Discontinuity of Height Limits around the Borders in Era 2



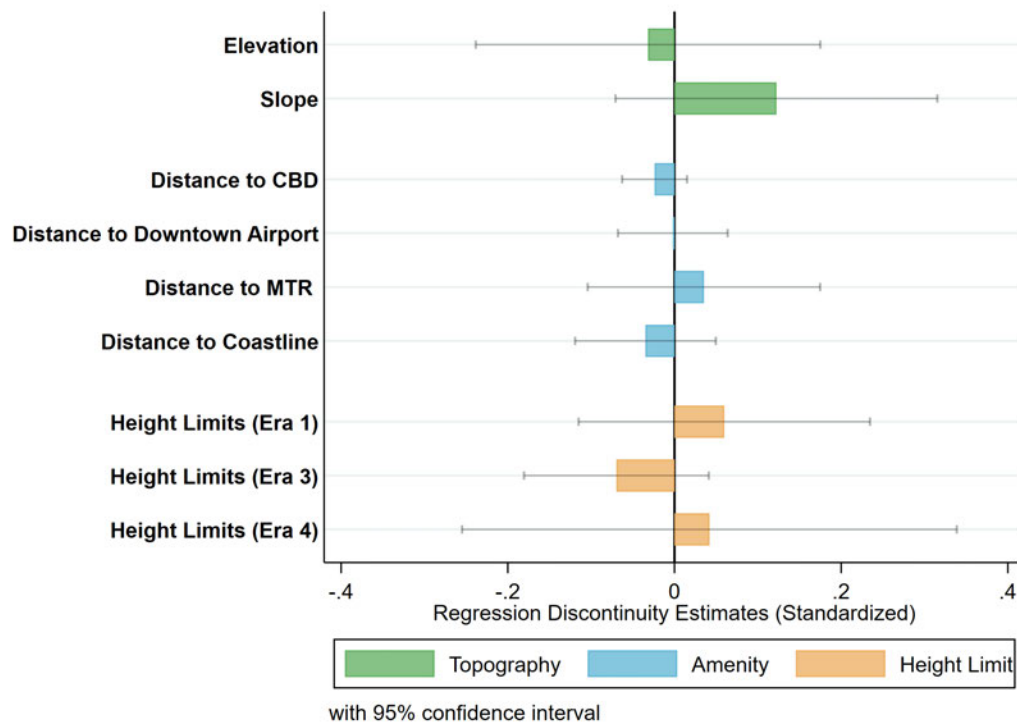
Notes: This figure shows the predicted regression line and the binned-average residuals, estimated using Equation (3) without controls. The dependent variable is the building height limits enforced in Era 2 (1989-1998, "Narrowed Flight Path"). All estimates have been adjusted by adding the sample mean of 79.3 meters above the Hong Kong Principal Datum (mPD) to provide a common reference point.

Figure 6: Comparison of Maximum Building Heights in Different Eras and the Height Limit in Era 2 within Grid Cells



Notes: This figure illustrates the binding nature of building height limits enforced during Era 2, focusing on grid cells within a 360-meter bandwidth of the updated flight path borders of Era 2 (1989-1998, "Narrowed Flight Path"). Panels A, B, C, and D show the maximum building heights in grid cells for the years 1988, 1998, 2008, and 2023, corresponding to Eras 1, 2, 3, and 4, respectively, as represented on the y-axis. The x-axis in all panels indicates the building height limits enforced during Era 2. The red line represents points where maximum building heights are equal to the Era 2 limits. Orange dots correspond to grid cells inside the flight path, while blue dots represent those outside it. Darker shades highlight grid cells that experienced new construction, leading to updated maximum building heights during the respective era. For comparison, 60 and 67 grid cells with maximum building heights exceeding 200 meters in Eras 3 and 4, respectively, are not plotted. Grid cells without buildings (maximum building height of 0) are omitted from all panels.

Figure 7: Continuity in Locational Fundamentals



Notes: This figure shows the standardized RD estimates from Equation (3) (without controls) for fundamental location characteristics, as well as the height limits enforced in Eras 1, 3, and 4, all using a 360-meter bandwidth. The means for these locational fundamentals are: elevation (17.1 mPD), slope (4.1 degrees), distance to the CBD (4.1 km), distance to the Downtown airport (1.9 km), distance to the nearest MTR station (0.6 km), distance to the coastline (1.1 km), height limits in Era 1 (55 mPD), height limits in Era 3 (486.5 mPD), height limit in Era 4 (76.9 mPD).

Tables

Table 1: Maximum Building Height in a Grid Cell

	(1)	(2)	(3)
Panel A. Regulatory Transition 1: First Upzoning in 1989			
A1. Maximum Building Height in a Grid Cell			
1 {Inside the Flight Path}, 1988	-2.234 (1.758)	-2.232 (1.658)	-2.591 (2.225)
1 {Inside the Flight Path}, 1998	-5.506*** (1.987)	-5.576*** (1.882)	-7.024*** (2.607)
A2. Log Ratio of Maximum Building Height between 1998 and 1988			
1 {Inside the Flight Path}	-0.062 (0.094)	-0.071 (0.095)	-0.127 (0.122)
Sample Mean in 1988 (mPD)	24.66	24.66	24.67
Panel B. Regulatory Transition 2: Second Upzoning in 1998			
B1. Maximum Building Height in a Grid Cell			
1 {Inside the Flight Path}, 2008	-1.242 (2.371)	-0.959 (2.340)	1.310 (3.230)
B2. Log Ratio of Maximum Building Height between 2008 and 1998			
1 {Inside the Flight Path}	0.162* (0.089)	0.174** (0.088)	0.283** (0.111)
Sample Mean in 1998 (mPD)	28.84	28.84	28.73
Panel C. Regulatory Transition 3: Downzoning in 2008			
C1. Maximum Building Height in a Grid Cell			
1 {Inside the Flight Path}, 2023	-2.505 (2.785)	-2.199 (2.713)	-1.179 (3.537)
C2. Log Ratio of Maximum Building Height between 2023 and 2008			
1 {Inside the Flight Path}	-0.045 (0.087)	-0.042 (0.088)	-0.112 (0.116)
Sample Mean in 2008 (mPD)	36.19	36.19	36.20
Border FE	X	X	X
Design Controls		X	X
Donut RD			X
Observations	12,669	12,669	11,591

Notes: Each cell in the table reports the coefficient β_1 , estimated using Equation (3) separately. This coefficient captures the difference in the outcome variable inside the updated flight path of Era 2 (1989–1998, “Narrowed Flight Path”) compared to outside it. Panel A presents the results for the first upzoning in 1989, Panel B for the second upzoning in 1998, and Panel C for the downzoning in 2008. The sample consists of grid cells within 360 meters of the nearest border, with each 30-by-30-meter grid cell as the unit of observation. Column (1) includes only border fixed effects, without incorporating design controls or excluding observations within the 60-meter donut outside the updated flight path. Column (2) adds design controls, including slope, elevation, distance to the CBD, and distance to the downtown airport. Column (3) further excludes grid cells within the 60-meter donut outside the flight path. Standard errors, clustered at the 150-by-150-meter grid square level, are reported in parentheses. “mPD” denotes meters above the Hong Kong Principal Datum.

*** $p < 0.01$, ** $p < 0.05$, * $p < 0.1$

Table 2: Building Volume and Footprint in a Grid Cell

	(1) Total Building Volume in a Grid Cell	(2) Total Building Footprint in a Grid Cell
Panel A. Regulatory Transition 1: First Upzoning in 1989		
A1. Building Feature in a Grid Cell		
1 {Inside the Flight Path}, 1988	-796.656 (818.836)	-24.899 (21.363)
1 {Inside the Flight Path}, 1998	-2,112.628** (990.844)	-25.334 (21.849)
A2. Log Ratio of Building Feature between 1998 and 1988		
1 {Inside the Flight Path}	-0.213 (0.314)	-0.088 (0.201)
Sample Mean in 1988	6,763 m ³	194 m ²
Panel B. Regulatory Transition 2: Second Upzoning in 1998		
B1. Building Feature in a Grid Cell		
1 {Inside the Flight Path}, 2008	1,591.767 (1,741.164)	-4.571 (22.220)
B2. Log Ratio of Building Feature between 2008 and 1998		
1 {Inside the Flight Path}	0.568** (0.257)	0.293* (0.153)
Sample Mean in 1998	8,447 m ³	220 m ²
Panel C. Regulatory Transition 3: Downzoning in 2008		
C1. Building Feature in a Grid Cell		
1 {Inside the Flight Path}, 2023	926.925 (1,821.661)	-6.612 (21.656)
C2. Log Ratio of Building Feature between 2023 and 2008		
1 {Inside the Flight Path}	-0.235 (0.272)	-0.118 (0.165)
Sample Mean in 2008	11,225 m ³	248 m ²
Border FE	X	X
Design Controls	X	X
Donut RD	X	X
Observations	11,591	11,591

Notes: Each cell in the table reports the coefficient β_1 , estimated using Equation (3) separately. This coefficient captures the difference in the outcome variable inside the updated flight path of Era 2 (1989–1998, "Narrowed Flight Path") compared to outside it. Panel A presents the results for the first upzoning in 1989, Panel B for the second upzoning in 1998, and Panel C for the downzoning in 2008. The sample consists of grid cells within 360 meters of the nearest border, excluding a 60-meter donut just outside the flight path border. Column (1) reports results for total building volume in a grid cell, including levels in different Eras and the log ratio between Eras. Column (2) presents results for total building footprint in a grid cell, similarly including levels in different Eras and the log ratio between Eras. Standard errors, clustered at the 150-by-150-meter grid square level, are reported in parentheses. "mPD" denotes meters above the Hong Kong Principal Datum.

*** $p < 0.01$, ** $p < 0.05$, * $p < 0.1$

Table 3: Log of Asset Price per sq ft of Floor Space

		(1)	(2)	(3)
Panel A. Era 2 - 1989-1998: Narrowed Flight Path				
Quality-Adjusted:	1 {Inside the Flight Path}, Era 2	-0.055 (0.053)	-0.051 (0.053)	-0.013 (0.061)
Quality-Unadjusted:	1 {Inside the Flight Path}, Era 2	-0.187* (0.106)	-0.202* (0.109)	-0.165 (0.123)
Panel B. Era 3 - 1998-2008: The Sky's the Limit				
Quality-Adjusted:	1 {Inside the Flight Path}, Era 3	-0.061 (0.05)	-0.030 (0.050)	-0.042 (0.066)
Quality-Unadjusted:	1 {Inside the Flight Path}, Era 3	-0.139 (0.123)	-0.108 (0.115)	-0.101 (0.145)
Panel C. Era 4 - 2008-Present: Re-imposing Height Limits				
Quality-Adjusted:	1 {Inside the Flight Path}, Era 4	-0.048 (0.039)	-0.020 (0.038)	-0.034 (0.065)
Quality-Unadjusted:	1 {Inside the Flight Path}, Era 4	0.000 (0.077)	0.034 (0.078)	0.003 (0.109)
Flat Size Controls		X	X	X
Access to Public Facilities		X	X	X
Border FE		X	X	X
Year FE		X	X	X
Design Controls			X	X
Donut RD				X
Observations		122,619	122,619	114,415

Notes: Each column presents two sets of results—one with and one without controls for flat quality—based on Equation (4), using the log of asset price per square foot of floor space as the dependent variable. For each regression, "1{Inside the Flight Path}, Era 2" reports the coefficient β_1 , which captures the differences in asset price per sq ft of floor space across the borders during Era 2. "1{Inside the Flight Path}, Era 3" reports the sum of β_1 and $\beta_{4,1}$, capturing the differences across the borders during Era 3. "1{Inside the Flight Path}, Era 4" reports the sum of β_1 and $\beta_{4,2}$, capturing the differences across the borders during Era 4. The sample consists of transactions within 360 meters of the nearest border, with each transaction serving as the unit of observation. Column (1) includes only border and year fixed effects, without incorporating design controls or excluding observations within the 60-meter donut outside the updated flight path. Column (2) adds design controls, including slope, elevation, distance to the CBD, and distance to the downtown airport. Column (3) further excludes transactions within the 60-meter donut outside the flight path. All regressions include controls for flat size and access to public facilities. Standard errors, clustered at the 150-by-150-meter grid square level, are reported in parentheses.

*** $p < 0.01$, ** $p < 0.05$, * $p < 0.1$

Table 4: Other Flat Features

	(1) Building Age	(2) Availability of a Clubhouse	(3) Share of Households Living in Informal Housing	(4) Share of Households Living in Private Permanent Housing
Panel A. Era 2 - 1989-1998: Narrowed Flight Path				
1 {Inside the Flight Path}, Era 2	6.645* (3.378)	-0.141** (0.062)	2.331 (4.422)	-0.354 (8.437)
Sample Mean in Era 2	14	0.016	18.63%	63.8%
Panel B. Era 3 - 1998-2008: The Sky's the Limit				
1 {Inside the Flight Path}, Era 3	4.264 (4.563)	0.068 (0.171)	-6.235 (3.822)	12.516 (12.259)
Sample Mean in Era 3	18	0.270	5.92%	67.66%
Panel C. Era 4 - 2008-Present: Re-imposing Height Limits				
1 {Inside the Flight Path}, Era 4	-0.356 (5.702)	0.035 (0.178)	-7.392* (4.107)	11.126 (7.129)
Sample Mean in Era 4	21	0.419	5.74%	78.36%
Border FE	X	X	X	X
Year FE	X	X		
Design Controls	X	X	X	X
Donut RD	X	X	X	X
Observations	114,415	114,415	5,624	5,624

Notes: Columns (1) and (2) present results from separate regressions estimated using Equation (4), with building age and the availability of a clubhouse as the respective outcome variables. These regressions are estimated without controlling for flat size, quality, or access to public facilities. For each regression, "1 {Inside the Flight Path}, Era 2" reports the coefficient β_1 , which captures the differences in outcome variable across the borders during Era 2. "1 {Inside the Flight Path}, Era 3" reports the sum of β_1 and $\beta_{4,1}$, capturing the differences across the borders during Era 3. "1 {Inside the Flight Path}, Era 4" reports the sum of β_1 and $\beta_{4,2}$, capturing the differences across the borders during Era 4. The sample comprises transactions located within 360 meters of the border, excluding a 60-meter donut just outside the flight path border, with each individual transaction serving as the unit of observation. Each cell in Columns (3) and (4) reports the coefficient β_1 , estimated using Equation (3) separately. The sample includes grid cells within 360 meters of the nearest border, excluding those located in street blocks that cross borders and have a similar number of cells on both sides (ratio smaller than 75/25). The unit of observation is a 30-by-30-meter grid cell. Standard errors, reported in parentheses, are clustered at the 150-by-150-meter grid square level for Columns (1) and (2), and at the street block level for Columns (3) and (4).

*** p<0.01, ** p<0.05, * p<0.1

Table 5: Tests for Planners' Blight

	(1) Quality-Adjusted (Log) Asset Price per sq ft of Floor Space	(2) Quality-Unadjusted (Log) Asset Price per sq ft of Floor Space	(3) Building Age	(4) Availability of a Clubhouse
1 {Inside the Flight Path}, Early Era 2	0.077 (0.058)	-0.056 (0.110)	0.285 (2.550)	-0.005 (0.020)
1 {Inside the Flight Path}, Late Era 2	-0.013 (0.053)	-0.349*** (0.125)	7.678** (3.275)	-0.098** (0.049)
Flat Size Controls	X	X		
Access to Public Facilities	X	X		
Flat Quality Controls	X			
Border FE	X	X	X	X
Year FE	X	X	X	X
Design Controls	X	X	X	X
Donut RD	X	X	X	X
Observations	31,272	31,272	31,272	31,272

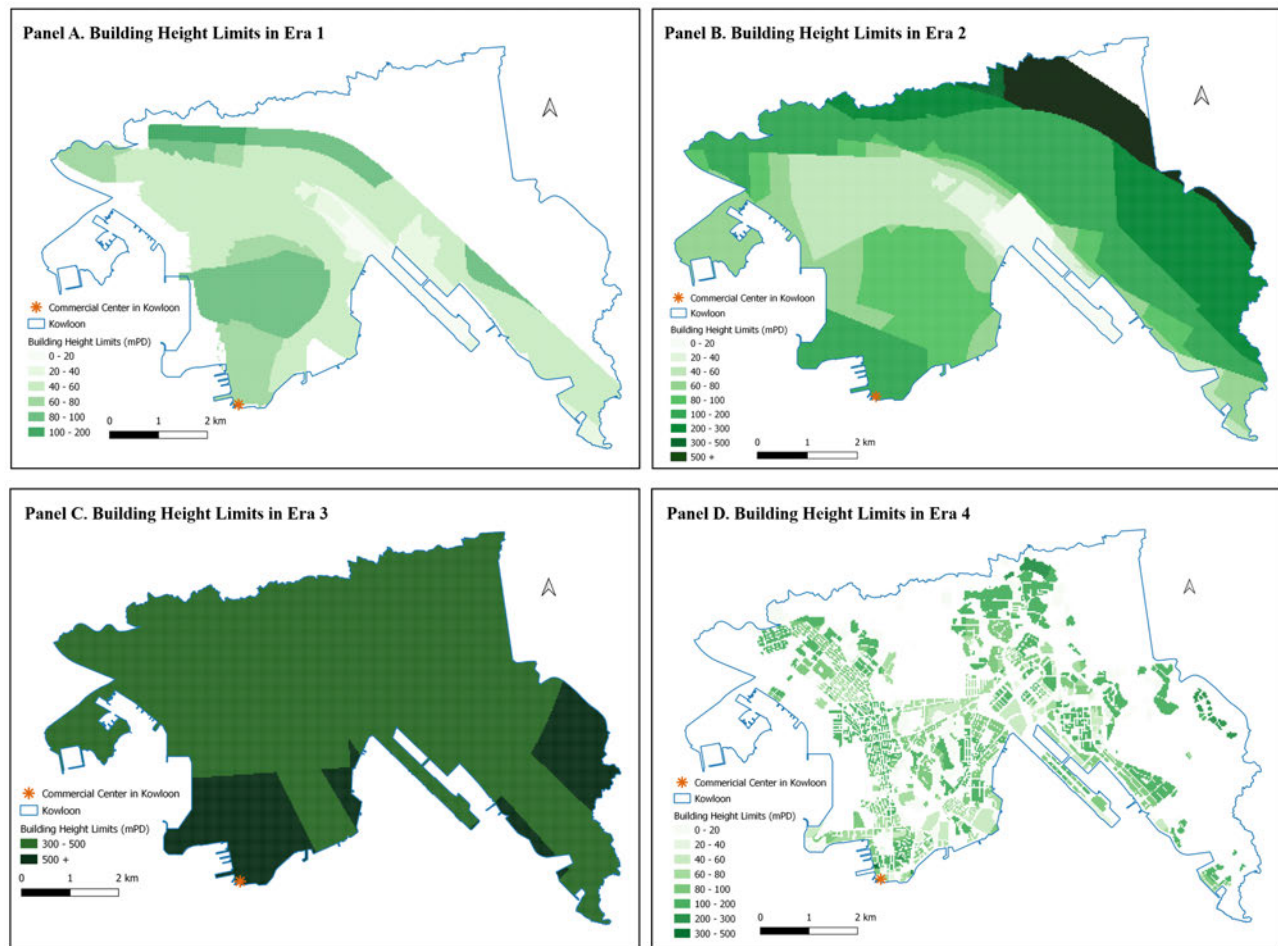
Notes: Each column presents results from a separate regression estimated using Equation (4). For each regression, "1 {Inside the Flight Path}, Early Era 2" reports the coefficient β_1 , which captures the differences in outcome variable across the borders during early Era 2 (1991-1994). "1 {Inside the Flight Path}, Late Era 2" reports the sum of β_1 and β_4 (representing the only post-period interaction), capturing the differences across the borders during late Era 2 (1995-1998). Column (1) includes controls for flat quality, such as building age, number of bedrooms, and number of living rooms, as detailed in Table A2. Column (2) excludes these quality controls. Columns (3) and (4) include only design controls. All regressions include both border and year fixed effects. The sample consists of flat transactions within 360 meters of the border during the period from 1991 to July 9, 1998, excluding a 60-meter donut just outside the flight path border. Standard errors, clustered at the 150-by-150-meter grid square level, are reported in parentheses.

*** p<0.01, ** p<0.05, * p<0.1

Appendix A Figures and Tables

A1. Figures

Figure A.1: Building Height Limits in Kowloon Across Different Eras



Notes: Panel A displays the building height limits enforced in Era 1 (1957-1989). Panel B shows the building height limits in Era 2 (1989-1998), right before the airport relocation. These height limits were completely removed after the airport relocation. Panel C illustrates the building height limits enforced in Era 3 (1998-2008), associated with the operation of the new airport. Panel D presents the building height limits only for land lots specifically regulated by the outline zoning plans in Era 4 (2008-present). In all four maps, the white areas within Kowloon indicate regions without specified and enforced building height limits during the corresponding era. In Era 1, the white areas along the western coastline were uninhabited oceans before extensive land reclamation. The white areas in the northeastern part of the map are mountainous regions.

Figure A.2: Binding Status of Height Limits in a Neighborhood Block

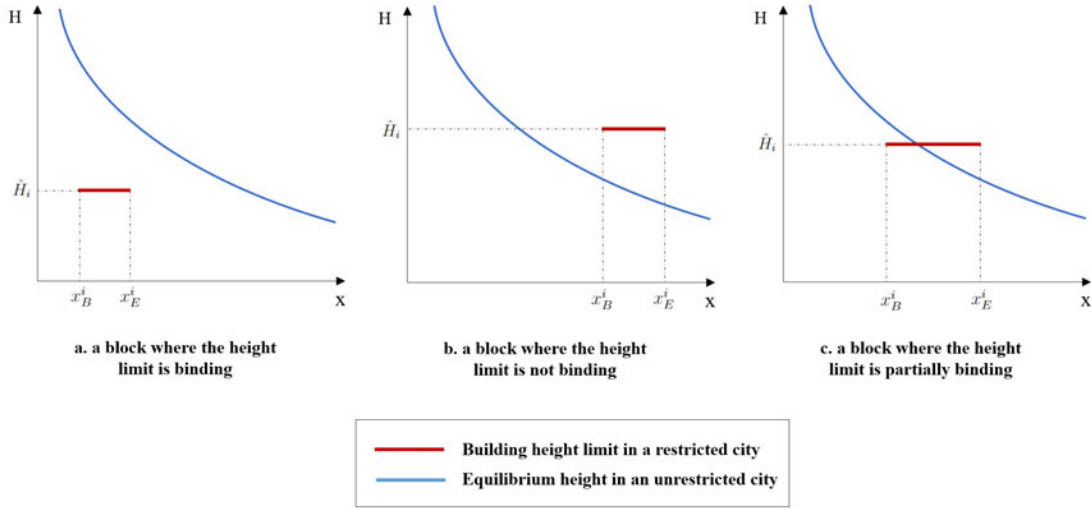
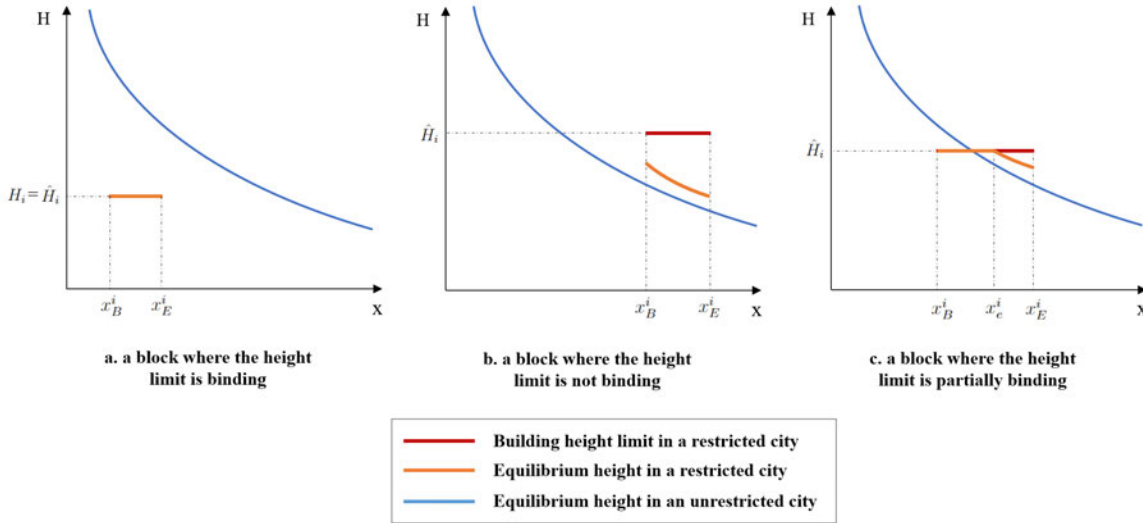
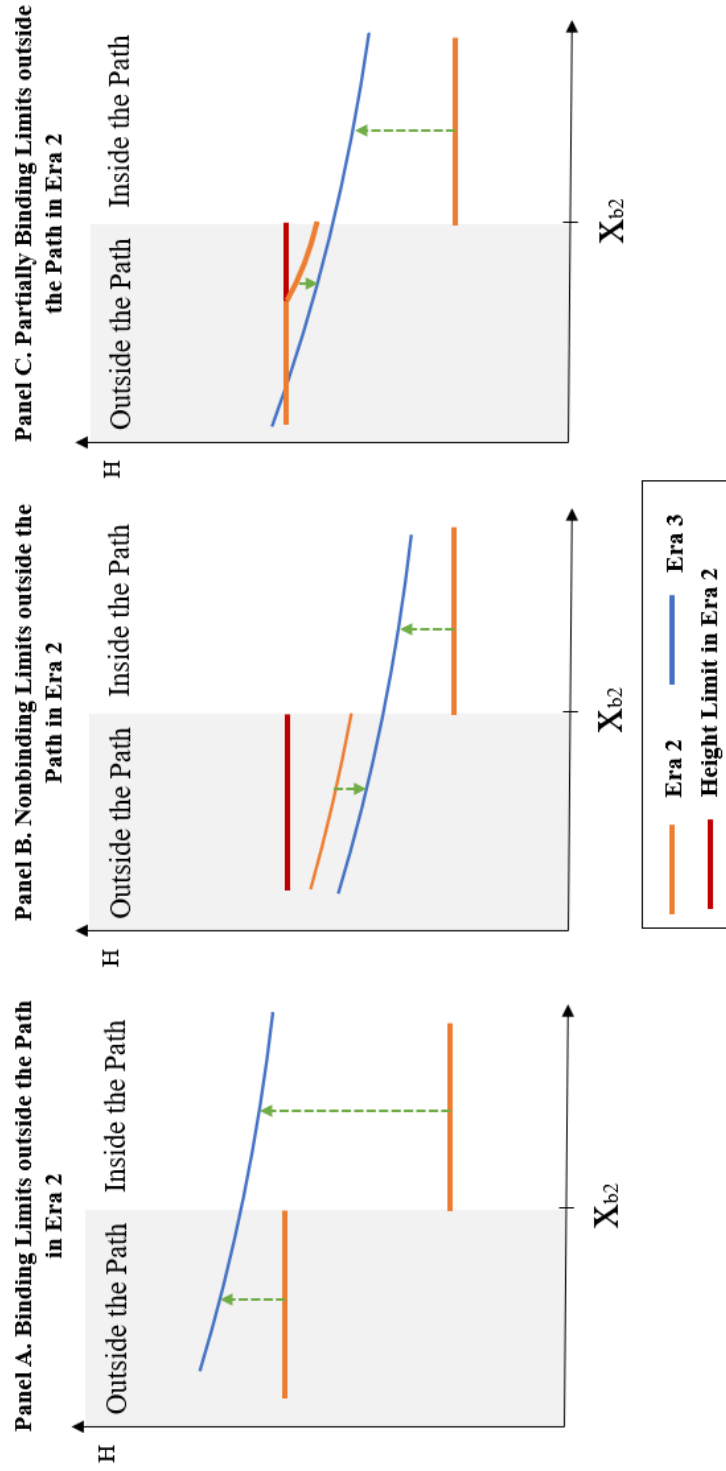


Figure A.3: Building Heights in Different Neighborhoods (Equilibrium with and without Height Limits)



Notes: \hat{H}_i represents the height limit enforced in the neighborhood block i , while H_i denotes the equilibrium height that developers choose to build in block i . x_B^i denotes the value of x where neighborhood block i begins, and x_E^i denotes the value of x where neighborhood block i ends ($x_B^i < x_E^i$). Additionally, the point x_e^i indicates the transition point where the height limit changes from binding to nonbinding ($x_e^i \in [x_B^i, x_E^i]$) in a neighborhood block i . In Panel c, within x_B^i and x_e^i , developers will construct buildings at the height limit; beyond x_e^i up to x_E^i , building heights remain below the height limits but higher than those in the unrestricted city.

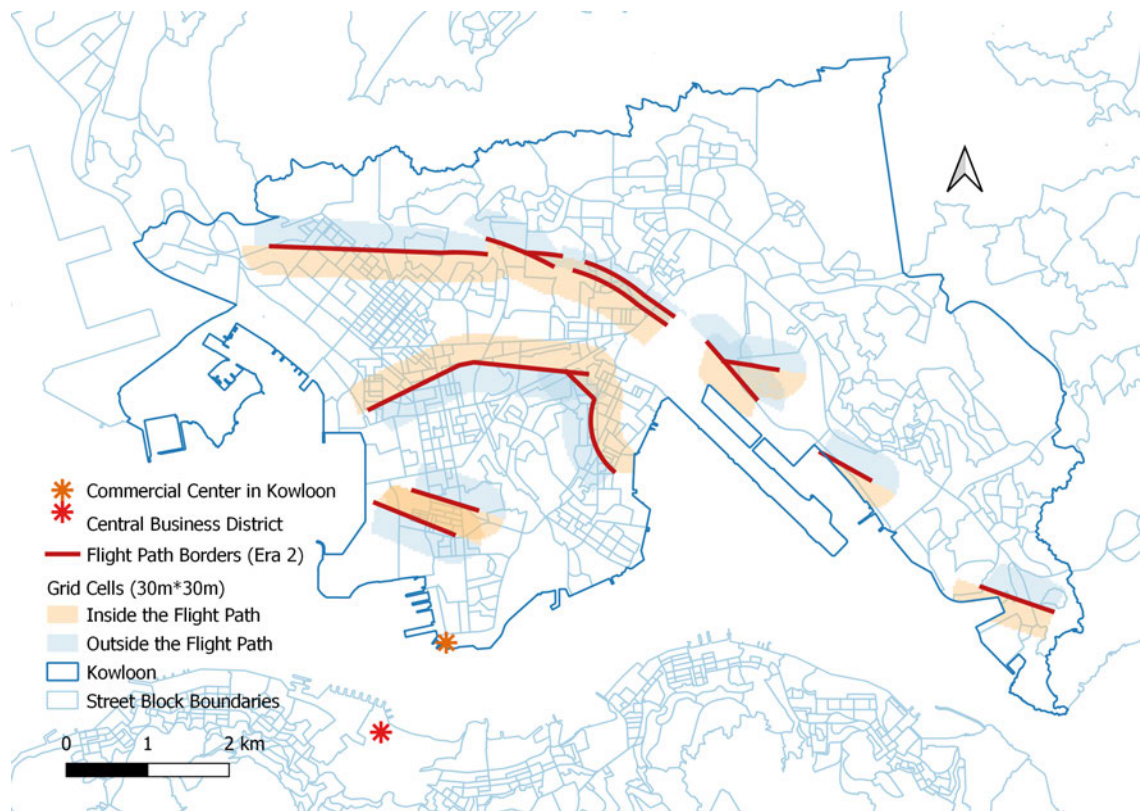
Figure A.4: Equilibrium Building Height across the Borders Before and After the Second Upzoning in 1998 Under Binding, Nonbinding, and Partially Binding Height Limits Outside the Path in Era 2



X_{b2} : Location of updated flight path borders in Era 2

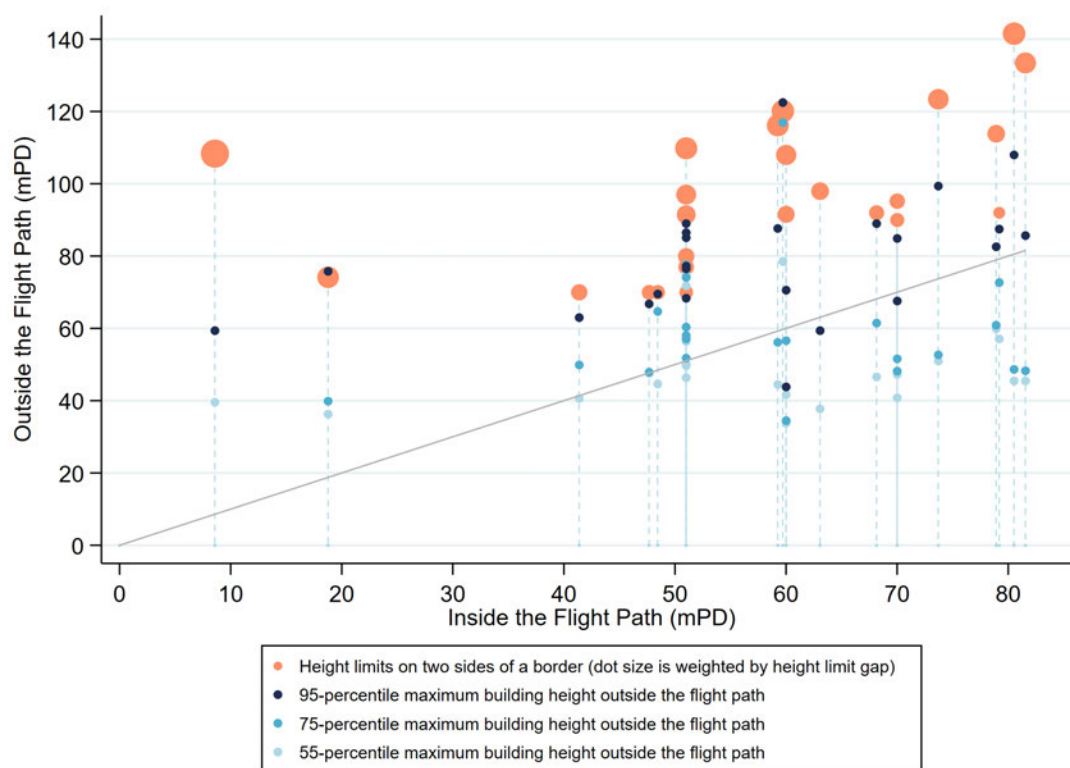
Notes: This figure shows the relative equilibrium building heights on both sides of the updated flight path borders of Era 2, denoted by x_{b2} , before and after the second upzoning in 1998, along with the associated changes. In Era 2, within the updated flight path, the height limits are assumed to be binding. Outside the updated flight path, the height limits can be one of three scenarios: binding (Panel A), nonbinding (Panel B), or partially binding (Panel C). Regardless of the scenario, neighborhoods inside the updated flight path are expected to experience a greater increase in equilibrium building heights following the second upzoning.

Figure A.5: Flight Path Borders in Era 2 that Satisfy All Criteria



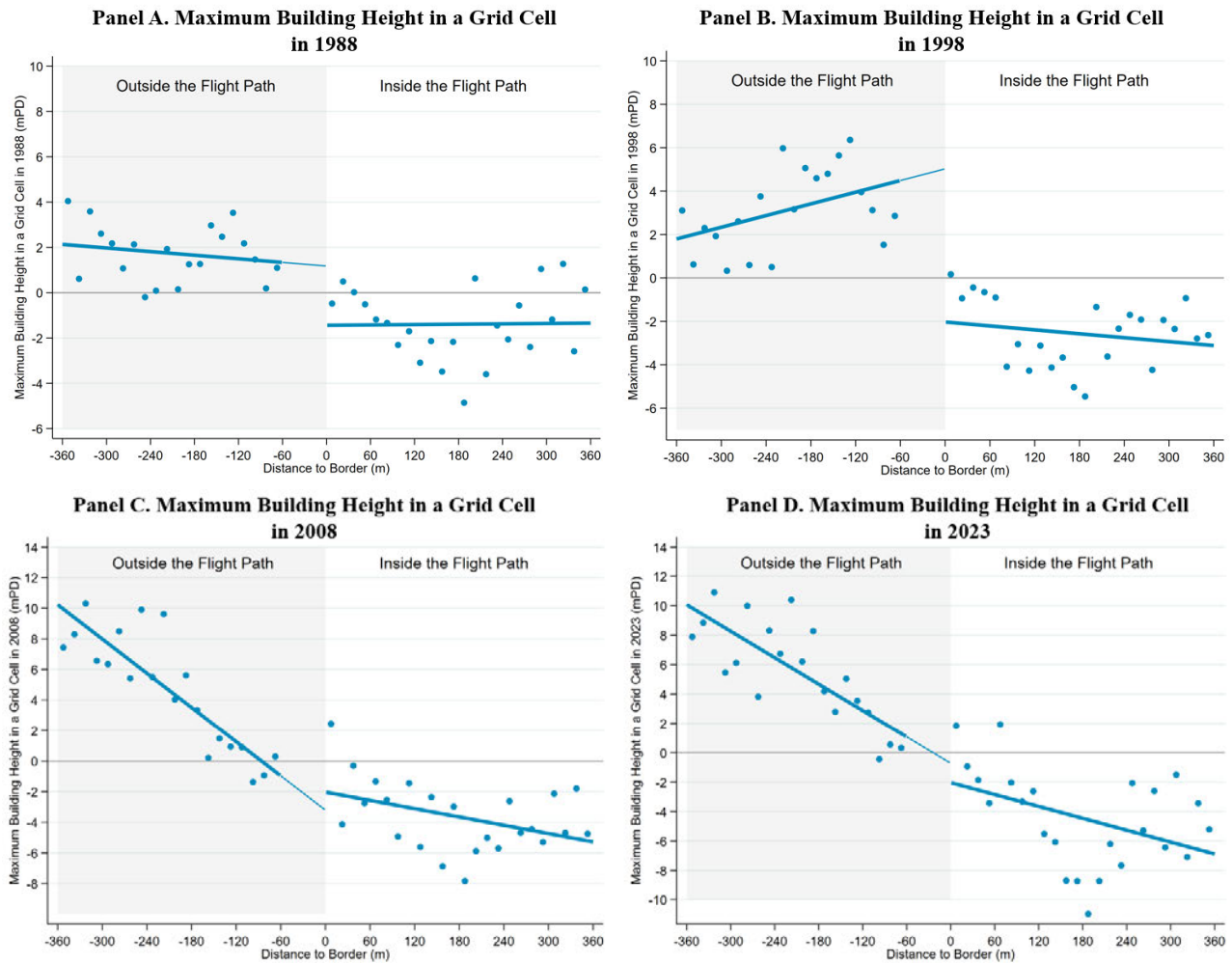
Notes: This figure plots all the 24 flight path borders in Era 2 that satisfy the following three criteria: 1) flight path borders that demarcate zones with a distinct difference in building height limits exceeding 10 meters in Era 2; and 2) the stricter side of the border must have a height limit of less than 80 meters; 3) the borders do not overlap with parks, depots, or oceans.

Figure A.6: Building Height Limits and Actual Building Height by Each Border in Era 2



Notes: This figure offers a detailed comparison of height limit and maximum building height for each updated flight path border in Era 2, illustrating the extent to which these borders were binding. Each orange dot represents a selected border, with the x-axis showing the building height limits inside the flight path and the y-axis showing the limits outside in Era 2. The size of each dot is weighted by the gap in height limits between the two sides of the border. The grey line indicates where the height limits on both sides of the border are equal. As shown, the height limits outside the flight path are consistently 10 to 90 meters higher than those inside, in accordance with my border selection criteria, which require a gap of more than 10 meters in height limits on either side of the border. Small blue dots are plotted on the vertical line connecting each orange dot with its corresponding x-axis value, representing different percentiles of maximum building height outside the flight path for each border in Era 2. The darkest blue dot represents the 95th percentile of maximum building height outside the flight path. Notably, most of these darkest blue dots are above the grey line, indicating that the height limits inside the flight path are binding, as developers chose to build taller in nearby neighborhoods just outside the flight path. Additionally, some of these darkest blue dots are close to or at the height limit outside the flight path, while others fall significantly below it, suggesting that the height limits outside the flight path are either binding or non-binding, depending on the case.

Figure A.7: Maximum Building Height in a Grid Cell around Borders in Each Era



Notes: This figure shows the predicted regression lines and the binned-average residuals, estimated using Equation (3), for maximum building height in a grid cell in 1988, 1998, 2008 and 2023, corresponding to Eras 1, 2, 3 and 4, respectively. The sample includes a 360-meter bandwidth on either side of the border, excluding a 60-meter donut just outside the flight path borders.

A2. Tables

Table A1: Summary Statistics for Building Sample

	Outside the Flight Path	Inside the Flight Path	Full Sample
	Mean	Mean	Mean
	(1)	(2)	(3)
<i>Characteristics</i>			
Distance to border (m)	206.227	177.041	190.077
Distance to metro (m)	593.571	652.576	626.222
Distance to coastline (m)	1108.522	1078.683	1092.011
Slope (degree)	5.12	3.132	4.02
Elevation (mPD)	21.641	13.234	16.989
Distance to CBD (m)	4170.912	4069.648	4114.876
Distance to the downtown airport (m)	1916.065	1917.079	1916.626
<i>Dependent Variables</i>			
<i>In 1988</i>			
Max. bldg. height (mPD)	25.399	24.074	24.666
Bldg. footprint (m ²)	185.772	200.041	193.668
Bldg. volume (m ³)	6790.065	6741.46	6763.169
<i>In 1998</i>			
Max. bldg. height (mPD)	31.233	26.713	28.732
Bldg. footprint (m ²)	212.188	226.37	220.036
Bldg. volume (m ³)	8988.106	8011.143	8447.494
<i>In 2008</i>			
Max. bldg. height (mPD)	40.353	32.854	36.203
Bldg. footprint (m ²)	247.86	248.896	248.433
Bldg. volume (m ³)	13126.894	9690.133	11225.127
<i>In 2023</i>			
Max. bldg. height (mPD)	48.788	38.488	43.088
Bldg. footprint (m ²)	272.069	270.492	271.197
Bldg. volume (m ³)	15440.85	11097.972	13037.673
Observations	5,177	6,414	10,591

Notes: This table reports the summary statistics of the key characteristics and dependent variables used in the main building footprint sample. The unit of observation is a 30m × 30m grid cell. Column (1) reports the sample mean for grid cells located within a 360-meter bandwidth on the less strict side of the border (outside the Era 2 flight path), excluding a 60-meter donut. Column (2) reports the sample mean for grid cells located within a 360-meter bandwidth on the stricter side of the border (inside the Era 2 flight path). Column (3) reports the overall sample mean. "mPD" refers to meters above the Hong Kong Principal Datum.

Table A2: Summary Statistics for Flat Transactions Sample

	Outside the Flight Path	Inside the Flight Path	Full Sample
	Mean	Mean	Mean
	(1)	(2)	(3)
Dependent Variable			
Asset price per sq ft of floor space (in HKD millions/sq ft)	.005	.004	.004
Design Features			
Distance to border (m)	223.18	188.695	202.908
Slope (degree)	2.435	1.241	1.733
Elevation (mPD)	9.875	7.567	8.518
Distance to CBD (m)	2779.425	2950.225	2879.83
Distance to the downtown airport (m)	2568.283	2090.828	2287.61
	602.049		
Flat Size Features			
Unit size (sq ft)	602.049	496.096	539.764
Dummy (using gross rather than net size)	.213	.137	.169
With a carpark	.057	.036	.044
Dummy (missing carpark info)	.234	.276	.259
With multiple floors	.004	.002	.003
Flat Quality Features			
Building age	15.619	20.082	18.243
Number of bedrooms	1.31	.676	.938
Dummy (missing bedrooms info)	.463	.682	.592
Number of living rooms	.972	.562	.731
Dummy (missing living rooms info)	.465	.684	.594
Unit floor	16.009	10.861	12.983
Dummy (missing floor info)	.001	0	0
With a clubhouse in the building	.337	.211	.263
With a swimming pool in the building	.333	.203	.256
Dummy (missing club house/swimming pool info)	.331	.462	.408
Dummy (first-hand transactions)	.202	.154	.174
Access to Public Facilities			
Distance to coastline (m)	838.271	819.972	827.514
Distance to MTR (m)	370.452	341.046	353.165
Distance to bus station (m)	82.714	83.57	83.217
Distance to green minibus station (m)	231.383	225.45	227.895
Distance to public primary school (m)	222.709	201.835	210.438
Distance to private primary school (m)	461.954	396.371	423.401
Distance to public secondary school (m)	294.625	324.788	312.357
Distance to private secondary school (m)	465.727	320.31	380.243
Distance to university (m)	573.295	756.207	680.82
Distance to park (m)	977.279	847.556	901.021
Distance to recreational ground (m)	260.359	252.478	255.726
Distance to street market (m)	408.925	373.149	387.894
Distance to health centers (m)	475.871	414.877	440.015
Distance to general clinics (m)	445.243	409.703	424.351
Distance to hospital (m)	788.467	864.745	833.307
Distance to specialist clinics (m)	669.435	757.614	721.271
Observations	47,156	67,259	114,415

Notes: This table presents the summary statistics of the key dependent variables and control variables used in the main private residential flat transactions sample from 1991 to 2020. The sample includes only borders with a minimum of 30 transactions on each side in Eras 2, 3, and 4. Each unique transaction serves as the unit of observation. Column (1) displays the sample mean for transactions located within a 360-meter bandwidth on the less strict side of the border (outside the Era 2 flight path), excluding a 60-meter donut. Column (2) displays the sample mean for transactions located within a 360-meter bandwidth on the stricter side of the border (inside the Era 2 flight path). Column (3) displays the overall sample mean.

Appendix B Theoretical Model

B1. City with Spatially Varying Building Height Limits

Let x_B^i denote the value of x where neighborhood block i begins, and x_E^i denote the value of x where neighborhood block i ends ($x_B^i < x_E^i$). Additionally, introduce a point x_e^i to indicate the transition point where the height limit changes from binding to nonbinding ($x_e^i \in [x_B^i, x_E^i]$) in a neighborhood block i . And There are n such blocks in the city, each with a fixed height limit of \hat{H}_i . Let u_m and \bar{x}_m represent the equilibrium utility and the distance from the periphery to the city center, respectively, for the city with spatially varying building height restrictions. The equilibrium conditions are given by the following:

$$r(\bar{x}_m, u_m) = r_a \quad (\text{B.1})$$

$$H_i(S(x_e^i, u_m)) = \hat{H}_i \quad (\text{B.2})$$

$$\sum_{i=1}^n \left(\int_{x_B^i}^{x_e^i} \theta x \frac{w \hat{H}_i}{\gamma q(x, u_m)} dx + \int_{x_e^i}^{x_E^i} \theta x \frac{w H_i(x, u_m)}{\gamma q(x, u_m)} dx \right) = N \quad (\text{B.3})$$

Specifically, Equation (B.2) stipulates that the building height freely chosen by developers at $x = x_e^i$, which is determined by the chosen structural density $S(x_e^i, u_m)$, equals the restricted building height \hat{H}_i enforced in this neighborhood block. This defines the point where the height limit becomes binding in neighborhood block i . When the entire neighborhood block is binding, x_e^i coincides with x_B^i , implying that $H_i = \hat{H}_i$ in the entire block. When the entire neighborhood block is nonbinding, $x_e^i = x_E^i$, indicating that no such transition point exists within this block.

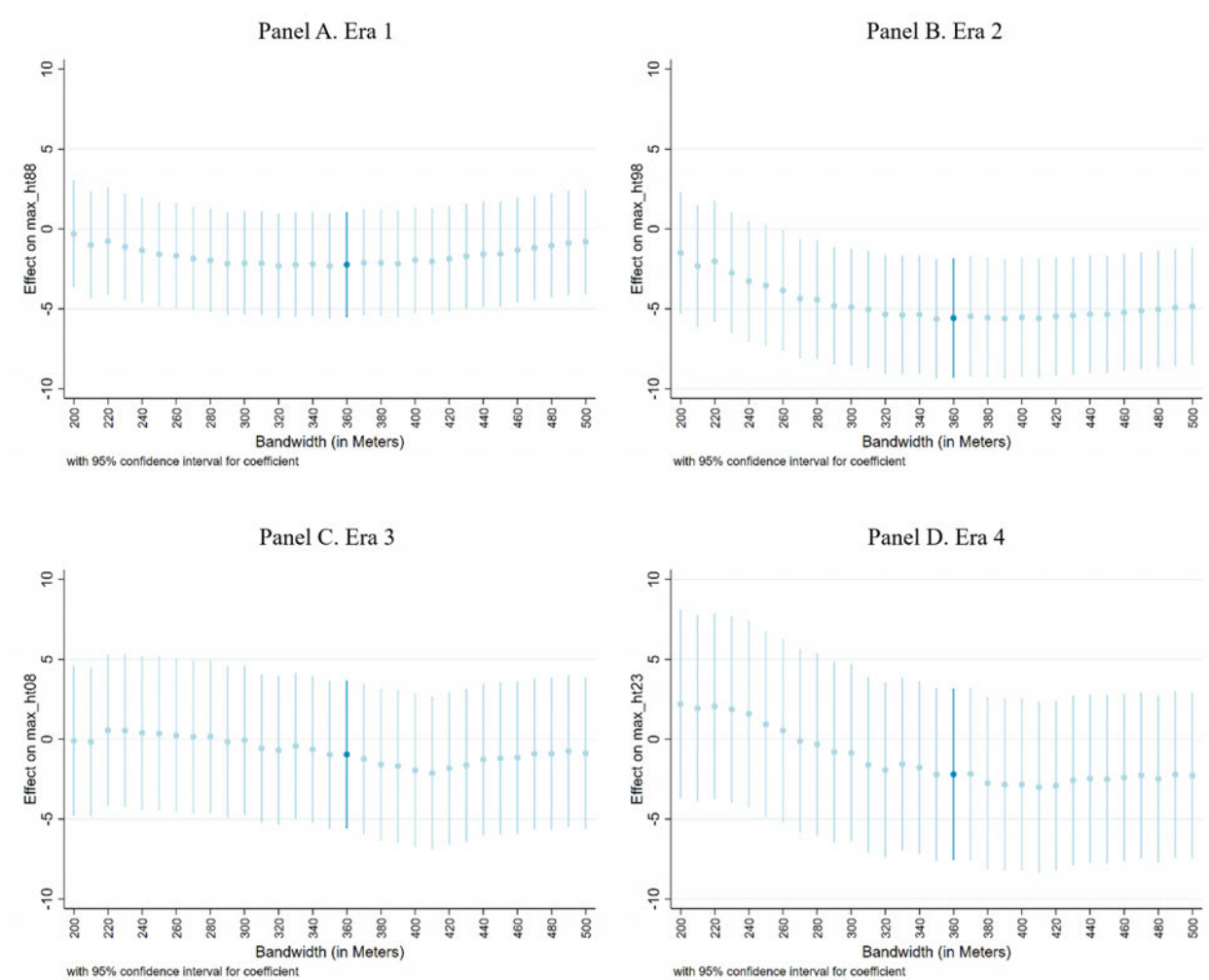
In Equation (B.3), the first integral sums up the population living in the parts of neighborhood blocks where the height limit is binding (from x_B^i to x_e^i), and the second integral sums up the population living in the parts of neighborhood blocks where the height limit is not binding (from x_e^i to x_E^i). The sum of these integrals equals the total population in the city. Note that when the entire neighborhood block is binding, x_e^i equals x_B^i , and thus the distance from x_e^i to x_B^i is 0, making the second integral for this neighborhood 0. Conversely, when the entire neighborhood block is not binding, x_e^i equals x_E^i , and thus the distance from x_B^i to x_e^i is 0, making the first integral for this neighborhood 0. Equation (B.3) can be considered a general form of Equation (2) in

the main text of the paper. If there are no binding building height limits in any of the neighborhood blocks, Equation (B.3) simplifies to Equation (2).

Appendix C Robustness

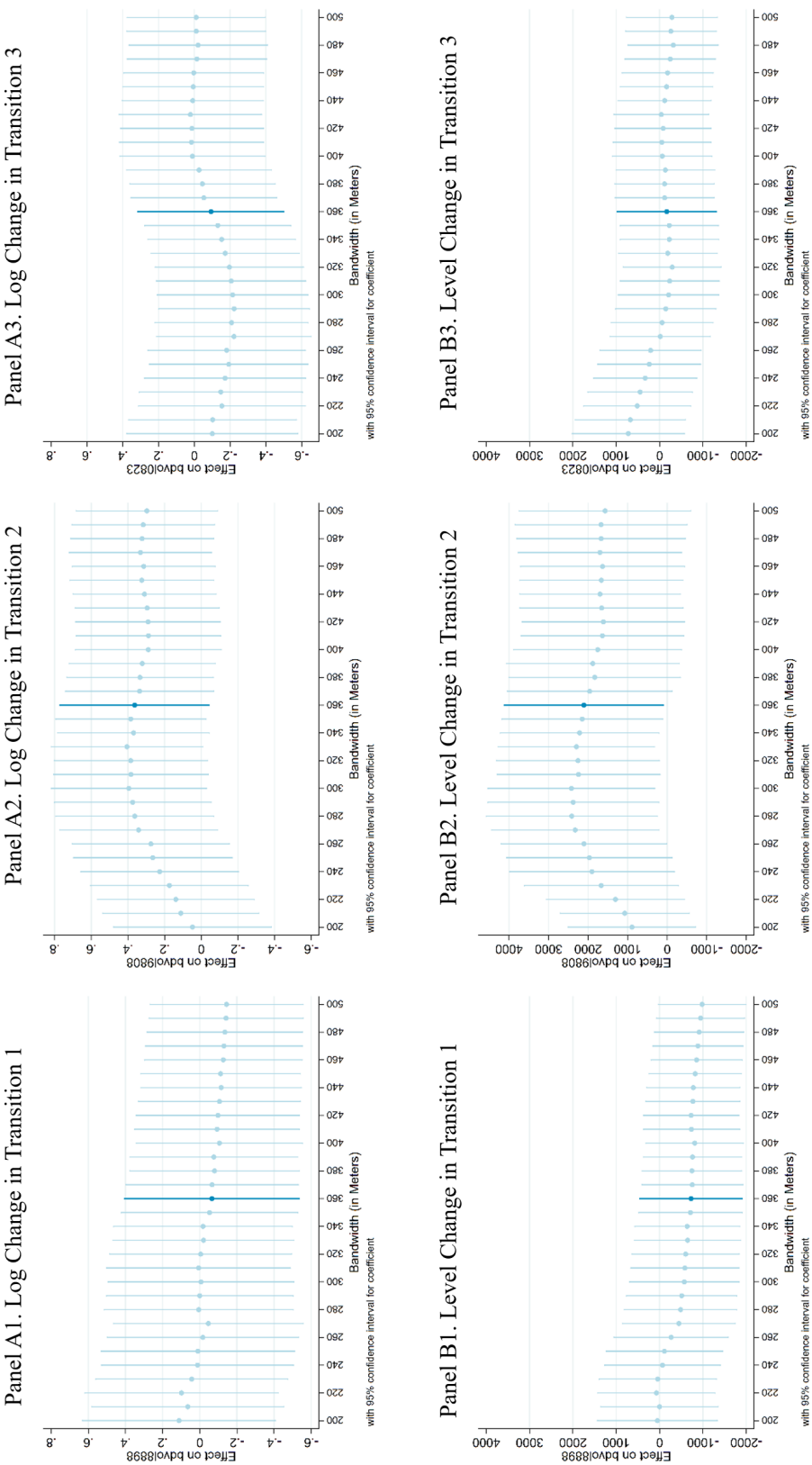
C1. Figures

Figure C.1: Robustness to the Selection of Bandwidth: Maximum Building Height



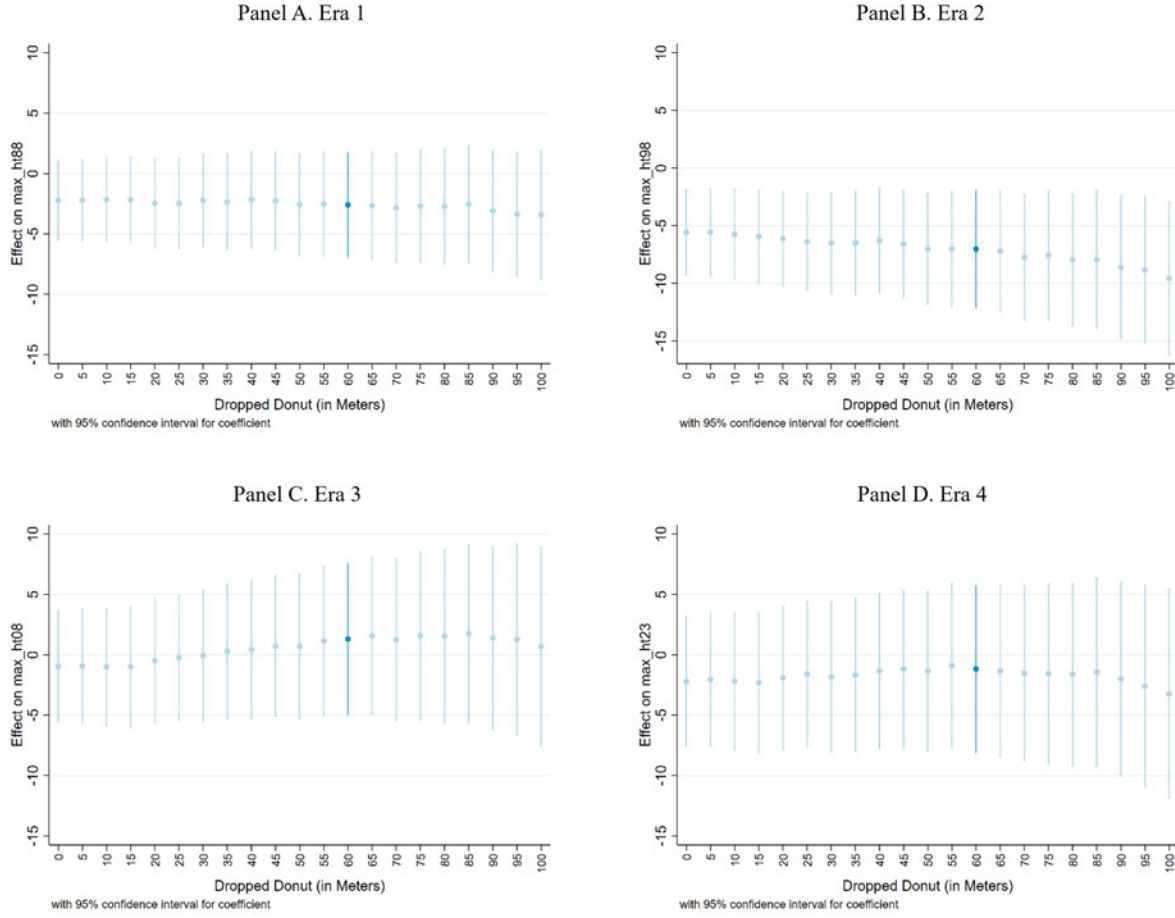
Notes: These figures illustrate the sensitivity of the coefficient β_1 from Equation (3) to various bandwidth selections. The dark blue dot and line represent the benchmark estimate and its confidence interval, with a bandwidth of 360 meters. Panel A displays the estimate using the maximum building height in a grid cell in Era 1, while Panels B, C, and D show the estimates using the maximum building height in a grid cell in Eras 2, 3, and 4, respectively.

Figure C.2: Robustness to the Selection of Bandwidth: Changes in Building Volume



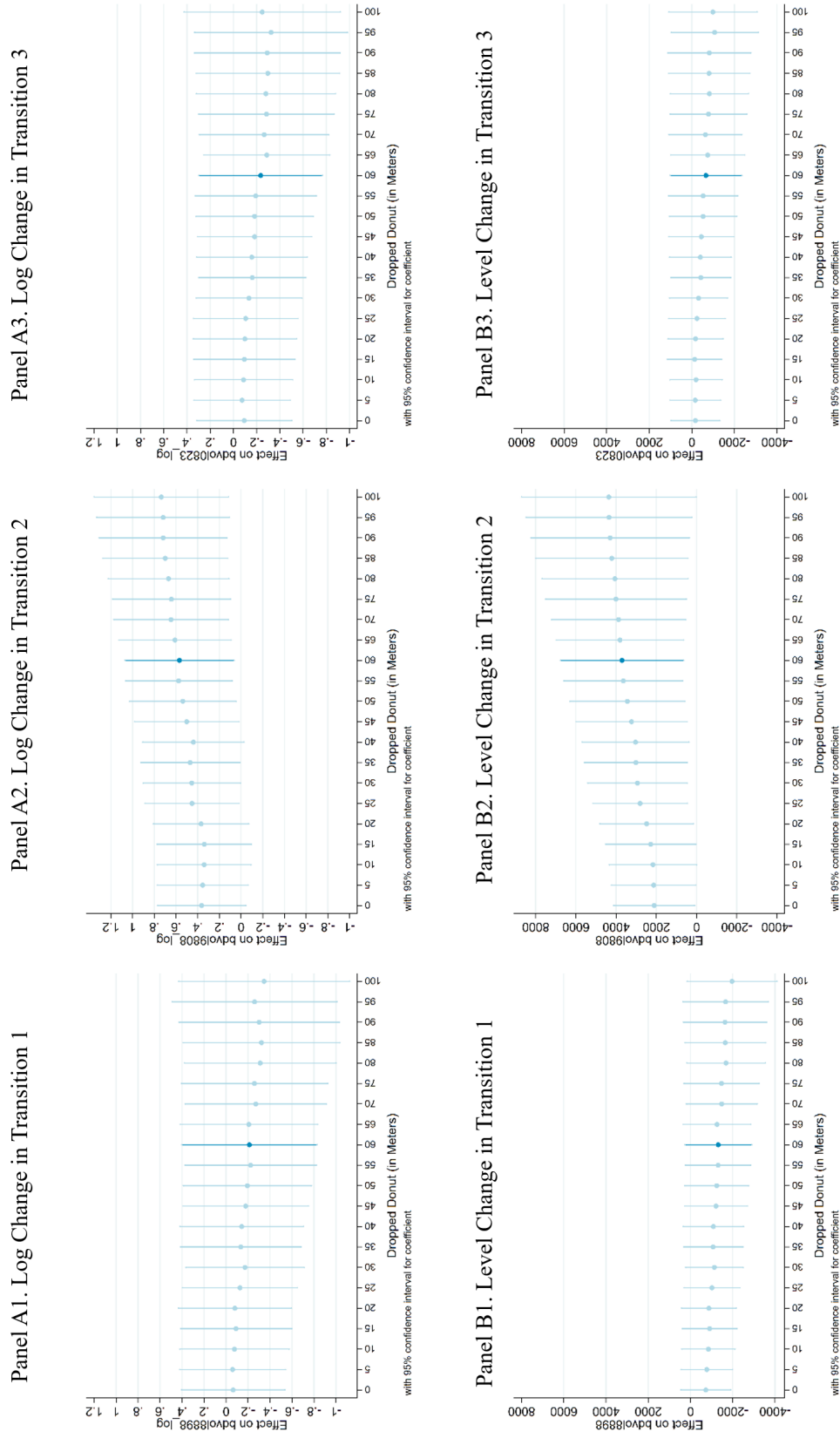
Notes: These figures illustrate the sensitivity of the coefficient β_1 from Equation (3) to various bandwidth selections. The dark blue dot and line represent the benchmark estimate and its confidence interval, with a bandwidth of 360 meters. Panels A1 to A3 display the estimates using the log changes in building volume in a grid cell in Transitions 1, 2, and 3, respectively. Panels B1 to B3 show the estimates using the level changes in building volume in a grid cell in Transitions 1, 2, and 3, respectively.

Figure C.3: Robustness to Excluded Donut Sizes: Maximum Building Height



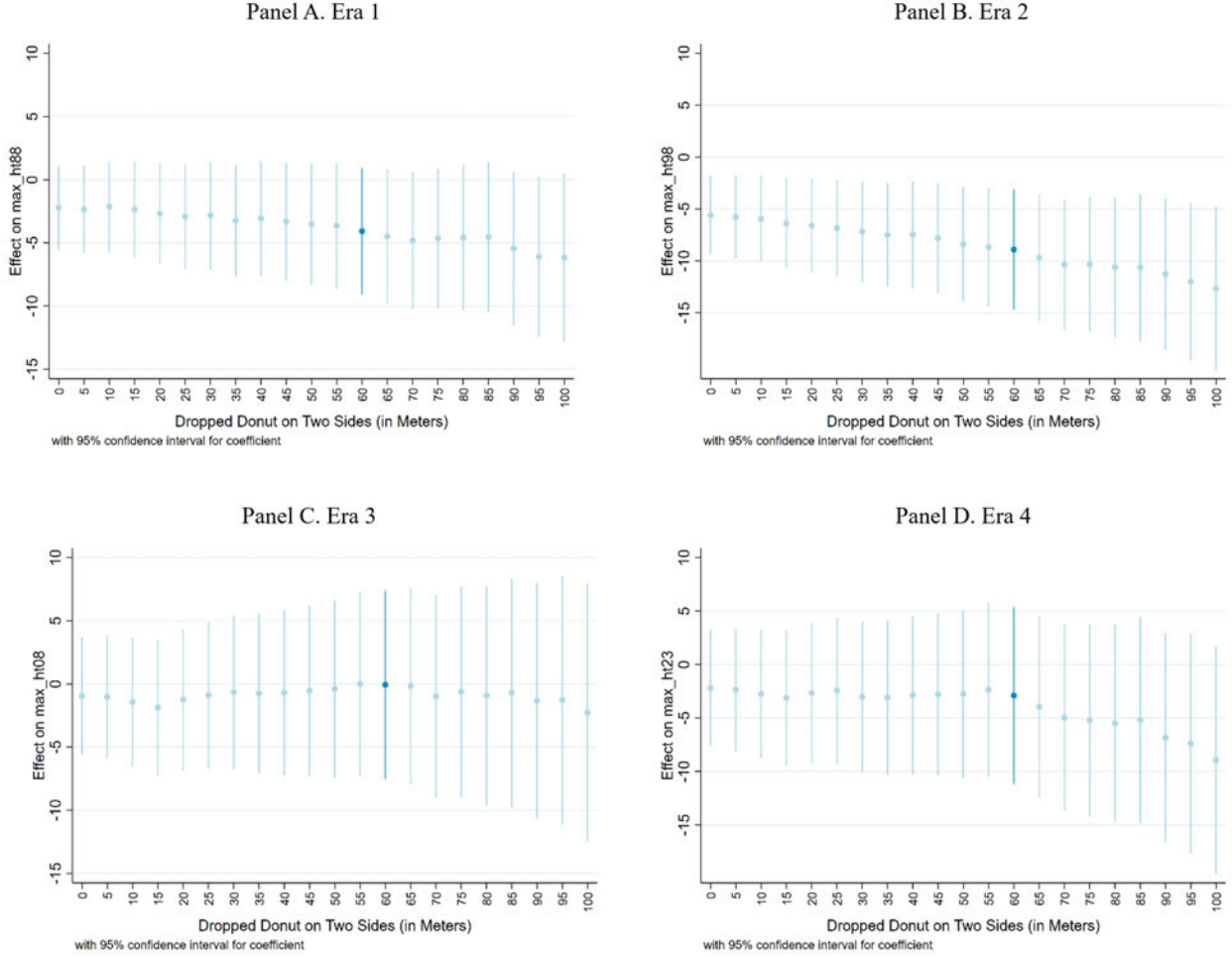
Notes: These figures illustrate the sensitivity of the coefficient β_1 from Equation (3) to various excluded donut sizes. The dark blue dot and line represent the benchmark estimate and its confidence interval, with a bandwidth of 360 meters and an excluded donut size of 60 meters just outside the flight path. Panel A displays the estimate using the maximum building height in a grid cell in Era 1, while Panels B, C, and D show the estimates using the maximum building height in a grid cell in Eras 2, 3, and 4, respectively.

Figure C.4: Robustness to Excluded Donut Sizes: Changes in Building Volume



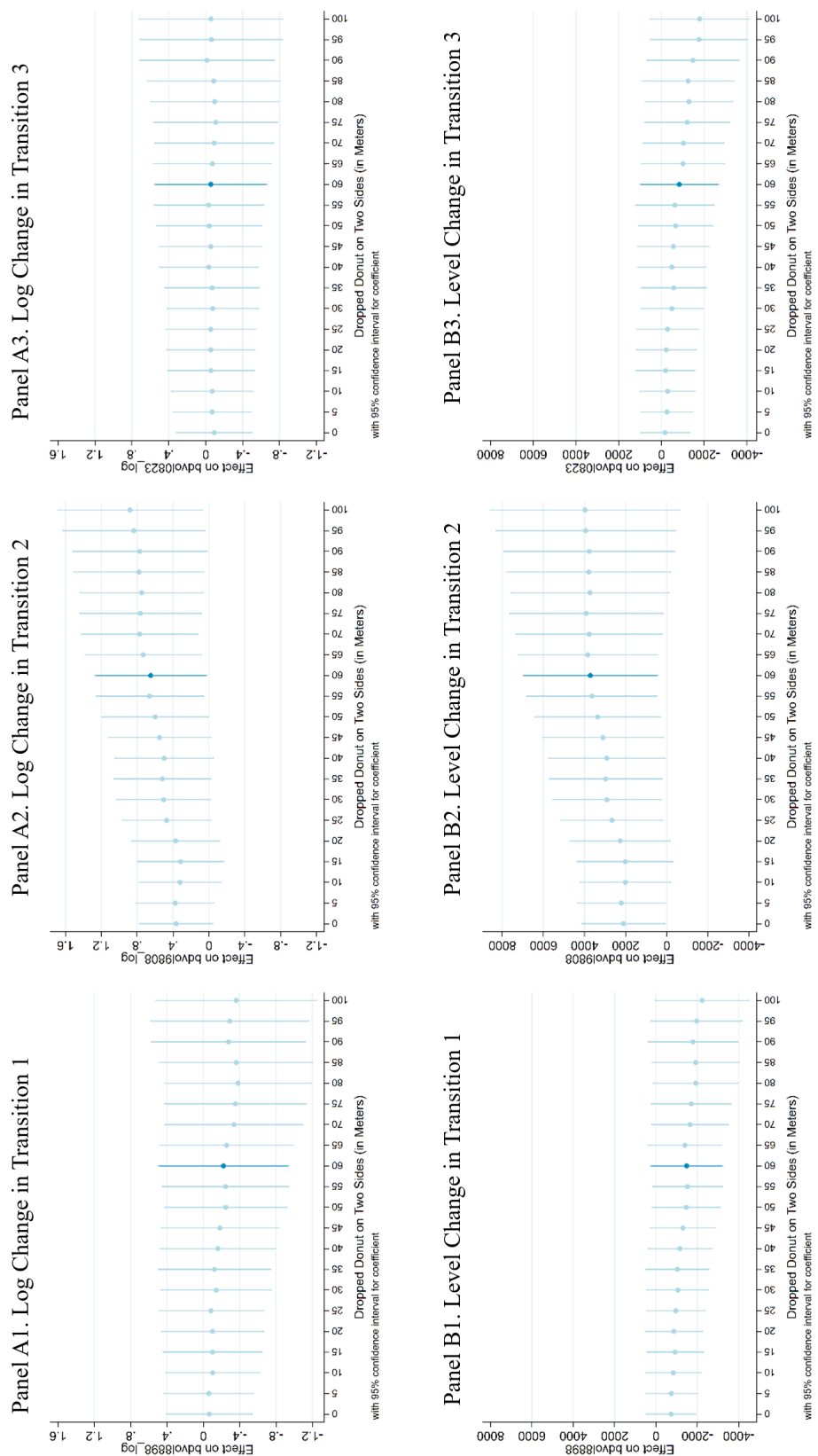
Notes: These figures illustrate the sensitivity of the coefficient β_1 from Equation (3) to various excluded donut sizes. The dark blue dot and line represent the benchmark estimate and its confidence interval, with a bandwidth of 360 meters and an excluded donut size of 60 meters just outside the flight path. Panels A1 to A3 display the estimates using the log changes in building volume in a grid cell in Transitions 1, 2, and 3, respectively. Panels B1 to B3 show the estimates using the level changes in building volume in a grid cell in Transitions 1, 2, and 3, respectively.

Figure C.5: Robustness to Excluding Donut Zones on Both Sides of the Border: Maximum Building Height



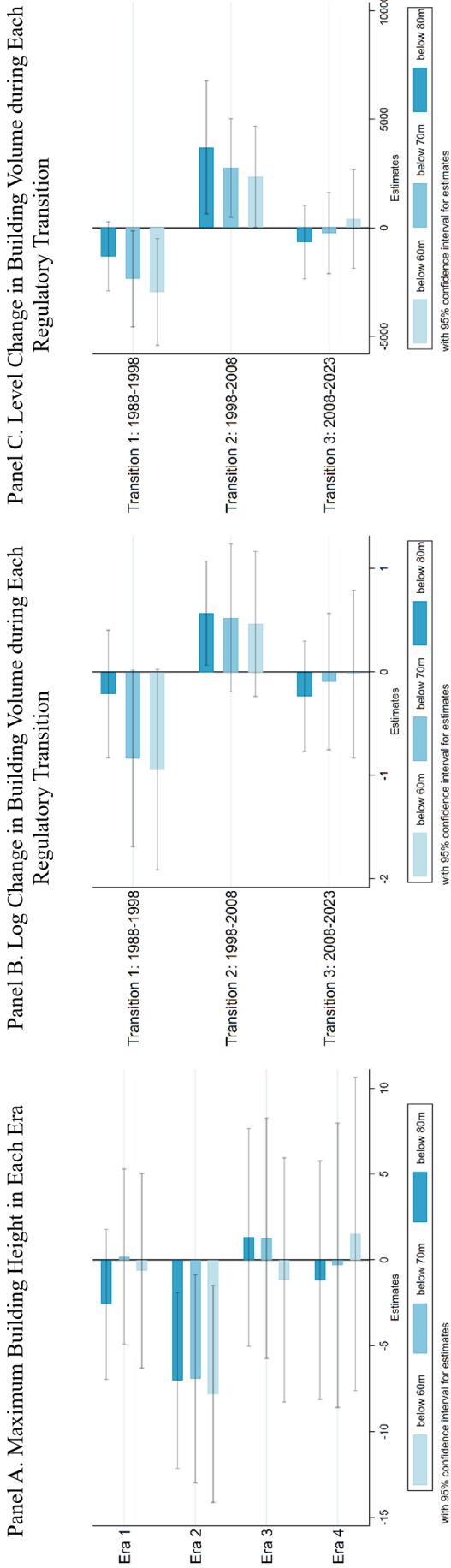
Notes: These figures illustrate the sensitivity of the coefficient β_1 from Equation (3) under various excluded donut sizes on both sides of the flight path borders. The dark blue dot and line represent the benchmark estimate and its confidence interval, using a bandwidth of 360 meters and excluding a 60-meter donut on each side of the flight path borders (totaling 120 meters). Panel A displays the estimate using the maximum building height in a grid cell in Era 1, while Panels B, C, and D show the estimates using the maximum building height in a grid cell in Eras 2, 3, and 4, respectively.

Figure C.6: Robustness to Excluding Donut Zones on Both Sides of the Border: Changes in Building Volume



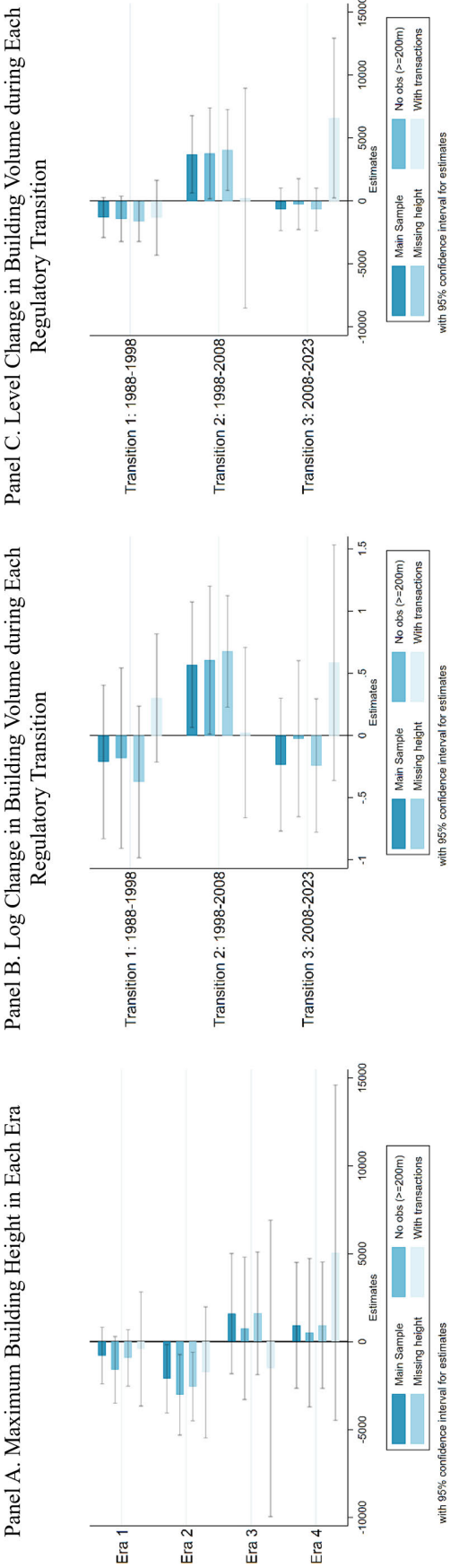
Notes: These figures illustrate the sensitivity of the coefficient β_1 from Equation (3) under various excluded donut sizes on both sides of the flight path borders. The dark blue dot and line represent the benchmark estimate and its confidence interval, using a bandwidth of 360 meters and excluding a 60-meter donut on each side of the flight path borders (totaling 120 meters). Panels A1 to A3 display the estimates using the log changes in building volume in a grid cell in Transitions 1, 2, and 3, respectively. Panels B1 to B3 show the estimates using the level changes in building volume in a grid cell in Transitions 1, 2, and 3, respectively.

Figure C.7: Robustness to Border Selection Criterion



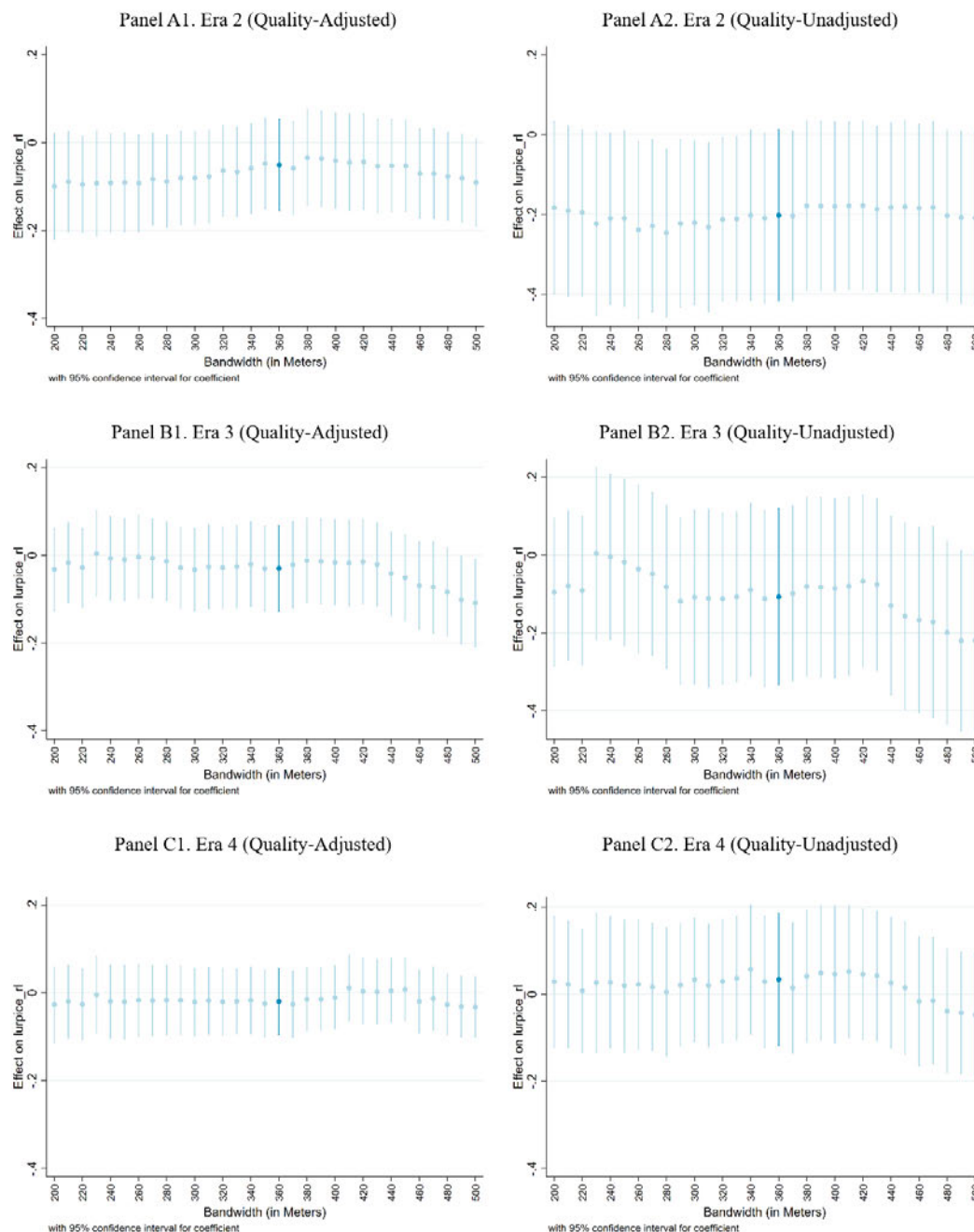
Notes: These figures illustrate the sensitivity of key estimates to the border selection criterion, specifically the height limit on the stricter side of the border (inside the flight path) set at 60, 70, or 80 meters (the main estimate uses 80 meters as the cut-off value). All the regressions use Equation (3), with a bandwidth of 360 meters and an exclusion of a 60-meter donut just outside the flight path. Panel A shows the estimate of β_1 from Equation (3), using the maximum building height in a grid cell for each era as the outcome variable. Panel B uses log changes in building volume during each regulatory transition. Panel C uses level changes in building volume during each regulatory transition.

Figure C.8: Robustness to Missing Data



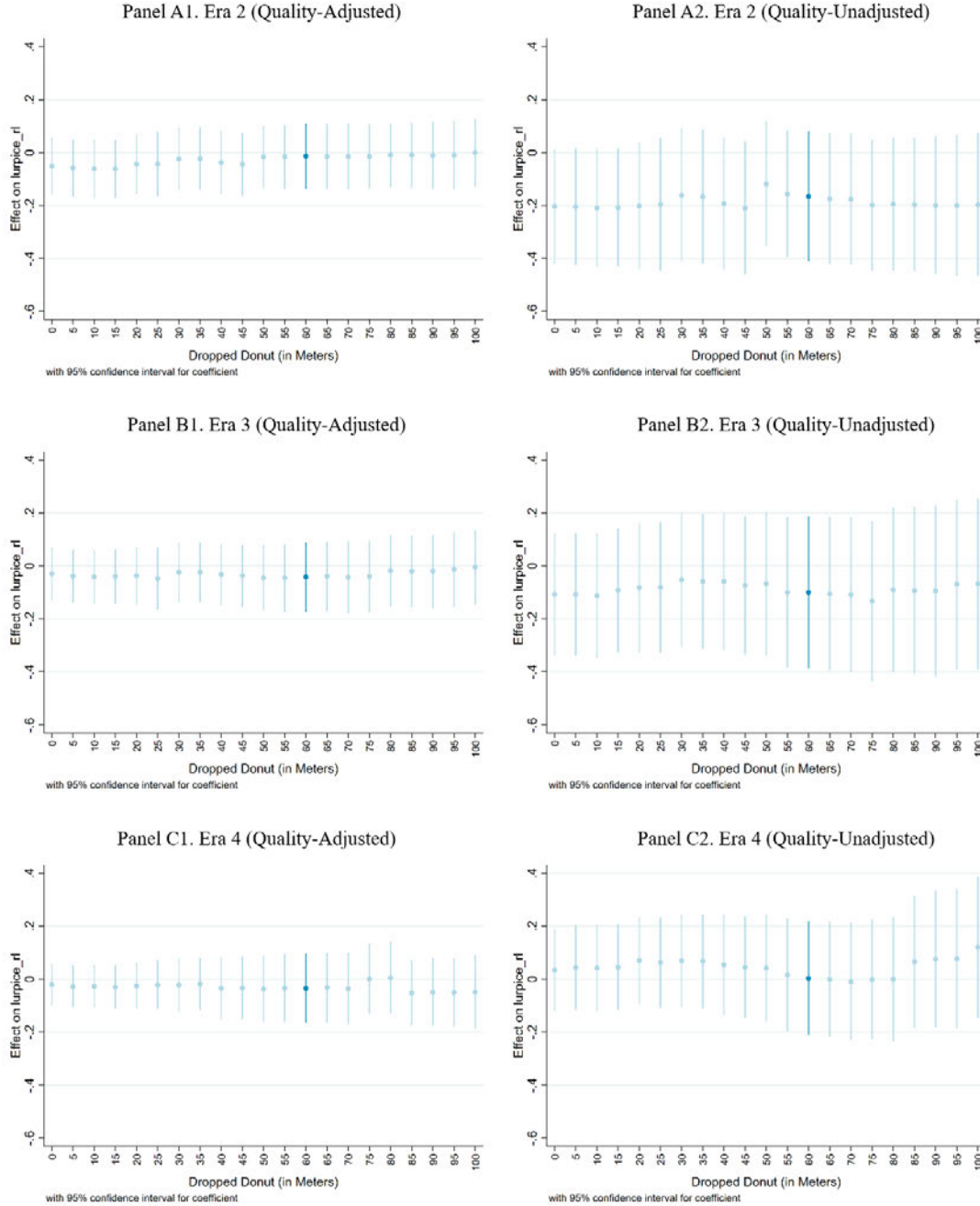
Notes: These figures illustrate the sensitivity of key estimates to missing data. All regressions use Equation (3), with a bandwidth of 360 meters and an exclusion of a 60-meter donut just outside the flight path. "No obs (>200m)" represents a sample excluding borders without observations for bandwidths larger than 200 meters (7 out of 24 selected borders have no observations beyond this distance due to the small building height limit zone). "Missing height" represents a sample excluding observations with missing building height information (in the main sample, missing height information was imputed using the average height of nearby buildings). "With transactions" represents a sample only including borders with flat transactions on both sides of the border in each Era and grid cells where flat transactions are located. Panel A shows the estimate of β_1 from Equation (3), using the maximum building height in a grid cell for each era as the outcome variable. Panel B uses log changes in building volume during each regulatory transition. Panel C uses level changes in building volume during each regulatory transition.

Figure C.9: Robustness to the Selection of Bandwidth: Log of Asset Price per sq ft of Floor Space



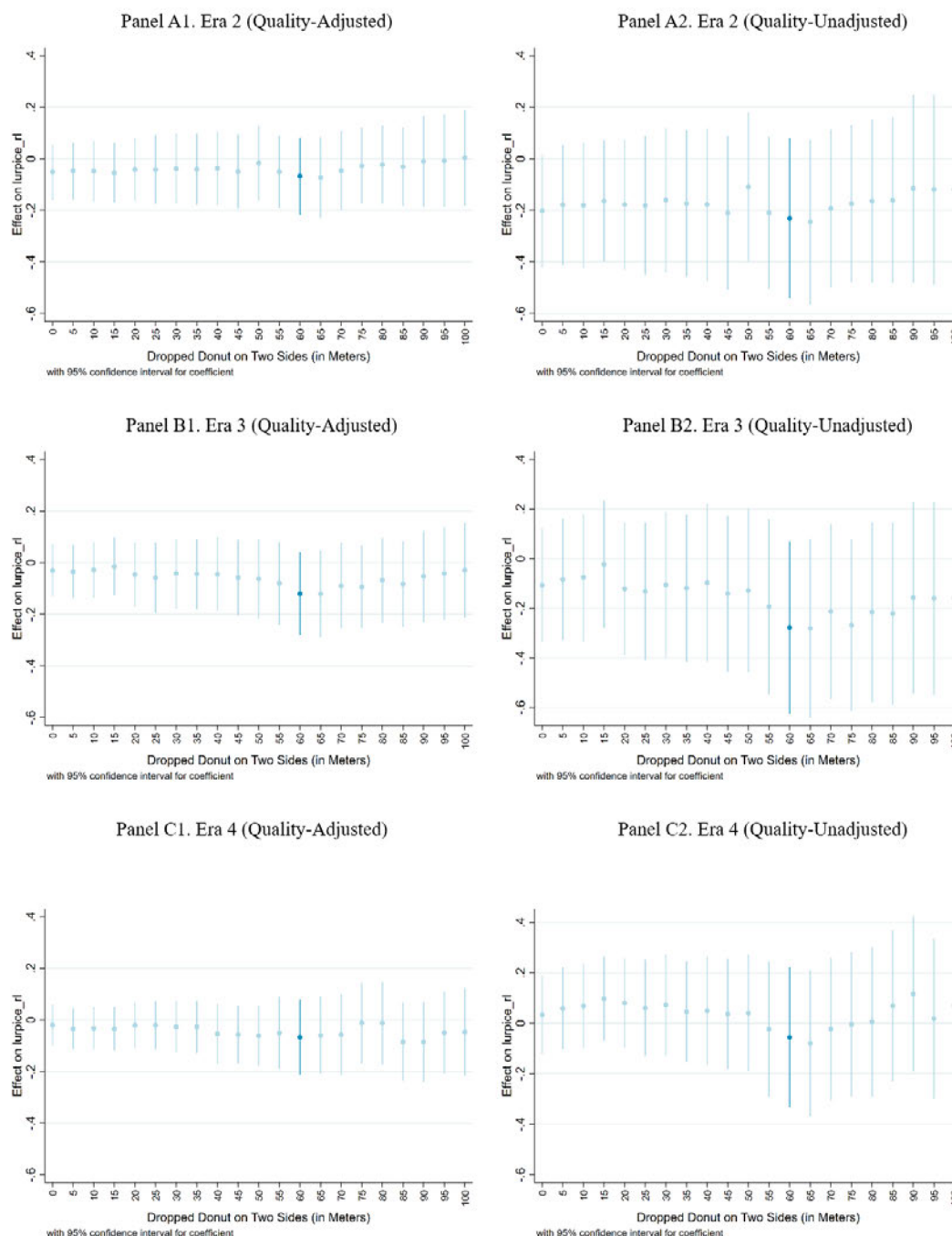
Notes: These figures illustrate the sensitivity of the differences in quality-adjusted and quality-unadjusted (log) asset prices per sq ft of floor space across the borders in different Eras, as analyzed in Equation (4), to various bandwidth selections. The dark blue dot and line represent the benchmark estimate and its confidence interval, with a bandwidth of 360 meters. Panels A1 and A2 display the estimates using the quality-adjusted and quality-unadjusted floor space prices in Era 2, respectively. Similarly, Panels B1 and B2 show the estimates for Era 3, and Panels C1 and C2 for Era 4.

Figure C.10: Robustness to Excluded Donut Sizes: Log of Asset Price per sq ft of Floor Space



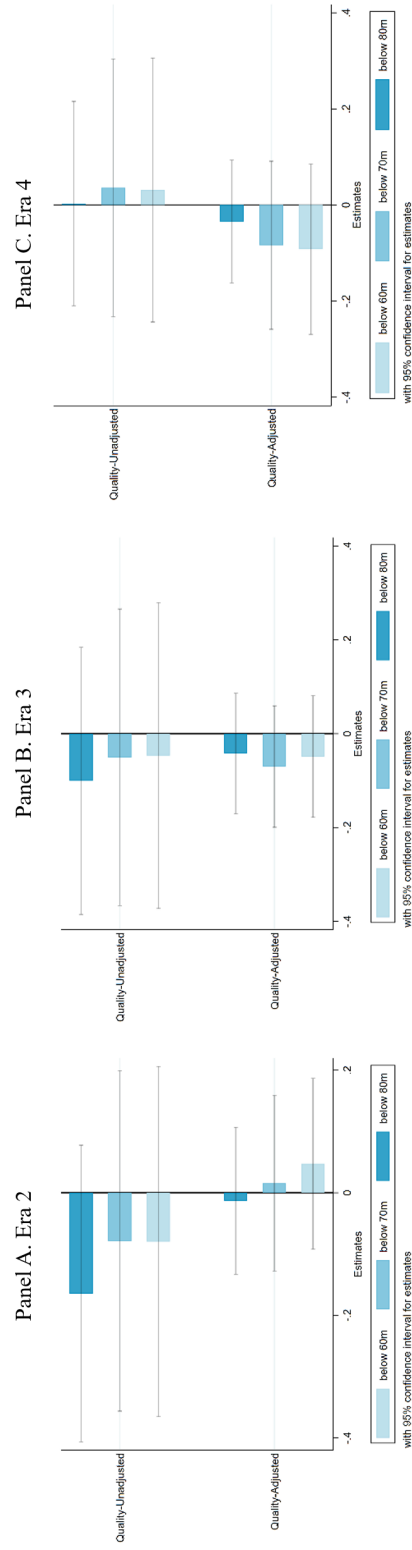
Notes: These figures illustrate the sensitivity of the differences in quality-adjusted and quality-unadjusted (log) asset prices per sq ft of floor space across the borders in different Eras, as analyzed in Equation (4), to various excluded donut sizes just outside the flight path. The dark blue dot and line represent the benchmark estimate and its confidence interval, with a bandwidth of 360 meters and an excluded donut size of 60 meters just outside the flight path. Panels A1 and A2 display the estimates using the quality-adjusted and quality-unadjusted floor space prices in Era 2, respectively. Similarly, Panels B1 and B2 show the estimates for Era 3, and Panels C1 and C2 for Era 4.

Figure C.11: Robustness to Excluding Donut Zones on Both Sides of the Border: Log of Asset Price per sq ft of Floor Space



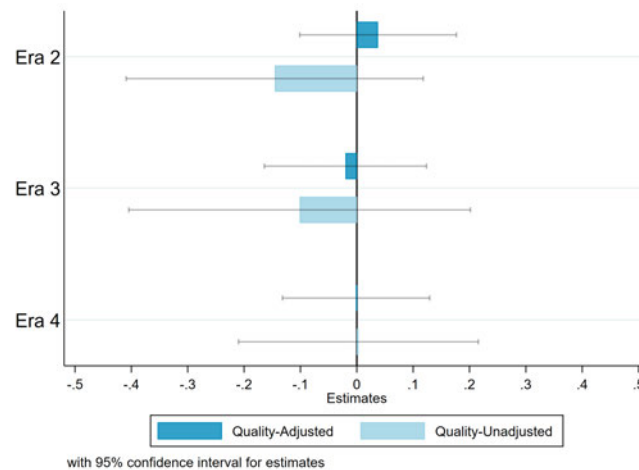
Notes: These figures illustrate the sensitivity of the differences in quality-adjusted and quality-unadjusted (log) asset prices per sq ft of floor space across the borders in different Eras, as analyzed in Equation (4), to various excluded donut sizes on both sides of the flight path borders. The dark blue dot and line represent the benchmark estimate and its confidence interval, using a bandwidth of 360 meters and excluding a 60-meter donut on each side of the flight path borders (totaling 120 meters). Panels A1 and A2 display the estimates using the quality-adjusted and quality-unadjusted floor space prices in Era 2, respectively. Similarly, Panels B1 and B2 show the estimates for Era 3, and Panels C1 and C2 for Era 4.

Figure C.12: Robustness to Border Selection Criterion: Log of Asset Price per sq ft of Floor Space



Notes: These figures illustrate the sensitivity of the differences in quality-adjusted and unadjusted (log) asset prices per sq ft of floor space across the borders to the border selection criterion, specifically the height limit on the stricter side of the border (inside the flight path) set at 60, 70, or 80 meters (the main estimate uses 80 meters as the cut-off value). All regressions use Equation (4), with a bandwidth of 360 meters and an exclusion of a 60-meter donut just outside the flight path. Panels A, B, C report estimates for Eras 2, 3, and 4, respectively.

Figure C.13: Robustness to Missing Data: Log of Flat Price per Unit



Notes: This figure illustrates the sensitivity of the differences in quality-adjusted and unadjusted (log) asset prices per sq ft of floor space across the borders to missing data. All regressions use Equation (4), with a bandwidth of 360 meters and an exclusion of a 60-meter donut just outside the flight path. The outcome variable used here is (log) real flat price per unit rather than (log) asset price per sq ft of floor space. In this analysis, all observations are retained, with unit size set to 0 if the information is unavailable, and a dummy variable is used to indicate observations without unit size information.

C2. Tables

Table C1: Maximum Building Height across Nonbinding Borders in Different Eras

	Maximum Building Height in a Grid Cell			
	(1) In 1988 (Era 1)	(2) In 1998 (Era 2)	(3) In 2008 (Era 3)	(4) In 2023 (Era 4)
1 {Inside the Flight Path}	-0.499 (3.475)	3.083 (3.786)	-0.458 (3.988)	-3.813 (4.300)
Sample Mean (mPD)	28.77	35.50	41.54	47.83
Border FE	X	X	X	X
Design Controls	X	X	X	X
Donut RD	X	X	X	X
Observations	14,856	14,856	14,856	14,856

Notes: Estimates from the regressions are based on Equation (3), using grid cells within a 360-meter bandwidth and excluding a 60-meter donut on the less restrictive side of identified non-binding borders (where building height limits are equal to or above 80 meters on the stricter side). Standard errors, shown in parentheses, are clustered by arbitrary 150 × 150-meter grid squares.

*** p<0.01, ** p<0.05, * p<0.1

Appendix D Data Sources, Processing and Choices

I have gathered extensive datasets while conducting fieldwork in Hong Kong. This appendix provides source information and processing details.

1. Airport-specific Building Height Limits

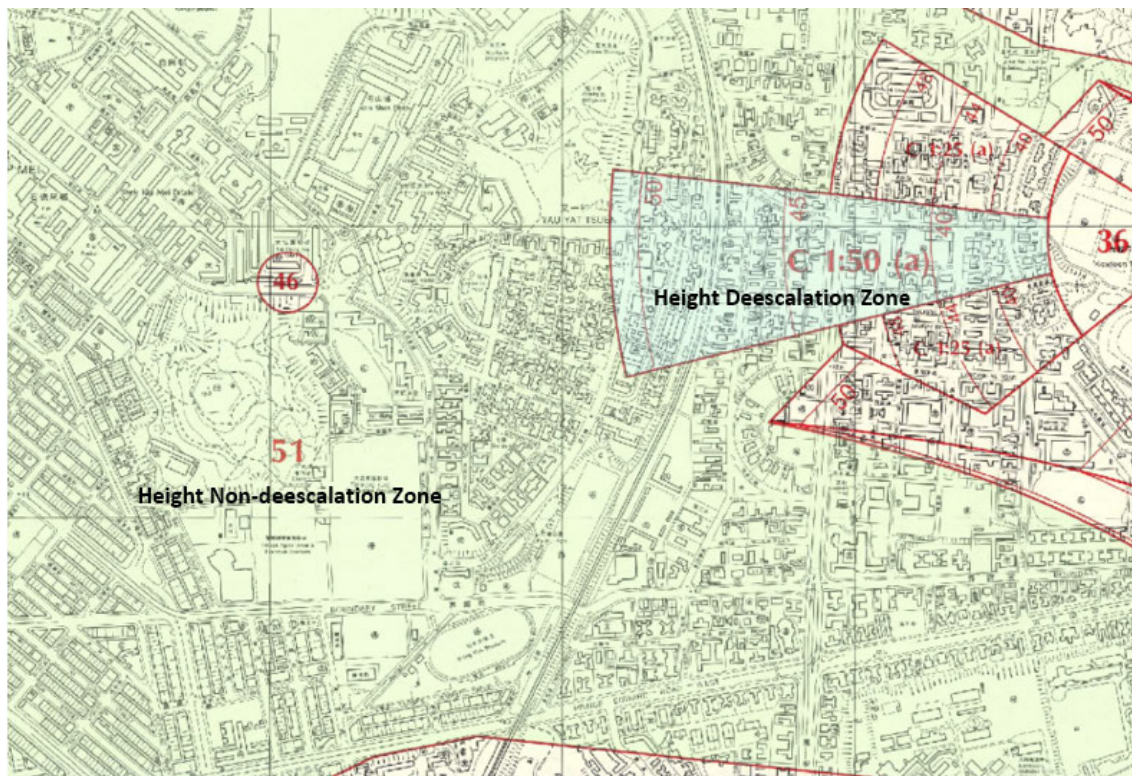
The Airport-specific building height limits are derived from Airport Height Control Maps, which were digitized from paper-based versions found in various Hong Kong libraries. Each map defines zones with distinct building height restrictions and provides the corresponding height limits within each zone. These maps classify zones into two primary categories: height deescalation zones and height non-deescalation zones. Height non-deescalation zones have fixed building height limits, while height deescalation zones contain variable limits based on specific climb or landing gradient ratios and anchored points (see illustration in Figure D.1). In cases where building height limits gradually change, often due to proximity to aircraft flight landing/take-off paths, the maps include geographical coordinates for anchor points and ratios for calculating height limits at specific locations using geometric methods. Importantly, maps issued from 1957 to 1996 are related to Kai Tak Airport's operations, while those issued from 1997 onward pertain to Chek Lap Kok Airport, Hong Kong's current airport.

- Airport Height Control Map (1957): Sourced from the Cartographica Laboratory and Library at the University of Hong Kong. This map represents the initial introduction of airport-specific height limits in Kowloon.
- Airport Height Control Map (1982): Acquired from the Government Records Service of Hong Kong and the Cartographica Laboratory and Library at the University of Hong Kong. This map provides more detailed information compared to the 1957 version.
- Airport Height Control Maps (1989): Obtained from the Government Records Service of Hong Kong, the Cartographica Laboratory and Library at the University of Hong Kong, and the Hong Kong Central Library. The 1989 map represents the

final building height limits enforced in Hong Kong before the closure of Kai Tak Airport. This version is consistent with the 1996 map.

- Airport Height Control Maps (1996): Obtained from the Cartographica Laboratory and Library at the University of Hong Kong. This version is consistent with the 1989 map.
- Airport Height Control Maps (1997): Sourced from the Cartographica Laboratory and Library at the University of Hong Kong. This map corresponds to the operation of the new airport, with building height limits in Kowloon exceeding 390 meters, as the increased distance from the new airport to Kowloon effectively eliminated airport-specific height restrictions in the Kowloon region.

Figure D.1: Examples of Height Deescalation and Non-Deescalation Zones



Notes: As shown in the figure, the height non-deescalation zone has a fixed building height limit of 51 meters. The height deescalation zone has a gradient ratio of 1/50, anchored at the point (a) (821485.4N, 837105.2E). Letter C indicates that the restricted height is defined by a conical surface passing through the height restriction contours shown.

2. Outline Zoning Plans

Outline Zoning Plans (OZPs) and corresponding maps for Kowloon's planning scheme areas since the mid-2000s were generously made available by the Cartographica Laboratory and Library at the University of Hong Kong and the Planning Department of Hong Kong. These vital resources contain details on the individual year and building height restrictions assigned to each planning scheme area when the government started integrating height limits into OZPs for urban planning.

3. Building Footprint Dataset

Data Sources and Initial Processing. The Building Footprint dataset for Hong Kong was acquired from the Hong Kong CSDI Portal in July 2023, courtesy of the Lands Department of Hong Kong. This comprehensive dataset encompasses details about the geographical coordinates, boundaries, maximum heights, construction years, building types (e.g., commercial or residential), and status (active, demolished, or under construction) of buildings constructed since the 1940s. Nevertheless, it's important to note that this dataset does come with certain limitations. Notably, there are instances of missing data related to building heights and construction years for select buildings (26.2% of the built-up area in this dataset lacks construction time information), and the demolition year is absent for all demolished structures.

In the Kowloon region, specifically, information regarding the completion year of the building structure is missing for about 26 percent of the total built area. To address these data gaps, I utilized satellite imagery and aerial photos of Kowloon from 1988, 1997, 1998, 2000, 2007, 2009, 2011, 2012, and 2023. I collaborated with a research assistant to manually collect and code information for buildings lacking completion year data, whether they were active or demolished. This coding included determining whether each building was constructed before January 1989, between January 1989 and July 1998, between July 1998 and Dec. 2007, or after Dec. 2007. Similarly, we coded information for currently demolished buildings, assessing whether the demolition occurred before January 1989, between January 1989 and July 1998, between July 1998 and Dec. 2007, or after Dec. 2007.

To ensure the accuracy of the data coding, the research assistant underwent a one-

month training period to align our judgments. Subsequently, the research assistant coded the entire Kowloon region dataset, with me reviewing 30 percent of the coded dataset each week to maintain consistency and accuracy. During this process, we also verified if there were any building footprints not captured by the government and identified very few such cases for years after 1988. However, in 1988, there were 2,330 missing building footprints, most of which were old public housing, slums, and storage warehouses. We manually digitized these structures and coded their building heights based on the height information of exactly the same structures nearby wherever possible.

This effort yielded comprehensive building footprint datasets at four significant time points for my analysis: Dec. 1988, July 1998, January 2008, and January 2023. Each dataset corresponds to the building footprints in Era 1, Era 2, Era 3, and Era 4, respectively.

A minor caveat of these maps is the missing height information, affecting 13.1% of the built-up area for the 1988 map, 6.4% for the 1998 map, 3.4% for the 2008 map, and 2.4% for the 2023 map. To address this, the heights of nearby buildings were used to impute the missing values.

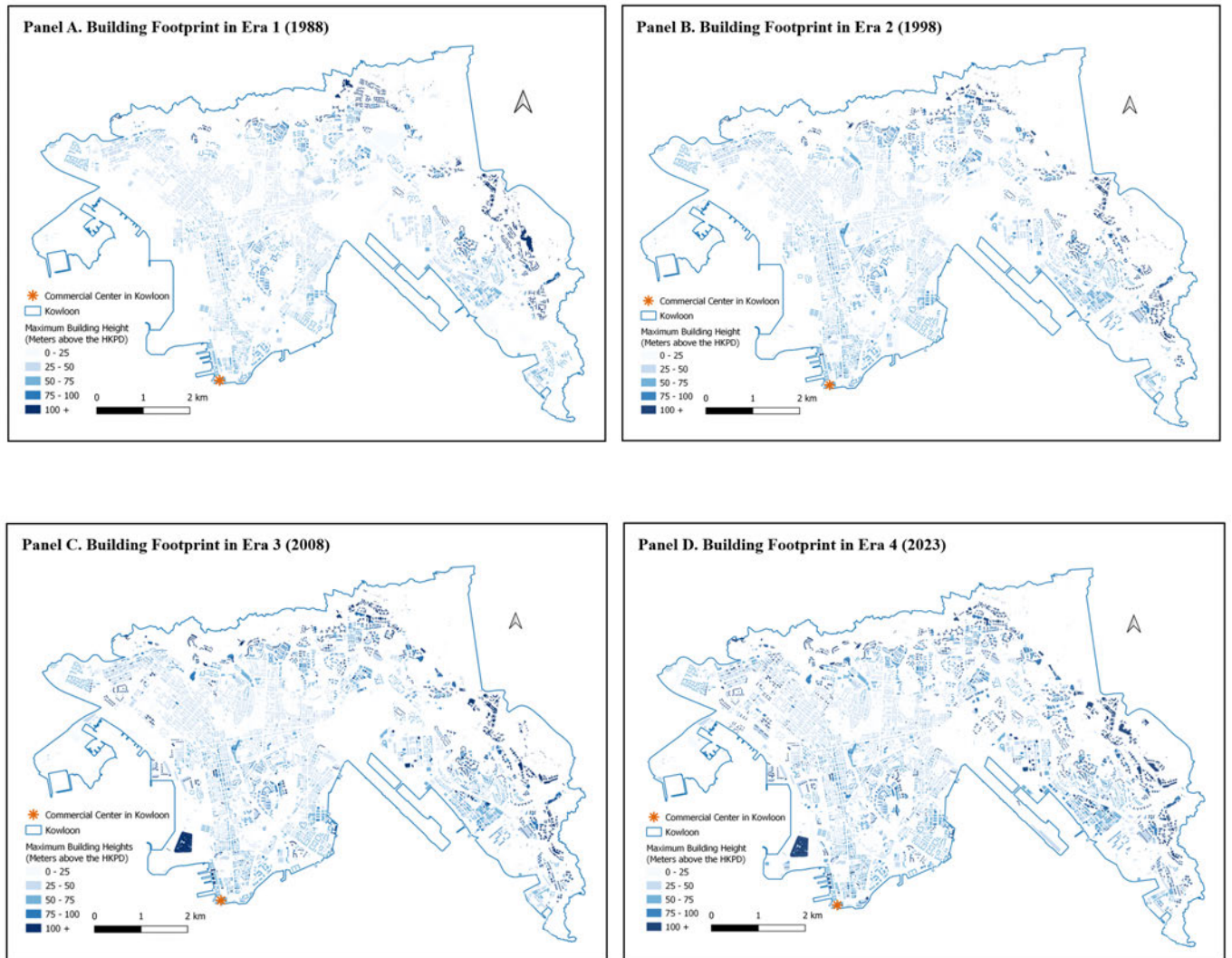
Figure D.2 shows building footprints and heights for each era. Panels A and B illustrate that buildings along the flight landing path to Kai Tak Airport were relatively low in height during Era 1 and Era 2. Between Era 1 and Era 2, taller buildings began to emerge just outside the narrowed flight path of Era 2, where height limits were modestly relaxed. Panels C and D reveal a notable expansion in building footprints and a significant increase in building heights in urban areas after the airport's relocation.

4. Satellite Imagery and Aerial Photos

The Satellite Imagery of Kowloon, Hong Kong was primarily obtained from two sources: Google Earth Pro and Hong Kong Map Service, depending on the specific years.

- Satellite Imagery from Google Earth Pro: Images from 2000, 2009, 2011, 2012, and 2023 were sourced from Google Earth Pro.
- Digital Aerial Photos (DAPs) from Hong Kong Map Service: Aerial photos captured from various altitudes and timeframes were accessed through the Hong Kong Map Service.

Figure D.2: Building Footprint Across Different Eras



- DAPs taken from 4,000 ft in Oct. 1988.
- DAPs taken from 10,000ft altitude in Nov. 1997.
- DAPs taken from 2,500ft, 3,500ft, and 4,000ft in July 1998.
- DAPs taken from 6,000ft in late November 2007.

The original format of each DAP lacks georeferencing. Therefore, my research assistants and I performed georeferencing on all these images for this building footprint dataset coding exercise.

5. Private Residential Flat Transactions

This cross-sectional dataset was acquired from EPRC Limited, a Hong Kong-based data vendor.⁴⁹ The dataset encompasses information on private residential flat transactions that occurred between 1991 and 2020.⁵⁰ It was compiled using electronic transaction data from the Land Registrar of Hong Kong, enriched with additional information such as flat unit and property characteristics. The unit of observation is the transaction identifier, and the dataset includes variables pertaining to transaction details, property features, and flat unit characteristics. Key variables include unique transaction identifiers, sale dates, transaction prices in millions, classification as first-/second-hand market transactions, building completion time, building facilities (e.g., swimming pool and/or clubhouse), building name, estate name, street name, district code, floor, unit, gross area in square feet, net area in square feet, number of bedrooms, and number of living rooms. To geocode each transaction, I used street names and building names. Geocoding for each transaction was performed using the Location Search API Service provided by the Hong Kong CSDI Portal. This API service identifies

⁴⁹I'm very grateful for the generous funding support from the Lincoln Institute of Land Policy, Institute of Humane Studies, the Trachtenberg School at GWU, and American Real Estate and Urban Economics Association, which made it possible to purchase this dataset (1991-2020) from EPRC Limited at a significantly discounted price.

⁵⁰Hong Kong has three main types of permanent housing: private permanent housing, public rental housing, and subsidized sale flats. These account for 56.8%, 28.5%, and 14.7% of the total housing stock, respectively (Census and Statistics Department of Hong Kong, 2022). According to the 2021 census, private permanent housing covers the following: private residential flats (45%), other quarters in private permanent housing, such as villas, bungalows, modern village houses, simple stone houses/traditional village houses, and all units of staff quarters (7.8%), and non-domestic quarters (0.8%). Notably, private residential flats - the focus of this dataset - constitute the largest proportion, encompassing flats and apartments in multi-story blocks or houses constructed by the private sector for residential purposes.

geographical locations in Hong Kong using addresses, building names, place names, or facility names. The geographical coordinates generated by this service are in the 1980 Hong Kong grid system (EPSG 2326) and were found to be more accurate for Hong Kong locations compared to Google or ArcGIS Pro's geocoding API services, based on checking exercises.

I excluded transactions involving buildings with an age of less than -3 years (since pre-sales of flat units rarely occur more than three years before completion) or transactions without available price information from the main sample. These exclusions account for 0% and 0.5% of the total transactions in Kowloon, respectively. Additionally, 23.6% of the transactions in Kowloon lack available unit size information. In my analysis, I excluded these transactions when analyzing floor space price per sq ft but also tested the sensitivity of the results by including all transactions using floor space price per unit. Transactions from 1991-1994 are extracted from Sales and Purchase Agreements (an earlier stage before the remaining balance is paid), while transactions from 1995-2020 are extracted from Assignments (marking the completion of a transaction) and constitute my main sample. For a detailed explanation, please refer to <https://www.clic.org.hk/en/topics/saleAndPurchaseOfProperty>.

For each transaction, I deflated the flat price using two methods: the annual CPI with 2010 as the base year (sourced from the World Bank) and the private domestic property price index released by the Rating and Valuation Department of Hong Kong, with 1999 as the base year. My results are robust to the use of either method.

6. Census/By-Census: Population and Demographics Data by Street Blocks

The street block-level socioeconomic characteristics dataset provides the finest geographical level of information available in Hong Kong, offering valuable insights into residents' profiles by education, income, employment status, and various economic indicators at the street block level every five years. This analysis uses data from 1996 to 2021, all sourced from the Census and Statistics Department of Hong Kong. These data are matched with the corresponding street block boundary maps for each census/by-census year, sourced from the Planning Department of Hong Kong. Key statistics used

for my analysis include population counts and shares by type of housing for each street block. To integrate this dataset with others, I assigned the street block-level statistics to all $30\text{m} \times 30\text{m}$ grid cells whose centroids are located within each specific street block.

- 1996: provided by the Census and Statistics Department of Hong Kong
- 2006: Census and Statistics Department of Hong Kong, downloaded from Hong Kong CSDI Portal
- 2016: Census and Statistics Department of Hong Kong, downloaded from Hong Kong CSDI Portal

7. Street Block Boundary Maps

In Hong Kong, the Planning Department employs the Tertiary Planning Unit/Street Block (TPU/SB) system for town planning. The Census and Statistics Department groups adjacent SBs with small populations into Large Street Block Groups for data dissemination. However, due to rapid population changes in small areas, TPU or SB boundaries may vary across different census/by-census years, even if they share the same TPU or SB code.

The street block boundary maps are sourced from the Planning Department of Hong Kong. Digital versions of street block boundary maps are readily available for the census/by-census years 2006 and 2016. However, official digitized versions of the 1996 LSBG boundary maps are not in existence. Hence, I collaborated with my research assistants to digitize the paper version of this map for research purposes.

8. Topography

- Elevation map: sourced from the Lands Department of Hong Kong
- Slope map: produced by Morgan & Guénard (2020) and downloaded from https://figshare.com/articles/dataset/Hong_Kong_climate_vegetation_and_topography_rasters/6791276?file=12353300

9. Location of Public Facilities

The Hong Kong CSDI Portal offers shapefiles containing information on the locations of schools, mass transit railways (MTR) stations, hospitals, parks, and other public facilities in Hong Kong. These shapefiles include the geographical coordinates of each location. I use the geographical coordinates of these public facilities to calculate the distance between each private residential flat unit and the nearest public facility. This generates a set of variables that capture the relative distance of flat units to the nearest public facilities and supplements the dataset on private residential housing transactions. I also use the geographical coordinates of metro stations and their construction times to calculate the distance from each grid cell's centroid to the nearest metro stations prior to the airport closure.